Biotechnology Advances 37 (2019) 107360

Contents lists available at ScienceDirect

Biotechnology Advances

journal homepage: www.elsevier.com/locate/biotechadv

Research review paper

A field of dreams: Lignin valorization into chemicals, materials, fuels, and health-care products

Judith Becker, Christoph Wittmann*

Institute of Systems Biotechnology, Saarland University, Campus A1.5, 66123 Saarbrücken, Germany

ARTICLE INFO

Keywords:
Aromatics
Lignocellulose
Laccase
Peroxidase
Catechol
Biotransformation
Cis,cis-muconic acid
Pseudomonas putida
Corynebacterium glutamicum
Amycolatopsis sp.
Sphingomonas paucimobilis

ABSTRACT

Lignin is one of the most abundant renewable resources on earth and is readily produced as a sidestream during biomass fractioning. So far, these large quantities of lignin have been severely underutilized, thereby wasting this valuable renewable. Recent technological advances in lignin recovery, breakdown, and conversion have now started forming the first sustainable value chains to take advantage of lignin. Microbial cell factories, inspired by nature's miscellaneous set of lignin-degrading microbes, are at the heart of these novel processes. Recent success stories in which the enzymes and pathways of these microbes were harnessed for biobased production from lignin hold great promise for a sustainable upgrading of this renewable polymer into value-added compounds.

1. Introduction

Lignin is the second most abundant polymer on earth. It naturally occurs as an integral part of lignocellulose in plants to give them rigidity and structure (Fig. 1) (Abdelaziz et al., 2016; Kohlstedt et al., 2018; Schutyser et al., 2018). Globally, the amount of available lignin in the biosphere is approximately 300 billion tons, with an annual increase of approximately 20 billion tons, thus providing an extensive carbon resource for sustainable production processes (Fernandez-Rodriguez et al., 2017). Chemically, lignin is a complex polymer assembled from aromatic building blocks, the phenylpropanoids (Fig. 2A), and can be regarded as a chemical treasure. However, it has remained the most underutilized renewable until today.

Technically, lignin accumulates as a coproduct of the cooking and pulping processes applied for biomass fractionation in different industrial sectors (Rinaldi et al., 2016; Van den Bosch et al., 2018) (Fig. 2B). Kraft pulping—the dominant pulping process today — produces approximately 130 million tons of lignin per year (Rinaldi et al., 2016; Van den Bosch et al., 2018). In addition, we can expect very large streams of lignin waste from second-generation biofuel plants. The US Energy Independence and Security Act of 2007 requires the mandatory use of 36 billion gallons of biofuels by 2022 (Chen and Wan, 2017). Interestingly, more than half of this amount will be provided from lignocellulosic biomass, leading to approximately 62 million tons of waste lignin in the US alone (Chen and Wan, 2017).

So far, the major fraction of technical lignin — approximately 140 million tons per year — is simply burned (Fig. 3A). The typical on-site generation of heat and power (Rinaldi et al., 2016; Van den Bosch et al., 2018), however, realizes only the energetic value of lignin. Therefore, lignin valorization has started to attract significant attention to make better use of this important renewable (Fig. 2B). Lignin valorization promises to kill two birds with one stone: a hand-in-hand production of added-value chemicals, materials and fuels from a global nonedible renewable resource instead of petroleum and much better economics of existing lignocellulosic processes in the biofuel and the pulp and paper industries (Chen and Wan, 2017; Liu et al., 2018).

Admittedly, lignin is difficult to break down due to the strong bonds between its building blocks, and its composition varies from plant to plant (Sanderson, 2011). Nevertheless, promising approaches have stimulated technological advances in lignin breakdown, such as hydrogenolysis, hydrothermal liquefaction, and hydrothermal carbonization, which provide mixed aromatic compounds, bio-oil and carbon materials from lignin, as recently indicated by (Cao et al., 2018; Ponnusamy et al., 2019). Moreover, the direct use of polymeric sulfonated forms of lignin from different pulping processes (Fig. 2B) yields low-value additives for concrete, glue, absorbers, emulsions, fertilizers, and photocatalyst supports (Cao et al., 2018; Khan et al., 2018; Naseem et al., 2016; Schutyser et al., 2018). In addition, the chemical

* Corresponding author at: Campus A1.5, 66123 Saarbrücken, Germany.
E-mail addresses: judith.becker@uni-saarland.de (J. Becker), christoph.wittmann@uni-saarland.de (C. Wittmann).

https://doi.org/10.1016/j.biotechadv.2019.02.016
Received 28 November 2018; Received in revised form 18 February 2019; Accepted 22 February 2019
Available online 06 April 2019

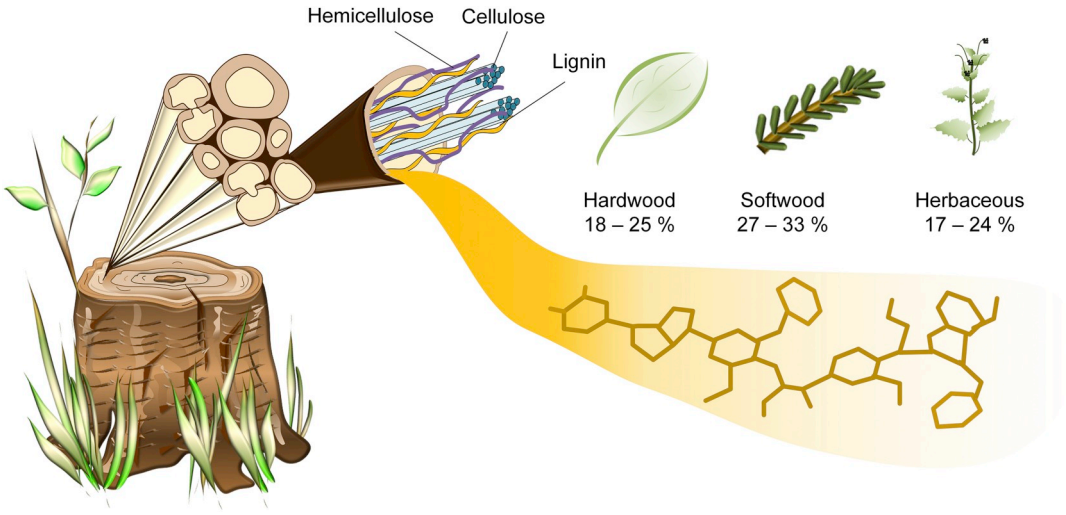

Fig. 1. Occurrence of lignin in nature. Terrestrial plants contain substantial fractions of lignocellulose, comprising cellulose, hemicellulose and lignin as polymeric constituents. Lignin itself is mainly composed of three phenyl alcohol subunits. Lignin content and composition differ depending on the plant source.

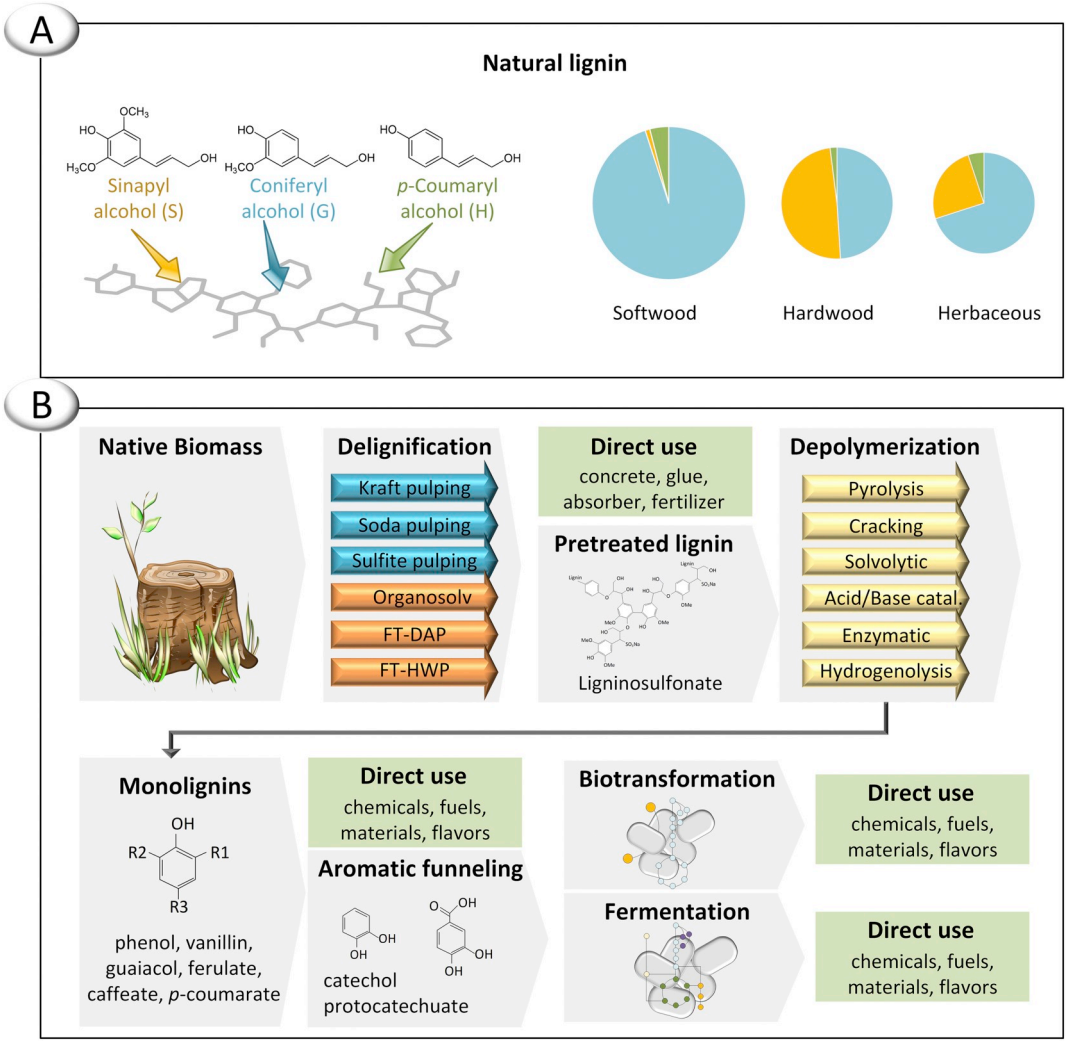

Fig. 2. Natural lignin – Composition and valorization. (A) Occurrence and composition of lignin in nature. The plant types differ in their relative lignin content (indicated by the size of the circle) and the relative fraction of the phenylpropanoid constitutes (S, G, H) (indicated by the segment size). Values on average lignin content and composition are taken from (Brunow, 2010). (B) Value chain for the production of lignin-derived compounds comprising delignification, depolymerization and upscaling. Blue arrows denote alkaline delignification processes, orange arrows denote acidic delignification processes. FT-DAP: flow-through diluted acid pretreatment, FT-HWP: flow-through diluted water pretreatment.

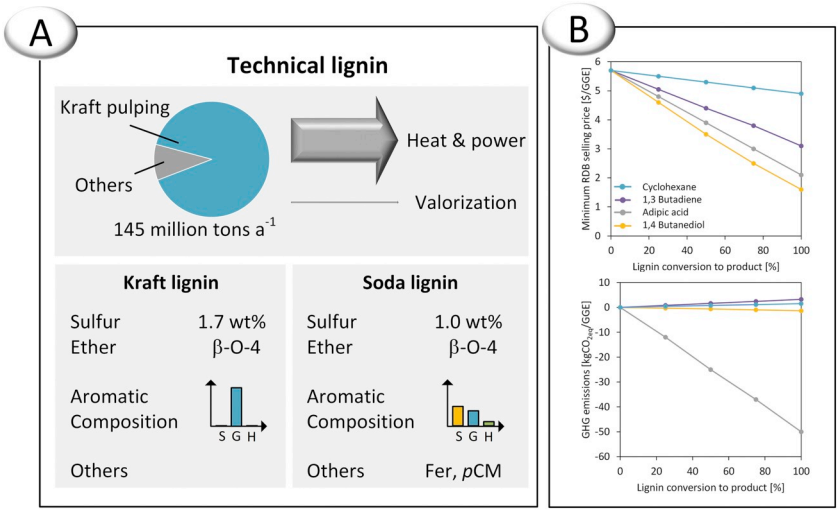

Fig. 3. Technical lignin – Composition and impact of valorization on selling prices and greenhouse gas emission. (A) Production, utilization and selected characteristics of technical lignin produced by Kraft pulping and soda pulping. Data are taken from (Constant et al., 2016; Rinaldi et al., 2016; Van den Bosch et al., 2018) (B) Minimum renewable diesel blendstock (RDB) price (top) and greenhouse gas (GHG) emission (bottom) as a function of lignin conversion to selected coproducts. GGE: gallon gasoline equivalent. Figure 3B was adapted from (Davis et al., 2013).

processing of lignin provides access to products of higher value. A prominent example is vanillin, an industrially established flavor and fragrance molecule that is derived through oxidative alkaline treatment of softwood lignin (Abdelaziz et al., 2016).

Furthermore, recent studies (Barton et al., 2018; Kohlstedt et al., 2018) have impressively demonstrated the potential to use microbes for the biochemical conversion of lignin into value-added products (Fig. 2B). As the masterpiece of lignin valorization, cascade routes produce platform chemicals for commercial plastics such as adipic acid, *cis,cis*-muconic acid (MA) and terephthalic acid from lignin at scales up to the pilot scale (Kohlstedt et al., 2018; Vardon et al., 2015). Beneficially, these processes not only promise sustainable green alternatives to fossil routes but also enhance the efficiency of the various existing second generation biorefineries. It is important to note that economic considerations reveal a tremendous potential to reduce the price for second generation biofuel and reduce associated greenhouse gas emissions, given a better valorization of the lignin fraction of lignocellulosic biomass beyond energy applications (Corona et al., 2018; Davis et al., 2013). Such calculations hold for industrial chemicals such as adipic acid, 1,4-butanediol, and cyclohexane and promise a unique win-win situation (Fig. 3B).

Clearly, the overall success in using lignin as a renewable resource requires a fully integrated value chain that efficiently bridges lignin recovery and depolymerization and (bio)chemical conversion of the obtained carbon feedstock into added-value products. Our review describes this lignin value chain and highlights recent developments and trends in this most promising field.

2. Natural lignin—Occurrence, biosynthesis and breakdown in nature

2.1. Chemical structure

In nature, lignin has evolved as an important structural compound, mainly in terrestrial plants. In addition to cellulose and hemicellulose, lignin is one of the three major constituents of lignocellulose, the woody part of plants (Fig. 1). In this case, lignin functions as a structural stabilizer, a water pipeline inside plants, and a barrier against microbial decay (Brunow, 2010; Linger et al., 2014). Chemically, lignin is composed of mainly three phenylpropanoid units: the monolignols coniferyl alcohol (G), sinapyl alcohol (S) and *p*-coumaryl alcohol (H) (Fig. 2A) (Abdelaziz et al., 2016; Cao et al., 2018; Wang et al., 2018a). The assembly of these units into lignin polymers occurs via reactive radical intermediates, which are generated by laccases and peroxidases (Schutyser et al., 2018). The resulting linkages between the monolignols comprise carbon-carbon and ether bonds (Fig. 4) and result in the complex tridimensional structure of lignin. Approximately 50-80 % of all interunit bonds are β-O-4 ether bonds (Chen and Wan, 2017; Van den Bosch et al., 2018). In addition, subunits are connected by α-O-4 linkages, β-5 linkages, β-β linkages, 5-5 linkages and biphenyl and diaryl ether structures (Brunow, 2010; Chen and Wan, 2017; Ponnusamy et al., 2019; Schutyser et al., 2018; Van den Bosch et al., 2018). Depending on the plant type, both lignin content and composition can vary substantially (Figs. 1, 2A). Softwood has the highest lignin content and is mainly composed of coniferyl units (G-type lignin) (Fig. 2A). In contrast, hardwood lignin is almost equally composed of coniferyl and sinapyl alcohol (G/S-type lignin), whereas lignin of grass, herbaceous, and angiosperm plants also contains *p*-coumaryl alcohol units (G/S/H-type lignin) (Brunow, 2010; Martinez et al., 2005; Ponnusamy et al., 2019). The distribution and occurrence of the different monolignols determine the amount and type of the interunit linkages: monolignols with ortho-methoxy-groups cannot form 5-5 and β-5 carbon-carbon bonds. Consequently, hardwood lignin with a high amount of S-units (two methoxy-substituted ortho groups) contains a lower fraction of carbon-carbon bonds than G-rich (one methoxy-substituted ortho group) softwood lignin (Chen and Wan, 2017; Schutyser et al., 2018).

2.2. Microbial ligninolysis—the initial step of lignin breakdown

White-rot and brown-rot fungi (Table 1) have long been considered the only organisms that can metabolize lignin (Brunow, 2010; Bugg et al., 2011). However, several studies recently reported on bacterial lignin-degraders of the genera *Streptomyces*, *Pseudomonas*, *Rhodococcus*, *Amycolatopsis*, *Oceanimonas*, *Comamonas*, *Pandoraea* and *Paenibacillus* from different environments (Majumdar et al., 2014; Numata and Morisaki, 2015; Palazzolo and Kurina-Sanz, 2016; Salvachua et al., 2015; Vyas et al., 2018) (Table 1). The relative activity and specificity of the different lignin-degraders can be easily monitored using an UV/vis assay (Ahmad et al., 2010). In a comparative study, the fungus *Phanerochaete chrysosporium* revealed the highest and broadest ligninolytic activity (Ahmad et al., 2010). Bacterial degraders were found to be more specific. *Nocardia autotrophica* degraded only milled wood lignin (MWL) of pine, *Pseudomonas putida* strain 33015 specifically degraded miscanthus MWL, whereas *Rhodococcus* RHA1 degraded different types of lignin (Ahmad et al., 2010).

In general, the ligninolytic activity of fungi and bacteria relies on a cocktail of oxidative enzymes (laccases and peroxidases) and some accessory enzymes such as H_2O_2-generating oxidases (Fig. 4) (Abdelaziz et al., 2016; Brunow, 2010; de Gonzalo et al., 2016; Palazzolo and

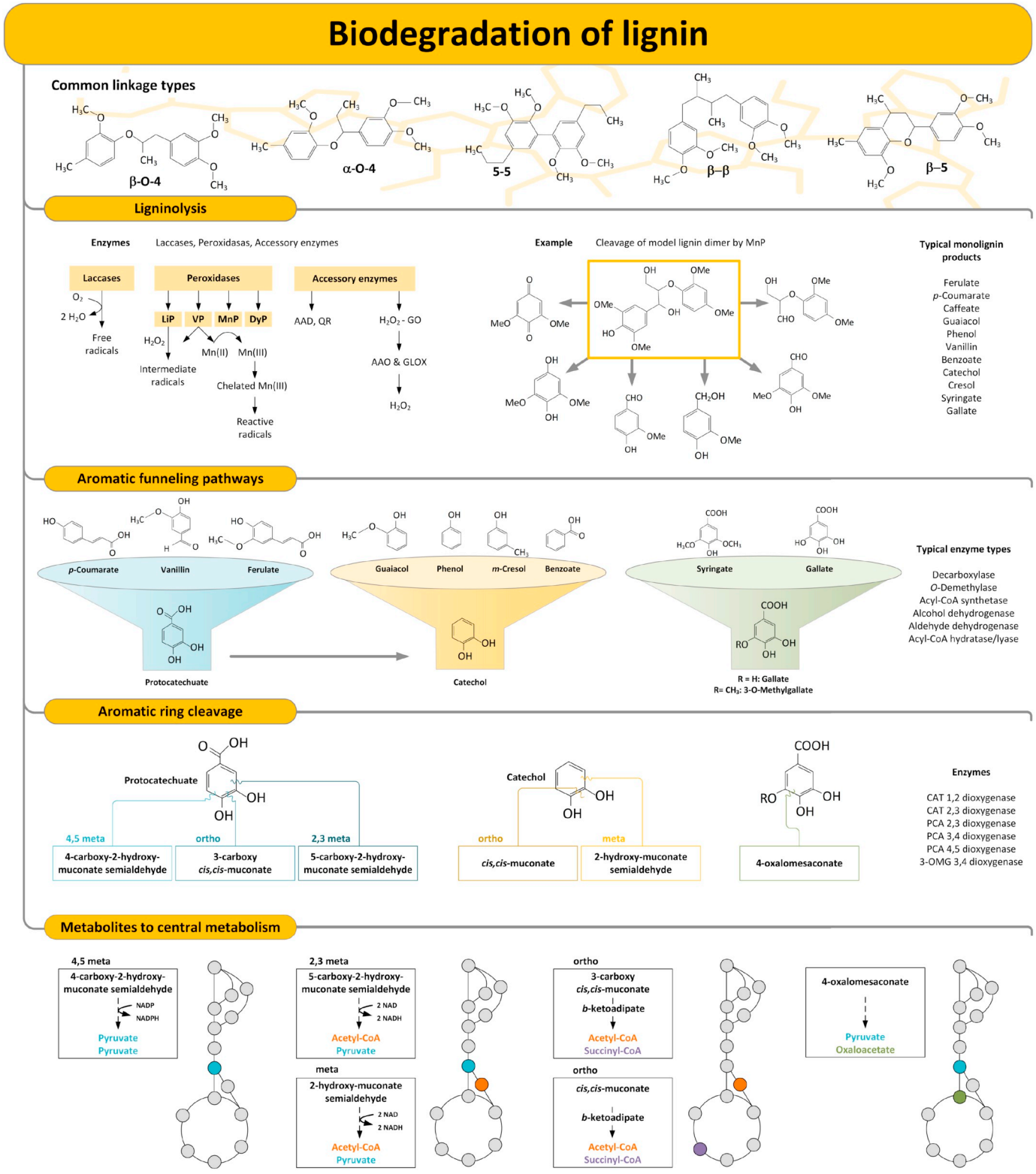

Fig. 4. Biodegradation of lignin. Common linkages in lignin are cleaved by the activity of laccases and peroxidases – partly relying on accessory enzymes – to provide a variety of monolignins. Aromatics from G-type and H-type lignin are then funneled via the key intermediates protocatechuate (PCA) and catechol (CAT), which are crosslinked in some microbes. The entry point of carbon into the central metabolism depends on the position of aromatic ring opening (ortho, meta). Aromatics from S-type lignin are degraded via gallate and 3-O-methylgallate (3-OMG). As common intermediate of further catabolism, 4-oxalomesaconate is formed directly by ring cleavage of gallate, or ring cleavage of 3-OMG and subsequent elimination of the methyl-group. Parts of the figure are adapted from (Abdelaziz et al., 2016; Dashtban et al., 2010; Hofrichter, 2002; López et al., 2017).

H_2O_2-GO: H_2O_2 generating oxidases, AAD: aryl alcohol dehydrogenase, AAO: aryl alcohol oxidase, GLOX: glyoxal oxidase, QR: quinone reductase.

Table 1
Overview of a selection of known microbes expressing enzymes with ligninolytic activity.

Organism	Enzymes	Carbon source/substrate	Reference
Fungi			
Phanerochaete chrysosporium	LiP, MnP	MWL of pine, wheat miscanthus, β-1, β-O-4 lignin model compounds	(Ahmad et al., 2010; Glenn et al., 1986; Glenn and Gold, 1985; Kirk et al., 1984; Tien and Kirk, 1984)
Lepista nuda	MnP, laccase	MWL of pine, wheat	(Ahmad et al., 2010; Erden et al., 2009)
Serpula lacrymans	LiP	MWL of pine	(Ahmad et al., 2010; Eastwood et al., 2011)
Schizophyllum commune	MnP, laccase	MWL of pine	(Ahmad et al., 2010; Wengel et al., 2006; Zhou et al., 2014)
Fusarium oxysporum	LiP, laccase	Kraft black liquor, veratryl alcohol	(Abdelaziz et al., 2016; Kumari et al., 2002)
Aspergillus terreus	LiP	Veratryl alcohol	(Kumari et al., 2002)
Penicillium citrinum	LiP	Veratryl alcohol	(Kumari et al., 2002)
Dichomitus squalens	Intracellular β-etherase	β-O-4 lignin model compound	(Marinovic et al., 2018)
Bacteria			
Streptomyces coelicolor	Laccase	MWL of pine, wheat miscanthus, ethanosolv lignin, β-O-4 lignin model compound	(Ahmad et al., 2010; Majumdar et al., 2014)
Streptomyces viridosporus	LiP, laccase	Wheat straw, ethanosolv lignin, β-O-4 lignin model compound	(Abdelaziz et al., 2016; Gottschalk et al., 2008; Majumdar et al., 2014)
Rhodococcus erythropolis	Laccase, peroxidase	MWL of pine, wheat miscanthus, APL, kraft lignin	(Abdelaziz et al., 2016; Ahmad et al., 2010; Salvachua et al., 2015)
Rhodococcus jostii	Laccase, MnP, DyP	MWL of pine, wheat miscanthus, APL, kraft lignin, model *β*-aryl ether lignin dimers, wheat straw lignocellulose	(Ahmad et al., 2011; Ahmad et al., 2010; Roberts et al., 2011; Sainsbury et al., 2013; Salvachua et al., 2015; Vignali et al., 2018)
Pseudomonas putida	Laccase, MnP, LiP	MWL of miscanthus, APL, Kraft lignin	(Ahmad et al., 2010; Salvachua et al., 2015; Xu et al., 2018)
Arthrobacter globiformis	Perodixase	MWL of pine, wheat	(Ahmad et al., 2010)
Nocardia autotrophica	Peroxidase	MWL of pine	(Ahmad et al., 2010)
Amycolatopsis sp.	MnP, laccase	APL, ethanosolv lignin, β-O-4 lignin model compound	(Majumdar et al., 2014; Salvachua et al., 2015)
Acinetobacter sp.	Laccase, MnP, LiP	APL, b-O-4 lignin model compounds, veratrylglycerol-β-guaiacyl ether	(Ghodake et al., 2009; Salvachua et al., 2015; Vasudevan and Mahadevan, 1990, 1992)
Cupriavidus necator	Laccase, MnP	APL	(Salvachua et al., 2015)
Aneurinibacillus aneurinilyticus		Kraft lignin	(Chandra et al., 2007)
Bacillus atrophaeus	Laccase	Kraft lignin, guaicylglycerol-β-guaiacyl ether	(Huang et al., 2013)
Enterobacter lignolyticus	Peroxidase, laccase, DyP	Alkali lignin	(Deangelis et al., 2013; Orellana et al., 2017; Shrestha et al., 2017)
Klebsiella pneumoniae	MnP, LiP, laccase, catalase-peroxidase	Kraft lignin	(Hochman and Goldberg, 1991; Kumar and Chandra, 2018; Xu et al., 2018)
Oceanimonas doudoroffii	Peroxidase	Lignin	(Brennan et al., 2017; Numata and Morisaki, 2015)
Sphingomonas paucimobilis	β-Etherase, hydrolase, extradiol dioxygenase, O-demethylase, decarboxylase	Lignin-derived biaryls, guaicylglycerol-β-guaiacyl ether, biphenyls	(Kuatsjah et al., 2017; Masai et al., 2007a; Peng et al., 1998; Peng et al., 1999; Takahashi et al., 2018; Yoshikata et al., 2014)
Ochrobactrum tritici	LiP, MnP, laccase	Kraft lignin	(Xu et al., 2018)

Kurina-Sanz, 2016; Vyas et al., 2018). Peroxidases directly act on lignin and lignin fragments but are also interestingly capable of attacking lignin from a distance (de Gonzalo et al., 2016). For the latter, the enzymes generate radical mediators that can penetrate the recalcitrant structure of lignin and initiate depolymerization (de Gonzalo et al., 2016). Depending on their catalytic reaction type, the peroxidases are classified as manganese peroxidases (MnPs), lignin peroxidases (LiPs), versatile peroxidases (VPs) and dye-decolorizing peroxidases (DyPs) (Chen and Wan, 2017).

MnPs are heme-containing enzymes and attack lignin structures in catalytic cycles via reactive Mn^{3+} ions (Abdelaziz et al., 2016; Chen and Wan, 2017; Hofrichter, 2002). The ability to produce and secrete MnPs is widespread among fungi (Table 1) (Hofrichter, 2002). Meanwhile, their production from bacterial degraders has also been proven (Table 1) (Salvachua et al., 2015). LiPs are activated by H_2O_2 and attack lignin via intermediate radicals, whereas VPs somehow combine the catalytic strategy of MnPs and LiPs (Abdelaziz et al., 2016; Chen and Wan, 2017). DyPs are structurally different from other peroxidases (Abdelaziz et al., 2016; Chen and Wan, 2017) and occur in fungi and bacteria (Table 1) (Chen and Wan, 2017; Salvachua et al., 2015). They typically exhibit a very broad substrate spectrum and are mainly active at acidic pH values (de Gonzalo et al., 2016). Recently, the *Rhodococcus jostii* DyPB was overexpressed in *Escherichia coli* and characterized. It efficiently oxidized aromatic lignin monomers and, furthermore, cleaved guaiacylglycerol-beta-guaiacyl ether, a model molecule for β-O-4 linkages (Vignali et al., 2018).

In addition to peroxidases, laccases play a major role in lignin degradation. They have a lower redox potential than peroxidases. Accordingly, they cleave only phenolic lignin units (Bugg et al., 2011; Chen and Wan, 2017; Majumdar et al., 2014) unless there are redox mediators such as vanillin and *p*-coumarate present (Abdelaziz et al., 2016).

While most ligninolytic enzymes are secreted, a recent study first described an intracellular β-etherase capable of cleaving a dimeric lignin model compound (Marinovic et al., 2018). The enzyme was found in the white-rod basidiomycete *Dichomitus squalens* and showed selective activity on the β-O-aryl ether bond under mild reaction conditions, making this enzyme attractive for biotechnological application (Marinovic et al., 2018). The product spectrum of the initial degradation step of lignin is diverse and comprises a variety of monolignins, including ferulate, *p*-coumarate, phenol, vanillin, guaiacol and cresols (Fig. 4) (Abdelaziz et al., 2016). As described below, microbes and their enzymes have been successfully used to mediate lignin breakdown and increase its bioavailability for subsequent bioconversions.

2.3. Catabolism of lignin-derived aromatics—the second step of lignin breakdown

As described above, the natural degradation of the lignin polymer is reserved for some specialized fungi and bacteria that are able to cleave

Table 2
Genes and enzymes described in various strains for degradation of aromatic compounds via funneling pathways.

Substrate	Product	Gene	Enzyme	Organism	Reference
Eugenol					
Eugenol	Coniferyl alcohol	*ehyAB*	Eugenol hydroxylase	*Pseudomonas* sp. strain HR199	(Overhage et al., 2002)
		vaoA	Vanillyl alcohol oxidase	*Penicillium simplicissimum* CBS 170.90	(Overhage et al., 2003)
Coniferyl alcohol	Coniferyl aldehyde	*calA*	Coniferyl alcohol dehydrogenase	*Pseudomonas* sp. strain HR199	(Overhage et al., 2002)
Coniferyl aldehyde	Ferulate	*calB*	Coniferyl aldehyde dehydrogenase	*Pseudomonas* sp. strain HR199	(Overhage et al., 2002)
				Pseudomonas putida KT2440	(Jimenez et al., 2002)
Ferulate					
Ferulate	Feruloyl-CoA	*fcs*	Acyl-CoA synthetase	*Pseudomonas* sp. strain HR199	(Overhage et al., 1999b)
				Pseudomonas putida KT2440	(Jimenez et al., 2002; Plaggenborg et al., 2003)
				Rhodococcus opacus PD630	(Plaggenborg et al., 2006)
		ferA	Acyl-CoA synthetase	*Sphingomonas paucimobilis* SYK-6	(Masai et al., 2002; Masai et al., 2007a)
Feruloyl-CoA	Vanillin + acetyl-CoA	*ech*	Enoyl-CoA hydratase/aldolase	*Pseudomonas* sp. strain HR199	(Overhage et al., 1999b)
				Pseudomonas putida KT2440	(Jimenez et al., 2002; Plaggenborg et al., 2003)
				Rhodococcus opacus PD630	(Plaggenborg et al., 2006)
Feruloyl-CoA	Vanillin + acetyl-CoA	*ferB, ferB2*	Enoyl-CoA hydratase/aldolase	*Sphingomonas paucimobilis* SYK-6	(Masai et al., 2002; Masai et al., 2007a)
Ferulate	Feruloyl-CoA	*phdA*	Acyl-CoA ligase	*Corynebacterium glutamicum*	(Kallscheuer et al., 2016)
Feruloyl-CoA	3-Hydroxyferuloyl-CoA	*pdhE*	Acyl-CoA hydratase	*Corynebacterium glutamicum*	(Kallscheuer et al., 2016)
3-Hydroxyferuloyl-CoA	3-Oxoferuloyl-CoA	*pdhB*	3-Hydroxyacyl-CoA dehydrogenase	*Corynebacterium glutamicum*	(Kallscheuer et al., 2016)
3-Oxoferuloyl-CoA	Vanillate + acetyl-CoA	*pdhC*	3-Oxoacyl-CoA ketohydrolase	*Corynebacterium glutamicum*	(Kallscheuer et al., 2016)
Vanillin					
Vanillin	Vanillate	*vdh*	Vanillin dehydrogenase	*Pseudomonas* sp. strain HR199	(Overhage et al., 1999a)
				Pseudomonas putida KT2440	(Jimenez et al., 2002; Plaggenborg et al., 2003)
				Rhodococcus opacus PD630	(Plaggenborg et al., 2006)
Vanillin	Vanillate	*ligV*	Vanillin dehydrogenase	*Sphingomonas paucimobilis* SYK-6	(Masai et al., 2007b)
Vanillate					
Vanillate	Protocatechuate	*vanA* *vanB*	Vanillate-*O*-demethylase	*Pseudomonas* sp. strain HR199	(Priefert et al., 1997)
				Acinetobacter baylyi	(Fischer et al., 2008)
				Corynebacterium glutamicum	(Merkens et al., 2005)
Vanillate	Protocatechuate	*ligM*	Vanillate-*O*-demethylase	*Sphingomonas paucimobilis* SYK-6	(Abe et al., 2005; Masai et al., 2007a; Nishikawa et al., 1998)
Vanillate	Guaiacol		Vanillate decarboxylase	*Streptomyces setonii (Amycolatopsis)*	(Pometto et al., 1981; Sutherland et al., 1983)
				Streptomyces sp.	(Alvarez-Rodriguez et al., 2003)
				Bacillus subtilis	(Alvarez-Rodriguez et al., 2003)
p-Coumarate					
p-Coumarate	*p*-Coumaryl-CoA	*fcs*	Acyl-CoA synthetase	*Pseudomonas putida* KT2440	(Jimenez et al., 2002)
p-Coumaryl-CoA	4-Hydroxybenzaldehyde + acetyl-CoA	*ech*	Enoyl-CoA hydratase/aldolase	*Pseudomonas putida* KT2440	(Jimenez et al., 2002)
4-Hydroxybenzaldehyde	4-Hydroxybenzoate	*vdh*	Aldehyde dehydrogenase	*Pseudomonas putida* KT2440	(Jimenez et al., 2002)
p-Coumarate	*p*-Coumaryl-CoA	*phdA*	Acyl-CoA ligase	*Corynebacterium glutamicum*	(Kallscheuer et al., 2016)
p-Coumaryl-CoA	3-Hydroxycoumaryl-CoA	*pdhE*	Acyl-CoA hydratase	*Corynebacterium glutamicum*	(Kallscheuer et al., 2016)
3-Hydroxycoumaryl-CoA	3-Oxocoumaryl-CoA	*pdhB*	3-Hydroxyacyl-CoA dehydrogenase	*Corynebacterium glutamicum*	(Kallscheuer et al., 2016)
3-Oxocoumaryl-CoA	4-Hydroxybenzoate + acetyl-CoA	*pdhC*	3-Oxoacyl-CoA ketohydrolase	*Corynebacterium glutamicum*	(Kallscheuer et al., 2016)
4-Hydroxybenozate	Protocatechuate	*pobA*		*Acinetobacter baylyi*	(Fischer et al., 2008)
				Pseudomonas putida KT2440	(Jimenez et al., 2002)
				Corynebacterium glutamicum	(Huang et al., 2008)
p-Cresol					
p-Cresol	4-Methylbenzylphosphate	*creHI*	4-Methylbenzylphosphate synthase	*Corynebacterium glutamicum*	(Du et al., 2016)
4-Methylbenzylphosphate	Benzylalcohol 4-phosphate	*creJEF*	P450 monooxygenase	*Corynebacterium glutamicum*	(Du et al., 2016)
Benzylalcohol 4-phosphate	4-Hydroxybenzylalcohol	*creD*	Universal phosphohydrolase	*Corynebacterium glutamicum*	(Du et al., 2016)
Benzylalcohol 4-phosphate	Benzylaldehyde 4-phosphate	*creG*	4-Hydroxybenzylalcohol dehydrogenase	*Corynebacterium glutamicum*	(Du et al., 2016)
		creJEF	P450 monooxygenase		

(*continued on next page*)

Table 2 (*continued*)

Substrate	Product	Gene	Enzyme	Organism	Reference
p-Hydroxybenzylalcohol	*p*-Hydroxybenzaldehyde	*creG*	4-Hydroxybenzylalcohol dehydrogenase	*Corynebacterium glutamicum*	(Du et al., 2016)
Benzylaldehyde 4-phosphate	Benzoate 4-phosphate	*creC*	Benzylaldehyde 4-phosphate dehydrogenase	*Corynebacterium glutamicum*	(Du et al., 2016)
		creJEF	P450 monooxygenase		
p-Hydroxybenzaldehyde	4-Hydroxybenzoate	*creC*	Benzylaldehyde 4-phosphate dehydrogenase	*Corynebacterium glutamicum*	(Du et al., 2016)
Benzoate 4-phosphate	4-Hydroxybenzoate	*creD*	Universal phosphohydrolase	*Corynebacterium glutamicum*	(Du et al., 2016)
p-Cresol	*p*-Hydroxybenzylalcohol	*pchC* *pchF*	*m/p*-Cresol methylhydroxylase	*Pseudomonas putida*	(Chen et al., 2014; Keat and Hopper, 1978b)
p-Hydroxybenzylalcohol	*p*-Hydroxybenzaldehyde	*pchC* *pchF*	*m/p*-Hydroxybenzylalcohol dehydrogenase *p*-Cresol methylhydroxylase	*Pseudomonas putida*	(Chen et al., 2014; Keat and Hopper, 1978a)
p-Hydroxybenzaldehyde	4-Hydroxybenzoate	*pchA*	*p*-Hydroxybenzaldehyde dehydrogenase	*Pseudomonas putida*	(Chen et al., 2014)
m-Cresol					
m-Cresol	*m*-Hydroxybenzylalcohol		*m/p*-Cresol methylhydroxylase	*Pseudomonas putida*	(Hopper and Taylor, 1975)
m-Hydroxybenzylalcohol	*m* -Hydroxybenzaldehyde		*m/p*-Hydroxybenzylalcohol dehydrogenase	*Pseudomonas putida*	(Hopper and Taylor, 1975; Keat and Hopper, 1978a)
m-hydroxybenzaldehyde	3-Hydroxybenzoate		*m/p*-Hydroxybenzaldehyde dehydrogenase	*Pseudomonas putida*	(Hopper and Taylor, 1975)
m-cresol	3-Methylcatechol		Monooxygenase	*Pseudomonas putida*	(Hopper and Taylor, 1975)
o-Cresol					
o-Cresol	2-Methylcatechol		Monooxygenase	*Amycolatopsis sp.*	(Barton et al., 2018)
Caffeic acid					
Caffeic acid	Caffeoyl-CoA	*fcs*	Acyl-CoA synthetase	*Pseudomonas putida* KT2440	(Jimenez et al., 2002)
Caffeoyl-CoA	Protocatechuic aldehyde + acetyl-CoA	*ech*	Enoyl-CoA hydratase/aldolase	*Pseudomonas putida* KT2440	(Jimenez et al., 2002)
Protocatechuic aldehyde	Protocatechuate	*vdh*	Aldehyde dehydrogenase	*Pseudomonas putida* KT2440	(Jimenez et al., 2002)
Caffeic acid	Caffeoyl-CoA	*phdA*	Acyl-CoA ligase	*Corynebacterium glutamicum*	(Kallscheuer et al., 2016)
Caffeoyl-CoA	3-Hydroxycaffeoyl-CoA	*pdhE*	Acyl-CoA hydratase	*Corynebacterium glutamicum*	(Kallscheuer et al., 2016)
3-Hydroxycaffeoyl-CoA	3-Oxocaffeoyl-CoA	*pdhB*	3-Hydroxyacyl-CoA dehydrogenase	*Corynebacterium glutamicum*	(Kallscheuer et al., 2016)
3-Oxocaffeoyl-CoA	Protocatechuate + Acetyl-CoA	*pdhC*	3-Oxoacyl-CoA ketohydrolase	*Corynebacterium glutamicum*	(Kallscheuer et al., 2016)
Protocatechuate					
Protocatechuate	3-Carboxy *cis,cis*-muconate	*pcaGH*	Protocatechuate 3,4-dioxygenase	*Corynebacterium glutamicum* *Pseudomonas putida* KT2440 *Acinetobacter baylyi* *Streptomyces setonii (Amycolatopsis)*	(Shen and Liu, 2005) (Jimenez et al., 2002) (Fischer et al., 2008) (Pometto et al., 1981)
Protocatechuate	4-Carboxy-2-hydroxy- muconate semialdehyde	*ligAB*	Protocatechuate 4,5-dioxygenase	*Sphingomonas (Pseudomonas) paucimobilis*	(Barry and Taylor, 2013; Noda et al., 1990)
Protocatechuate	5-Carboxy-2-hydroxy- muconate semialdehyde	*praA*	Protocatechuate 2,3-dioxygenase	*Paenibacillus* sp. strain JJ-1b	(Kasai et al., 2009)
Protocatechuate	Catechol	*aroY*	Protocatechuate decarboxylase	*Enterobacter cloacae* *Klebsiella aerogenes*	(Yoshida et al., 2010) (Grant and Patel, 1969)
Benzoate					
Benzoate	Benzoate diol	*benABC*	Benzoate 1,2-diogygenase	*Acinetobacter baylyi* *Pseudomonas putida* KT2440 *Corynebacterium glutamicum* *Streptomyces setonii*	(Fischer et al., 2008) (Jimenez et al., 2002) (Shen et al., 2005) (Park and Kim, 2003)
Benzoate diol	Catechol	*benD*	Benzoate diol dehydrogenase	*Pseudomonas putida* KT2440 *Corynebacterium glutamicum* *Streptomyces setonii*	(Jimenez et al., 2002) (Shen et al., 2005) (Park and Kim, 2003)
Phenol					
Phenol	Catechol	*phe* *dmpKLMNOP*	Phenol hydroxylase Phenol hydroxylase	*Corynebacterium glutamicum* *P. putida* CF600	(Chen et al., 2018)
Guaiacol					
Guaiacol	Catechol	*gcoA*	Aromatic O-demethylase	*Streptomyces setonii (Amycolatopsis)*	(Mallinson et al., 2018)

(*continued on next page*)

Table 2 (*continued*)

Substrate	Product	Gene	Enzyme	Organism	Reference
Guaiacol	Catechol		Aromatic O-demethylase	*Rhodococcus rhodochrous*	(Eltis et al., 1993; Karlson et al., 1993)
Catechol					
Catechol	*cis,cis*-Muconate	*catA*	Catechol 1,2-dioxygenase	*Acinetobacter baylyi*	(Fischer et al., 2008)
				Pseudomonas putida KT2440	(Jimenez et al., 2002)
				Amycolatopsis	(An et al., 2000; Barton et al., 2018; Pometto et al., 1981)
				Corynebacterium glutamicum	(Shen et al., 2005)
				Sphingobium scionense WP01	(Muthu et al., 2018)
Catechol	*cis,cis*-Muconate	*clcA*	(Methyl)-catechol 1,2-dioxygenase	*Sphingobium scionense* WP01	(Muthu et al., 2018)
Catechol	2-Hydroxy-muconate semialdehyde	*xylE*	Catechol 2,3-dioxygenase	*Pseudomonas putida*	(Harayama and Rekik, 1990)
				Sphingobium scionense WP01	(Muthu et al., 2018)
Syringaldehyde					
Syringaldehyde	Syringate	*desV*	Syringaldehyde dehydrogenase	*Sphingomonas paucimobilis* SYK-6	(Kamimura et al., 2017)
Syringate					
Syringate	3-O-Methylgallate	*desA*	Syringate O-demethylase	*Sphingomonas paucimobilis* SYK-6	(Masai et al., 2007a)
Syringate	3-O-Methylgallate		Syringate O-demethylase	*Pseudomonas* sp.	(Donnelly and Dagley, 1980; Sparnins and Dagley, 1975)
3-O-Methylgallate	2-Pyrone-4,6-dicarboxylate	*ligAB* *desZ*	Protocatechuate 4,5-dioxygenase	*Sphingomonas paucimobilis* SYK-6	(Kasai et al., 2005; Masai et al., 2007a)
2-Pyrone-4,6-dicarboxylate	4-Oxalomesaconate	*ligI*	2-Pyrone-4,6-dicarboxylate hydrolase	*Sphingomonas paucimobilis* SYK-6	(Kasai et al., 2005; Masai et al., 2007a)
3-O-Methylgallate	4-Carboxy-2-hydroxy-6-methoxy-6-oxohexa-2,4-dienoate	*desZ*	3-O-Methylgallate 3,4-dioxygenase	*Sphingomonas paucimobilis* SYK-6	(Kasai et al., 2005; Masai et al., 2007a)
3-O-Methylgallate	4-Carboxy-2-hydroxy-6-methoxy-6-oxohexa-2,4-dienoate		3-O-Methylgallate 3,4-dioxygenase	*Pseudomonas* sp.	(Donnelly and Dagley, 1980; Sparnins and Dagley, 1975)
3-O-Methylgallate	Gallate	*ligM*	Vanillate/3-O-methylgallate O-demethylase	*Sphingomonas paucimobilis* SYK-6	(Abe et al., 2005; Masai et al., 2007a)
Gallate					
Gallate	4-Oxalomesaconate	*desB*	Gallate dioxygenase	*Sphingomonas paucimobilis* SYK-6	(Kasai et al., 2005; Masai et al., 2007a; Sugimoto et al., 2014)
		ligAB	Protocatechuate 4,5-dioxygenase		
Gallate	4-Oxalomesaconate	*galA*	Gallate dioxygenase	*Pseudomonas* sp.	(Nogales et al., 2005; Sparnins and Dagley, 1975)

the complex three-dimensional structure. However, as soon as structurally simple aromatics are released from the ligninolysis process, various other microbes come into play (Table 2). These microbes exhibit a set of convergent catabolic pathways to funnel the mixture of aromatic compounds, released in the first step of lignin breakdown, into central intermediates. Interestingly, aromatics from G-type and H-type lignin are funneled into only two metabolites: protocatechuate and catechol, whereas S-type lignin-derived aromatics degradation occurs via a non-interacting branch (Fig. 4) (Jimenez et al., 2002; Linger et al., 2014; Masai et al., 2007a; Shen et al., 2012).

Enzymes typically involved in the breakdown of aromatics to protocatechuate and catechol comprise acyl-CoA synthetases, acyl-CoA hydratases/lyases, decarboxylases and alcohol and aldehyde dehydrogenases (Table 2) (Abdelaziz et al., 2016). Some of them are promiscuous and equally responsible for the degradation of different aromatics. For example, in *Pseudomonas,* the assimilation routes for ferulate, coumarate and caffeate share the enzymes Fcs (acyl-CoA synthetase), Ech (enoyl-CoA hydratase) and Vdh (aldehyde dehydrogenase) (Table 2). Several microbes can decarboxylate protocatechuate into catechol via the activity of protocatechuate decarboxylase, making catechol a central hub (Table 2, Fig. 4) (Grant and Patel, 1969; Yoshida et al., 2010).

The further breakdown of catechol and protocatechuate is initiated by cleavage of their aromatic ring (Fig. 4). The major catabolic route, i.e., the β-ketoadipate pathway relies on ortho-cleavage of the ring structure of protocatechuate and catechol using dioxygenases (Grund et al., 1990; Johnson and Beckham, 2015; Shen and Liu, 2005). In addition, some microbes possess meta-cleaving dioxygenases (Table 2) and degrade aromatic compounds in a β-ketoadipate-independent manner (Heinaru et al., 2000; Kasai et al., 2009; Noda et al., 1990). The different ring-cleavage modes inherently produce different metabolites and are thereby associated with different entry points of carbon into the central metabolism and impacting redox metabolism (Fig. 4), which has relevance for biotechnological upgrading of lignin (Johnson et al., 2017). Although we find common features for aromatic degradation (Fig. 4, Table 2), some peculiarities have evolved in different microbes. For example, (i) eugenol is metabolized by eugenol hydroxylase in *Pseudomonas* (Overhage et al., 1999a), whereas *Penicillium simplicissimum* CBS 170.90 uses vanillyl alcohol oxidase (de Jong et al., 1992; Overhage et al., 2003); (ii) *C. glutamicum* operates unconventional catabolic pathways for *p*-cresol (Du et al., 2016) and the phenylpropanoids ferulate, *p*-coumarate and caffeate (Kallscheuer et al., 2016); and (iii) *Amycolatopsis* possesses a rare pathway for vanillin degradation via guaiacol (Sutherland et al., 1983) that is different from the pathways of other organisms (Table 2) (Jimenez et al., 2002; Shen et al., 2012). Guaiacol is then converted into catechol (Barton et al., 2018; Sutherland et al., 1983) by the activity of a recently discovered promiscuous cytochrome P450 aromatic O-demethylase (Mallinson et al., 2018) before entering the β-ketoadipate pathway. A similar degradation pathway for guaiacol is present in *Rhodococcus rhodochrous* strain 116. The promiscuous O-demethylase P450RR1 also acts on other ortho-substituted phenols, including o-cresol, 2-chlorophenol and 2-ethoxyphenol (Eltis et al., 1993; Karlson et al., 1993).

Although initial studies on aromatic degradation date back to the 1970s (Hopper and Taylor, 1975; Keat and Hopper, 1978a) research papers continuously report on novel findings, enzyme variants and alternative pathways, thereby increasingly complementing and completing the picture of aromatic compound metabolism (Du et al., 2016; Kallscheuer et al., 2016; Mallinson et al., 2018; Muthu et al., 2018). The immense repertoire of enzymes for the cleavage of lignin and the assimilation of its aromatic building blocks (Table 2) has found its first promising applications in the processing of technical lignin and lignin-derived depolymerization products, as discussed below.

3. Technical lignin—recovery and depolymerization

Technical lignin is the starting material of valorization. In recent years, different approaches have been developed to recover technical lignin from biomass and industrial streams and further depolymerize it. Here, we briefly discuss such technical aspects of lignin production and processing. For a more detailed understanding of these methods, the reader is addressed to excellent recent reviews (Abdelaziz et al., 2016; Ponnusamy et al., 2019; Schutyser et al., 2018; Van den Bosch et al., 2018; Vyas et al., 2018).

3.1. Lignin recovery from delignification

Technical lignins, presently available on the market, are largely recovered from the cooking liquors of pulping (delignification) processes. Today, they are mainly commercialized by MeadWestvaco Cooperation and Borregaard Industries (Pye, 2010; Schutyser et al., 2018). The most important delignification processes are kraft, soda and sulfite pulping (Abdelaziz et al., 2016; Pye, 2010; Schutyser et al., 2018). Sulfite pulping is a process of cooking wood at 140 – 170 °C in an alkaline, a pH neutral or an acidic environment, depending on the added sulfite salt (Abdelaziz et al., 2016; Schutyser et al., 2018). The ether bonds within the lignin structure are thereby hydrolyzed and subsequently sulfonated by the sulfite ions (SO_3^{-2}) in the liquor. Sulfite pulping produces fully water-soluble, highly degraded lignosulfonates with a sulfur content of 4 – 7 wt% (Abdelaziz et al., 2016; Schutyser et al., 2018; Van den Bosch et al., 2018). Established in 1874, sulfite pulping became the dominant process for wood delignification until kraft pulping was established in 1930s (Pye, 2010).

During the kraft process, the biomass is cooked for several hours at 155 – 175°C in an aqueous solution of NaOH and Na_2S (white liquor) (Abdelaziz et al., 2016; Schutyser et al., 2018). The thus-formed hydroxide (OH^-) and hydrosulfide (HS^-) anions crack the aromatic ether bonds in the lignin structure and release low-molecular-weight thiolignin oligomers (Abdelaziz et al., 2016; Pye, 2010; Schutyser et al., 2018). In the strongly alkaline environment of the cooking process, these thiolignin fragments are soluble, but they can be precipitated upon acidification of their black liquor (Abdelaziz et al., 2016; Pye, 2010; Schutyser et al., 2018). The obtained lignin has a sulfur content of approximately 1 - 3 wt%; is highly condensed, with only a few β-O-4 ether linkages remaining; and consists only of G-type aromatics (Fig. 3A) (Constant et al., 2016; Schutyser et al., 2018).

Similar to kraft and sulfite pulping, soda pulping involves cooking biomass at 160 – 170°C. The cooking is carried out in the presence of soda (NaOH) and—optionally—anthraquinone, the latter increasing the efficiency by promoting reductive ether bond cleavage (Abdelaziz et al., 2016; Schutyser et al., 2018; Van den Bosch et al., 2018). Soda lignin has a low sulfur content; is highly condensed, with very few remaining β-O-4 ether bonds; is composed of S- and G-type aromatics and might contain additional components such as ferulates and coumarates (Fig. 3A) (Constant et al., 2016; Pye, 2010; Schutyser et al., 2018).

There are far more methods for biomass processing and delignification, which provide a variety of diverse lignins differing in composition, impurities, solubility and chemical structure (Abdelaziz et al., 2016; Constant et al., 2016; Schutyser et al., 2018; Van den Bosch et al., 2018). The markets and applications of these products are largely determined by the structures of the various forms of technical lignins recovered from the different pulping operations (Pye, 2010), and the structure also influences the choice of depolymerization method (Abdelaziz et al., 2016). Indeed, an increase in carbon-carbon bonds in technical lignins at the expense of carbon-ether bonds impedes lignin breakdown, as most depolymerization methods fail to cleave the carbon-carbon bonds (Schutyser et al., 2018).

3.2. Depolymerization

Depolymerization of the complex lignin structure is a key element for the biotechnological upgrading of lignin. Carbon must be made bioavailable for microbial production hosts, which requires a breakdown of lignin into low-molecular-weight mono- or oligolignins. The depolymerization methods are as diverse as the delignification methods and have been intensively reviewed (Abdelaziz et al., 2016; Ragauskas et al., 2014; Schutyser et al., 2018; Van den Bosch et al., 2018). Among these methods, certain approaches provide high fractions of phenolic monomers, including vanillin, guaiacol, *p*-coumarate, benzoate and catechol, which are of particular relevance for downstream biochemical conversion processes, as illustrated below in the application examples.

3.2.1. Thermal and chemical depolymerization

Thermochemical processes include hydrogenolysis, hydrolysis, alkaline oxidation, and fast pyrolysis. The process temperatures range from 100°C to 600°C, and depolymerization is partly supported by base, metal and acid catalysts or even carried out in supercritical fluids (Kang et al., 2013; Pinkowska et al., 2012; Van den Bosch et al., 2018; Wahyudiono and Goto, 2011). The products obtained from hydrothermal depolymerization are diverse and depend on the method used and the type of lignin (Kang et al., 2013). One of these processes, namely, oxidative depolymerization of lignin from sulfite pulping, has been commercialized for the production of vanillin (see chapter 5). At present, the Norwegian company Borregaard holds a monopoly position in the production of lignin-derived vanillin (Fache et al., 2016; Van den Bosch et al., 2018). Their process uses O_2 as an oxidizing agent in an environment of concentrated NaOH solution.

For the use of depolymerized lignin for biotechnological purposes, the production of high fractions of small aromatics, including acids (vanillate, ferulate, *p*-coumarate, (hydroxy)-benzoate), aldehydes (vanillin, benzaldehyde) and phenolic monomers (catechol, guaiacol, phenol, cresol), is highly desirable. In this regard, a recent study described base-catalyzed depolymerization of organosolv and soda lignin at 300°C, 90 bar and 4 wt% NaOH (Fernandez-Rodriguez et al., 2017). The overall yield of phenolics was only approximately 20 – 23 wt% because of the high repolymerization reaction. Catechols thereby formed the major fraction of aromatic monomers, followed by phenols, cresols and guaiacols (Fernandez-Rodriguez et al., 2017). Another study investigated in more detail how the process parameters influence the catechol yield (Schuler et al., 2017). To this end, kraft lignin was depolymerized at different temperatures (250°C, 300°C, 350°C, 400°C, 450°C) and reaction times in the presence of 1 wt% KOH as catalyst. Catechol production was most efficient at 300°C. Lower temperatures did not properly support depolymerization, whereas gasification impaired the catechol yield at higher temperatures (Schuler et al., 2017). As the initial step of a whole value chain from lignin to nylon, hydrothermal conversion of kraft pine lignin was carried out in demineralized water for 1 h at 395°C (Kohlstedt et al., 2018). This procedure provided an aromatic mixture mainly comprising catechol and phenol with some traces of cresols (Kohlstedt et al., 2018). Variation in the reaction temperature (330°C, 350°C, 370°C) and the vessel pressure (130, 165, 210 bar) enabled the production of guaiacol-rich hydrolysates (Barton et al., 2018). The decreased temperature increased the guaiacol fraction but did so at the expense of the overall aromatic yield (Barton et al., 2018). In general, the yield of such processes still suffers from the undesired repolymerization of lignin, which accounts for up to 30 – 45 % of the initially deployed lignin (Fernandez-Rodriguez et al., 2017; Schutyser et al., 2018) and remains to be optimized.

3.2.2. Enzyme-based depolymerization

As shown, challenges in thermal, chemical and physical depolymerization of lignin are yield and catalyst selectivity (Schutyser et al., 2018; Xu et al., 2014), so lignin depolymerization with enzymes and microbes is regarded as potentially advantageous (Ponnusamy et al., 2019). Indeed, initial studies demonstrated lignin depolymerization using bacterial consortia (Bilal et al., 2018; Wu and He, 2013) and individual strains (Chai et al., 2014; Deangelis et al., 2013). Admittedly, such microbial depolymerization processes are highly time consuming and, at present, hardly feasible for industrial-scale applications. Similarly, access to efficient enzymes for the depolymerization of lignin remains a great challenge. White-rot fungi, the main natural producers of peroxidases and laccases, are hard to cultivate, and the complex regulation of their biosynthetic pathways makes fungus-based enzyme production an ambiguous business (Martani et al., 2017). Moreover, most enzymes function under ambient and moderate conditions or even in an acidic environment (de Gonzalo et al., 2016), where most technical lignins are poorly soluble (Constant et al., 2016; Pye, 2010).

A milestone towards enzymatic lignin breakdown was the commercial production of an extremely alkaline lignin oxidase, MetZyme® LIGNO™, by the Finnish company MetGen Oy (Hämäläinen et al., 2018). This laccase of bacterial origin functions at pH values as high as 10-11 and at elevated temperature, offering a high value for biorefinery lignin valorization (Hämäläinen et al., 2018). In the future, the recombinant production of enzymes that work under extreme conditions thus appears highly attractive, and broadening the spectrum of enzymatic workhorses could bring enzyme-based lignin breakdown closer to industrial applicability.

4. Towards lignin biotechnology

Considering commercialization, a lignin-based biotechnology faces several challenges: the lignins, currently available in large quantities, e.g., from MeadWestvaco Cooperation and Borregaard Industries, mainly comprise sulfonated forms from kraft and sulfite pulping processes, which might not meet the required specifications for biotechnology applications (Pye, 2010; Schutyser et al., 2018). Recovered and pretreated lignin typically contains crude mixtures of different aromatics, of which many are toxic, and other inhibiting substances such as sulfite and may also exhibit extreme pH values. On the microbial producer side, the use of technical lignin therefore likely entails engineering stress tolerance (Buschke et al., 2013b; Kohlstedt et al., 2018; Wang et al., 2012), extending the substrate spectrum (Buschke et al., 2013b; Buschke et al., 2011; Sonoki et al., 2014; Vardon et al., 2015), and operating the routes of aromatic catabolism at a high level using, e.g., superior enzyme variants (Overhage et al., 2003; Sonoki et al., 2014), and streamlined pathway regulation (Becker et al., 2018a; Johnson et al., 2017).

4.1. Role of synthetic biology and systems metabolic engineering

Obviously, global and systematic engineering of microbial metabolism, i.e., systems metabolic engineering, is needed to achieve the desired strain performance (Becker et al., 2018b; Becker and Wittmann, 2015, 2018; Jinek et al., 2012; Kohlstedt et al., 2010; Ma et al., 2017; Martins-Santana et al., 2018). In recent years, systems metabolic engineering revolutionized strain breeding for the production of the following various products from sugars: amino acids and related compounds (Becker et al., 2011; Lee et al., 2007; Park et al., 2014; Rohles et al., 2016; Shin et al., 2016), organic acids (Becker et al., 2013a; Blazeck et al., 2014; Chu et al., 2015; Harder et al., 2016; Huang et al., 2014; Lange et al., 2017; Rohles et al., 2018; Saitoh et al., 2005; Tsuge et al., 2015), diamines (Chae et al., 2015; Kind et al., 2010a; Kind et al., 2010b; Kind et al., 2011; Kind et al., 2014; Mimitsuka et al., 2007; Qian et al., 2009, 2011; Schneider and Wendisch, 2010), and alcohols (Jojima et al., 2015; Shen et al., 2011; Smith et al., 2010). Systems-wide analysis of strains provided in-depth insights into regulatory and metabolic traits related to production, substrate use and cellular stress response (Adler et al., 2013; Adler et al., 2014; Busche et al., 2012; Buschke et al., 2013a; Hemme et al., 2014; Hoffmann et al., 2018; Kiefer et al., 2004; Kohlstedt et al., 2014; Krömer et al., 2004; Raivio

et al., 2013; Schwechheimer et al., 2018a; Schwechheimer et al., 2018b; Ukibe et al., 2009; Weber et al., 2005; Wittmann et al., 2002; Wittmann and Heinzle, 2002; Wittmann et al., 2004; Xiao et al., 2018). The technology platform for targeted and customized strain engineering is rapidly expanding and incorporates an increasing number of elements from synthetic biology. Beyond the traditionally used native control elements for gene expression, libraries of synthetic promoters, ribosomal binding sites and bicistronic elements are accessible (Jeschek et al., 2016; Kohlstedt et al., 2018; Liu et al., 2017; Mutalik et al., 2013; Rytter et al., 2014; Xu et al., 2019; Yim et al., 2013; Yim et al., 2016; Zhang et al., 2015). Their synthetic control architecture enables tunable expression, recruiting riboswitches as well as chemical and optical inducers, which can either be applied by the process operator or work in a situationally self-controlled manner by sensing products or substrates that appear during the course of the process (Rodrigues et al., 2014; Sankaran et al., 2019; Varman et al., 2018; Wu et al., 2018; Zhou and Zeng, 2015). In addition, the molecular biology toolbox for DNA synthesis and assembly and targeted and multiplex genome editing allows for ever faster execution and throughput of genetic modifications (Arazoe et al., 2018; Banno et al., 2018; Cho et al., 2017; Cho et al., 2013; Cook et al., 2018; Gibson, 2009; Gibson et al., 2009; Inokuma et al., 2017; Jinek et al., 2012; Mitsunobu et al., 2017; Moore et al., 2016; Nishizaki et al., 2007; Storch et al., 2017). Finally, yet importantly, the implementation of synthetic pathways is highly efficient, allowing a modular and flexible assembly of specialized designer bugs (Baumgärtner et al., 2014; Becker et al., 2013b; Heider et al., 2014; Paddon et al., 2013; Rodrigues et al., 2013; Rohles et al., 2018; Tsuruta et al., 2009). This approach involves the design and engineering of novel enzymes with desired properties, such as hybrid enzyme variants with improved tolerance (Kohler et al., 2018) and preferred substrate and cofactor specificity (Bommareddy et al., 2014; Hong et al., 2018; Lv et al., 2018).

Metabolic engineering has successfully been applied to prime some microbial hosts for lignin valorization. In particular, specific targets were addressed to establish or improve the production of chemicals, materials, fuels and flavors, as discussed in more detail below.

In addition, more general aspects of aromatic utilization were engineered. For example, protocatechuate and 4-hydroxybenzoate degradation was established in *E. coli* (Clarkson et al., 2017). While *E. coli* is a well-known industrial workhorse, its application in lignin valorization is strongly limited, as it is incapable of degrading most aromatic compounds. Heterologous expression of a nine-gene pathway from *P. putida* KT2440 removed this drawback and enabled growth on protocatechuate as sole carbon and energy source (Clarkson et al., 2017). After the growth was improved through evolutionary adaptation, the core protocatechuate pathway was extended to utilize 4-hydroxybenzoate by expression of the 4-hydroxybenzoate 3-monooxygenase gene *praI* from *Paenibacillus* sp. strain JJ-1B (Clarkson et al., 2017).

In addition, *E. coli* was equipped with an autoregulatory system for the production of catechol from vanillin (Wu et al., 2018). The design comprised heterologous expression of the genes *ligV* (vanillin dehydrogenase) and *ligM* (vanillate-O-demethylase) from *Sphingomonas paucimobilis* SKY-6 and *aroY* (protocatechuate decarboxylase) from *Klebsiella pneumoniae* under control of the vanillin-inducible ADH7 promoter. As an advantage for the use of aromatics, the expression of the genes was spontaneously induced in the presence of vanillin, thereby activating the synthetic pathway and converting the toxic substrate into less toxic compounds without requiring the addition of external inducers (Wu et al., 2018).

Similarly, a phenol-inducible promoter was developed by a hybrid promoter engineering approach recruiting the endogenous phenol-responsive promoter P_{emrR} and replacing its spacer region to create the engineered promoter variants P_{vtac}, P_{vtrc} and P_{vtic} (Varman et al., 2018). These inducible promoter systems can be beneficial for developing substrate-inducible and dynamic regulatory gene expression systems and provide flexibility in operating conditions (Varman et al., 2018).

In *C. glutamicum*, decoupling of the expression of the genes encoding the catechol-catabolizing enzymes from benzoate induction proved valuable for the production of *cis,cis*-MA (Becker et al., 2018a). Replacement of the natural promoter of *catA* by the constitutive promoter of the *tuf* gene, which encodes elongation factor tu, substantially increases *catA* expression, which is indicated by increased CatA activity, and thereby improves biotransformation efficiency using catechol as substrate (Becker et al., 2018a). The inherent complexity of aromatic pathway regulation was at least partly removed, which is a strategy that appears generally promising for the use of aromatics as a substrate for biobased production.

Beyond the cellular engineering of existing living organisms, successful reports on the design, creation and application of synthetic cells are rapidly increasing in number. Such systems aim at minimal complexity but maintain customized and modular programming via genetic circuits or synthetic genomes embedded inside living cells deprived of their native genomes, liposomes, or other types of compartments (Rampioni et al., 2019; Schwille et al., 2018; York-Duran et al., 2017). This progress displays a promising step towards a new era of biotechnology using fully synthetic cell constructs (Schwille et al., 2018).

4.2. Host selection

Ideally, a selected host already possesses all required metabolic traits for (i) substrate utilization and (ii) product synthesis, (iii) is genetically accessible, (iv) is known to perform at the industrial scale, and (v) exhibits general robustness. For lignin biotechnology, catabolic pathways for aromatic degradation and a natural robustness towards toxic substrates are particularly crucial. Moreover, a proven suitability for industrial-scale biotechnology applications is highly desirable. In this regard, *P. putida*, well known for its potential to assimilate and tolerate different aromatic compounds, appears to be an excellent logical choice (Dvorak et al., 2017; Nikel and de Lorenzo, 2018; Nikel et al., 2014). *C. glutamicum* is a rather newcomer in this field, but it is highly versatile, efficient and robust in using lignin-derived compounds (Becker et al., 2018a). Although widely used in industry, *E. coli* lacks aromatic catabolism as an essential trait for lignin biotechnology. Although this deficit can be overcome by elaborate genetic engineering (Clarkson et al., 2017; Overhage et al., 2003; Wu et al., 2018), *E. coli* still falls short of established cell factories such as *P. putida* and *C. glutamicum* in terms of pathway flexibility and tolerance (Buschke et al., 2013b; Nikel and de Lorenzo, 2014; Ramos et al., 2015; Shen et al., 2012). In contrast, other natural aromatic degraders, such as *Amycolatopsis, Sphingomonas* and *Rhodococcus*, have great potential from the perspective of substrate utilization and tolerance (Barton et al., 2018; Kosa and Ragauskas, 2012; Masai et al., 2012; Masai et al., 2007a; Mycroft et al., 2015; Plaggenborg et al., 2006; Takahashi et al., 2014) but bear the risk that they cannot be domesticated for large-scale application and might be recalcitrant towards genetic modification, though established methods for genome manipulation are continuously improving (Barton et al., 2018; Sonoki et al., 2018). Therefore, there is no easy identification of the “best” or “optimal” production host. There are pros and cons for each host that can make one host optimal, depending on the process. For example, for the production of bulk chemicals with high annual market demands, *P. putida* and *C. glutamicum* appear most attractive, as both strains combine many features that are most desired for industrial workhorses: high tolerance and robustness, versatile aromatic pathways, genetic accessibility, domesticated for industrial-scale application, fast growth, and high specific and volumetric productivity. For highly priced fine and specialty chemicals, including flavors and fragrances, rarely used and unconventional microbes might be more favorable than the typical species (Banerjee and Chattopadhyay, 2019). This alternative choice might also be relevant for the production of fatty acid methyl esters (FAMEs), which are known to be naturally produced in *Amycolatopsis* and *Rhodococcus* (Kosa and Ragauskas, 2012, 2013; Salvachua et al., 2015) but not in *P.*

putida and *C. glutamicum*.

4.3. Tolerance engineering

Strain robustness and tolerance have been issues since the early years of industrial biotechnology because the producer strains have to cope with the harsh conditions of large-scale fermentation processes, including pH, oxygen and substrate gradients and high concentrations of potentially toxic products.

The emerging field of lignocellulose biorefineries adds another issue: substrate toxicity. This toxicity might immediately relate to the carbon substrate itself, e.g., aromatic compounds; to organic and inorganic ingredients such as sulfate, sodium hydroxide, acetate and furfural; or to extreme pH regimes in the substrate stream (Buschke et al., 2013b; Rumbold et al., 2009; Wang et al., 2012).

As mentioned above, *P. putida* KT2440 exhibits a considerable tolerance towards many inhibitors (Nikel and de Lorenzo, 2014, 2018). Nevertheless, its tolerance towards catechol was even further increased by expression of a synthetic gene cassette consisting of the P_{cat} promoter and the genes *catA* and *catA2*, which encode the two native catechol 1,2-dioxygenases of *P. putida* KT2440 (Kohlstedt et al., 2018). This benefit is likely related to accelerated catechol degradation and thus detoxification of the cultivation environment. Moreover, the intracellular energy level was identified as a highly critical factor for cell survival (Kohlstedt et al., 2018). In line with this observation, genome-reduced strains of *P. putida* — missing, among other features, the energy-demanding flagellar machinery — showed a high oxidative stress tolerance along with an increased energy charge and NADPH/NADP ratio (Martinez-Garcia et al., 2014a; Martinez-Garcia et al., 2014b). In *Saccharomyces cerevisiae*, the tolerance to phenolic substances was improved by heterologous expression of the *lcc*2 laccase gene of *Trametes versicolor*. The engineered strain rapidly degraded coniferyl aldehyde and other phenolic fermentation inhibitors, enabling faster growth and ethanol production (Larsson et al., 2001). Overexpression of the native *GRE2* gene, encoding NADPH-dependent methylglyoxal reductase, could mediate toxicity tolerance in xylose-fermenting *S. cerevisiae*. Integration of a second gene copy resulted in the strain being less sensitive towards typical biomass-derived inhibitors such as glycoaldehyde, furfural, acetic acid and vanillin and exhibiting better ethanol production from lignocellulose hydrolysates (Jayakody et al., 2018).

As cellular responses to inhibitory compounds are often complex, the efficiency of genetically engineering single metabolic features might be limited. Here, adaptive evolution can help to achieve desired tolerance improvements. This approach mimics natural selection by fortifying genetic diversification in response to an imposed selective pressure (Becker et al., 2018b; Sauer, 2001). Comparative genome sequencing can then be used to identify beneficial modifications, allowing subsequent reverse metabolic engineering (Minty et al., 2011; Pfeifer et al., 2017; Portnoy et al., 2011). For *C. glutamicum,* adaptive evolution was successfully applied to increase the tolerance towards oxidative stress (Lee et al., 2013), thermal and solvent stress (Oide et al., 2015), and lignocellulose-derived inhibitors, including vanillin, syringaldehyde and 4-hydroxybenzaldehyde (Wang et al., 2018b). For the last case, genome sequencing and transcriptional profiling indicated that an improved NADPH supply for aldehyde inhibitor reduction contributed to the increased tolerance. Moreover, a point mutation in the global transcriptional regulator McbR was identified (Wang et al., 2018b). McbR plays a key regulatory role in sulfur assimilation, biosynthesis of methionine and cysteine, and oxidative stress metabolism (Krömer et al., 2008; Rey et al., 2005; Rey et al., 2003). Interestingly, superoxide dismutase is downregulated in *mcbR* deletion strains (Krömer et al., 2008), a feature that was recently related to aromatic tolerance in *Rhodococcus opacus* (Henson et al., 2018a). This lipid-accumulating microbe was also subjected to adaptive evolution to improve its tolerance towards phenol (Yoneda et al., 2016). Compared to that of the wild type, the phenol degradation pathway of the evolved strains was highly upregulated. As a consequence, the adapted *R. opacus* strains exhibited faster growth and higher lipid production along with an accelerated phenol consumption rate. A follow-up study suggested that tolerance is also mediated by a lipid composition changed in terms of the chain length and the number of double bonds of mycolic acids (Henson et al., 2018b).

In a recent study, *R. opacus* was challenged with different combinations of aromatic compounds, including phenol, guaiacol, vanillate, benzoate and 4-hydroxybenzoate, to force adaptation (Henson et al., 2018a). Evolution led to outstanding growth improvements of up to 1900 %. The identified mutations and transcriptional changes of several of the analyzed evolved strains revealed a certain pattern, with tolerance correlated to decreased activity of superoxide dismutase and activation of aromatic degradation and funneling pathways. Interestingly, these examples from evolutionary engineering yielded a similar tolerance mechanism, i.e., faster detoxification of the medium by upregulation of the assimilation route, as metabolic engineering did for improved catechol tolerance of *P. putida* (Kohlstedt et al., 2018). Therefore, one might conclude that a key feature towards aromatic tolerance is the operation of aromatic catabolism at a high level.

5. Added-value products from lignin

Meanwhile, different approaches use native and engineered microbes to convert lignin and its building blocks into voluminous bulk chemicals, smart biomaterials and high-value molecules using biotransformation and fermentation (Table 3).

5.1. Chemicals

5.1.1. Cis,cis-muconic acid

Progress with *cis,cis*-MA, a six-carbon di-unsaturated dicarboxylic acid, has emerged as the masterpiece of lignin valorization. The compound is a direct precursor for adipic acid and terephthalic acid, industrial mass chemicals for the market of commercial plastics (Becker et al., 2015; Polen et al., 2013; Vardon et al., 2016). Moreover, MA can be applied to the production of unsaturated polyamides (Suastegui et al., 2016) and unsaturated polyesters (Rorrer et al., 2016; Rorrer et al., 2017). Potential pathways from sugars suffer from an inherently low yield, which is an obvious hurdle regarding their industrial exploitation (Curran et al., 2013; Draths and Frost, 1994; Yu et al., 2014). The consideration of lignin-based feedstocks suddenly and strongly changed this picture. MA is a natural intermediate in the catabolism of lignin-derived aromatics in different microbes (Fig. 4). The compound immediately accumulates upon disruption of the degradation route at the muconate cycloisomerase point, which is downstream of the MA node (Mizuno et al., 1988; Schmidt and Knackmuss, 1984). The metabolic relatedness of MA and aromatic substrates thus enable stoichiometric conversion at 100 % yield (mol mol^{-1}) (van Duuren et al., 2011). In recent years, efforts on lignin-based MA and even lignin-based nylon have been impressively successful. Different microbes were tested and engineered towards industrial production (Barton et al., 2018; Becker et al., 2018a; Kohlstedt et al., 2018; Sonoki et al., 2018; van Duuren et al., 2011; Vardon et al., 2015).

5.1.1.1. Pseudomonas putida as production host. Based on its outstanding repertoire to degrade aromatics (Belda et al., 2016; Jimenez et al., 2002; Nikel and de Lorenzo, 2018), *Pseudomonas putida* has long been regarded as a potential producer of MA (van Duuren et al., 2011). In a pioneering study, chemical mutagenesis resulted in a mutant of *P. putida* KT2440 that accumulated MA when cultured on a glucose-benzoate mixture (van Duuren et al., 2011). Genome and transcriptome analysis of the obtained strain, *P. putida* KT2440 JD-1, revealed that MA production resulted from a point mutation in the transcriptional regulator *catR* that silenced the *cat* operon, involving muconate cycloisomerase (*catB*). Using the JD-1

Table 3
Biotechnological use of lignin and lignin-derived aromatics for the production of value-added compounds.

Microorganism	Substrate	Product	Method	Titer [g L^{-1}]	Yield [mol mol^{-1}]	Reference
Sphingobacterium sp. M4115	Benzoate	*cis,cis*-muconate	batch	0.56	29 %	(Wu et al., 2006)
Corynebacterium lilium ATCC21793	Benzoate	*cis,cis*-muconate	batch	1.4	4.7 %	(Imada et al., 1989)
Corynebacterium acetoacidophilum ATCC 13870	Benzoate	*cis,cis*-muconate	batch	2.5	8.5 %	(Imada et al., 1989)
Microbacterium ammoniaphilum ATCC 21645	Benzoate	*cis,cis*-muconate	batch	2.5	8.5 %	(Imada et al., 1989)
Brevibacterium flavum ATCC 13826	Benzoate	*cis,cis*-muconate	batch	2.6	8.8 %	(Imada et al., 1989)
Arthrobacter sp. T-8226-11	Benzoate	*cis,cis*-muconate	batch	4.5	91 %	(Imada et al., 1989)
Pseudomonas sp. mutant 1167	Benzoate	*cis,cis*-muconate	batch	7.2	61 %	(Xie et al., 2014)
Corynebacterium pseudodiphtheriticum M2128	Benzoate	*cis,cis*-muconate	fed batch	3.1	47 %	(Liu et al., 2003)
Pseudomonas putida ATCC 31916	Catechol	*cis,cis*-muconate	fed batch	5.3	100 %	(Maxwell, 1986, 1988, 1991)
Pseudomonas putida ATCC 31916	Toluene	*cis,cis*-muconate	fed batch	5.7	–	(Maxwell, 1982)
Pseudomonas sp. B13	Benzoate	*cis,cis*-muconate	fed batch	7.4	91 %	(Schmidt and Knackmuss, 1984)
Pseudomonas putida ATCC 31916	Toluene	*cis,cis*-muconate	fed batch	12.6	–	(Hsieh, 1984)
Pseudomonas putida ATCC 31916	Toluene	*cis,cis*-muconate	fed batch	15.0	–	(Hsieh, 1985)
Pseudomonas putida ATCC 31916	Toluene	*cis,cis*-muconate	fed batch	27.0	–	(Hsieh, 1990)
Pseudomonas putida BM014	Benzoate	*cis,cis*-muconate	fed batch	13.5	–	(Choi et al., 1997)
Pseudomonas putida BM014	Benzoate	*cis,cis*-muconate	fed batch	32.4	100 %	(Bang and Choi, 1995)
Pseudomonas putida KT2440-JD1	Benzoate	*cis,cis*-muconate	fed batch	18.5	100 %	(van Duuren et al., 2012)
Arthrobacter sp. T8626	Benzoate	*cis,cis*-muconate	fed batch	44.1	96 %	(Mizuno et al., 1988)
Pseudomonas sp. MP-D14	Toluene	*cis,cis*-muconate	batch	3.5	–	(Chua and Hsieh, 1990)
Pseudomonas sp. DCB-71	Toluene	*cis,cis*-muconate	fed batch	45.0	–	(Chua and Hsieh, 1990)
Escherichia coli pE*catA*$_{Pput}$	Catechol	*cis,cis*-muconate	fed batch	59.0	100 %	(Kaneko et al., 2011)
Pseudomonas putida KT2440-CJ103	Benzoate	*cis,cis*-muconate	batch	1.1[a]	93 %	(Vardon et al., 2015)
Pseudomonas putida KT2440-CJ103	Phenol	*cis,cis*-muconate	batch	0.6[a]	64 %	(Vardon et al., 2015)
Pseudomonas putida KT2440-CJ103	4-Hydroxybenzoate	*cis,cis*-muconate	batch	0.8[a]	53 %	(Vardon et al., 2015)
Pseudomonas putida KT2440-CJ103	*p*-Coumarate	*cis,cis*-muconate	fed batch	13.5	67 %	(Vardon et al., 2015)
Pseudomonas putida KT2440-CJ103	Lignin hydrolysate	*cis,cis*-muconate	batch	0.7	–	(Vardon et al., 2015)
Pseudomonas putida KT2440-CJ238	*p*-Coumarate	*cis,cis*-muconate	batch	2.8[a]	95 %	(Johnson et al., 2017)
Pseudomonas putida KT2440-CJ238	Ferulate	*cis,cis*-muconate	batch	0.7[a]	28 %	(Johnson et al., 2017)
Pseudomonas putida KT2440-MA1	Catechol	*cis,cis*-muconate	fed batch	64.2	100 %	(Kohlstedt et al., 2018)
Pseudomonas putida KT2440-MA9	Catechol-phenol mixture	*cis,cis*-muconate	batch	0.5[a]	100 %	(Kohlstedt et al., 2018)
Pseudomonas putida KT2440-MA9	Catechol-phenol mixture	*cis,cis*-muconate	fed batch	6.0	100 %	(Kohlstedt et al., 2018)
Pseudomonas putida KT2440-MA9	Lignin hydrolysate	*cis,cis*-muconate 3-methyl muconate	fed batch	13.0	100 %	(Kohlstedt et al., 2018)
Pseudomonas putida IDPC/pTS110	Vanillate	*cis,cis*-muconate	batch	0.2	3 %	(Sonoki et al., 2018)
Pseudomonas putida IDPC/pTS110	4-Hydroxybenzoate	*cis,cis*-muconate	batch	0.8	12 %	(Sonoki et al., 2018)
Pseudomonas putida IDPC/pTS110	Vanillate 4-Hydroxybenzoate	*cis,cis*-muconate	batch	1.3	19 %	(Sonoki et al., 2018)
Pseudomonas putida IDPC/pTS110	Lignin hydrolysate	*cis,cis*-muconate	fed batch	0.02	1 %	(Sonoki et al., 2018)
Amycolatopsis sp. ATCC 39116 MA-2	Guaiacol	*cis,cis*-muconate	fed batch	3.1	96 %	(Barton et al., 2018)
Amycolatopsis sp. ATCC 39116 MA-2	Lignin hydrolysate	*cis,cis*-muconate 2-methyl muconate	fed batch	0.2	72 %	(Barton et al., 2018)
Corynebacterium glutamicum MA-1	Catechol	*cis,cis*-muconate	batch	1.4	100 %	(Becker et al., 2018a)
Corynebacterium glutamicum MA-1	Phenol	*cis,cis*-muconate	batch	0.7	100 %	(Becker et al., 2018a)
Corynebacterium glutamicum MA-1	Benzoate	*cis,cis*-muconate	batch	2.8	100 %	(Becker et al., 2018a)
Corynebacterium glutamicum MA-2	Catechol	*cis,cis*-muconate	fed batch	85	100 %	(Becker et al., 2018a)
Corynebacterium glutamicum MA-2	Lignin hydrolysate	*cis,cis*-muconate	fed batch	1.8	100 %	(Becker et al., 2018a)
Escherichia coli vanAB-vdh-catA$_{Pput}$*aroY-kpdB*$_{Kpneu}$	Vanillin	*cis,cis*-muconate	batch	0.1[a]	70 %[a]	(Sonoki et al., 2014)
Sphingomonas paucimobilis SME257/ pTS084	Vanillate	*cis,cis*-muconate	batch	0.6	45 %	(Sonoki et al., 2018)
Sphingomonas paucimobilis SME257/ pTS084	Lignin hydrolysate	*cis,cis*-muconate	fed batch	0.03	45 %	(Sonoki et al., 2018)
Pseudomonas sp. HR199 Δ*vdh*	Eugenol	Vanillin	batch	0.4	45 %	(Overhage et al., 1999a)
Escherichia coli pSK*echE/Hfcs*	Ferulate	Vanillin	batch	0.3	7 %	(Overhage et al., 2003)
Streptomyces setonii	Ferulate	Vanillin	fed batch	6.4	68 %	(Muheim and Lerch, 1999)
Ralstonia eutropha H16 pBBR1-JO2*ehyABcalAcalB*	Eugenol	Ferulate	fed batch	3.5[a]	94 %	(Overhage et al., 2002)
Escherichia coli XL-1 Blue pSK*vaomPcalAmcalB*	Eugenol	Ferulate	fed batch	14.7	93 %	(Overhage et al., 2003)
Amycolatopsis sp. HR167 pRLE6SK*vaom*	Eugenol	Coniferyl alcohol	fed batch	4.7	–	(Overhage et al., 2006)
Rhodococcus jostii RHA1 *ligAB*	Straw lignocellulose	Pyridine-2,4-dicarboxylic acid	batch	0.08	–	(Mycroft et al., 2015)
Rhodococcus jostii RHA1 *praA*	Straw lignocellulose	Pyridine-2,5-dicarboxylic acid	batch	0.13	–	(Mycroft et al., 2015)
Pseudomonas putida KT2440-CJ112	Benzoate	Pyruvate	batch	0.7[a]	43 %	(Johnson and Beckham, 2015)
Pseudomonas putida KT2440-CJ113	Benzoate	Pyruvate	batch	0.6[a]	34 %	(Johnson and Beckham, 2015)
Pseudomonas putida KT2440-CJ115	*p*-Coumarate	Pyruvate	batch	0.5[a]	110 %	(Johnson and Beckham, 2015)
Pseudomonas putida KT2440-CJ116	*p*-Coumarate	Pyruvate	batch	2.0[a]	22 %	(Johnson and Beckham, 2015)
Pseudomonas putida KT2440-CJ120	Benzoate	Lactate	batch	0.4[a]	22 %	(Johnson and Beckham, 2015)
		Pyruvate		0.5[a]	21 %	
Pseudomonas putida KT2440-CJ127	Benzoate	Lactate	batch	0.5[a]	28 %	(Johnson and Beckham, 2015)
		Pyruvate		0.5[a]	24 %	
Pseudomonas putida KT2440-CJ124	*p*-Coumarate	Lactate	batch	0.5[a]	27 %	(Johnson and Beckham, 2015)
		Pyruvate		0.2[a]	4 %	

(*continued on next page*)

Table 3 (*continued*)

Microorganism	Substrate	Product	Method	Titer [g L^{-1}]	Yield [mol mol^{-1}]	Reference
Pseudomonas putida KT2440-CJ122	*p*-Coumarate	Lactate	batch	1.4[a]	76 %	(Johnson and Beckham, 2015)
		Pyruvate		1.4[a]	77 %	
Phanerochaete chrysosporium	Lignin	Succinate	batch	0.02	–	(Hong et al., 2017)
Pseudomonas putida	*p*-Coumarate	PHA	batch	0.16	34 %[b]	(Linger et al., 2014)
Pseudomonas putida	Ferulate	PHA	batch	0.17	39 %[b]	(Linger et al., 2014)
Pseudomonas putida	Lignin hydrolysate	PHA	batch	0.25	32 %[b]	(Linger et al., 2014)
Pseudomonas putida A514 *phaJ4-phaG-alkK*	Vanillin	PHA	batch	0.25	34 %[b]	(Wang et al., 2018c)
Pandoraea sp. ISTKB	4-Hydroxybenzoate	PHA	batch	0.25	47 % [b]	(Kumar et al., 2017)
Pandoraea sp. ISTKB	*p*-Coumarate	PHA	batch	0.17	41 % [b]	(Kumar et al., 2017)
Pandoraea sp. ISTKB	Vanillate	PHA	batch	0.07	33 % [b]	(Kumar et al., 2017)
Pandoraea sp. ISTKB	Kraft lignin	PHA	batch	0.02	21 %[b]	(Kumar et al., 2017)
Cupriavidus basilensis	Kraft lignin	PHA	fed batch	0.32	15 – 18 %[b]	(Shi et al., 2017)
Rhodococcus opacus PD630	Vanillate	Lipid	batch	0.24[a]	15 %[b]	(Kosa and Ragauskas, 2012)
Rhodococcus opacus PD630	4-Hydroxybenzoate	Lipid	batch	0.32[a]	20 %[b]	(Kosa and Ragauskas, 2012)
Rhodococcus opacus DSM1069	Kraft lignin	Lipid	batch	0.07	14 %[b]	(Wei et al., 2015)
Rhodococcus opacus PD630	Kraft lignin	Lipid	batch	0.15	–	(Zhao et al., 2016)
Rhodococcus opacus PD630	Lignin	Lipid	batch	1.83	18 %[a,b]	(Liu et al., 2018)

[a] estimated from reference
[b] given as wt/wt_{cdw}

strain and automatic pH-controlled benzoate feeding (van Duuren et al., 2012) enabled the production of MA at a titer of 18.5 g L^{-1} and a specific production rate of 0.6 g g^{-1} h^{-1} (Table 3).

More recently, MA production was upgraded using metabolically engineered strains. In a groundbreaking study, *P. putida* KT2440 was genetically modified to funnel a broad range of lignin aromatics, namely, protocatechuate, coniferyl alcohol, ferulate, vanillin, caffeate, *p*-coumarate, 4-hydroxybenzoate, benzoate, catechol, and phenol to MA (Fig. 5A) (Vardon et al., 2015). To this end, the protocatechuate branch of the β-ketoadipate pathway was linked to the catechol branch by heterologous expression of *aroY* from *Enterobacter cloacae*, which encodes protocatechuate decarboxylase. The implementation of *aroY* into the *pcaHG* locus, which encodes protocatechuate 3,4-dioxygenase, simultaneously disrupted the natural protocatechuate degradation route of *P. putida* to avoid loss of aromatics to central metabolism. The use of phenol was enabled by the expression of *dmpKLMNOP*, which encodes phenol monooxygenase in *Pseudomonas* sp. CF600. Moreover, MA degradation was eliminated, and *catA*, encoding the MA forming enzyme catechol 1,2 dioxygenase, was constitutively expressed. The design was realized via an expression cassette consisting of the *tac* promotor and an operon of the genes *catA* and *dmpKLMNOP*, which replaced the genomic section containing *catR*, *catBC*, and the native promoter of *catBCA*. The resulting strain, *P. putida* KT2440-CJ103, produced MA from different aromatics via the catechol and protocatechuate branches. The obtained molar yield ranged from 14 % (coniferyl alcohol) to 93 % (benzoate). For some of the substrates tested, the accumulation of pathway intermediates reduced the yield and indicated an inefficient conversion. In a fed-batch process using glucose as a growth substrate and *p*-coumarate as a biotransformation substrate, the CJ103 strain produced 13.5 g L^{-1} MA within 78.5 h (Table 3). MA was purified from the culture broth by activated carbon treatment and crystallization. Overall, 74 % of the produced MA was recovered at >97 % purity (Vardon et al., 2015). Pd/C-aided catalytic hydrogenation of MA then yielded biobased adipic acid (Vardon et al., 2015). As an important proof of concept, 0.7 g L^{-1} MA was produced from depolymerized lignin (Fig. 6A) (Vardon et al., 2015). Improved MA production efficiency using substrates of the protocatechuate branch was achieved by increasing the protocatechuate decarboxylase activity (Johnson et al., 2016). The strategy involved coexpression of *ecdBD* from *E. cloacae,* which encodes two accessory proteins. One of the enzymes likely supplies a flavin-derived cofactor utilized by protocatechuate decarboxylase, thereby enhancing its activity. The accumulation of protocatechuate was thereby reduced, and the specific MA production rate from coumarate increased by 50 % (Johnson et al., 2016).

Another seminal study substantially upgraded the metabolic performance of *P. putida* KT2440, brought MA production to the pilot scale and implemented the novel mutant in a cascade process to convert lignin to nylon for the first time (Kohlstedt et al., 2018). Because all lignin-based aromatics transforming towards MA inherently merge at catechol, a highly toxic intermediate, the catechol node was a bottleneck to be metabolically engineered. Upon deletion of *catCB*, a designated mutant, MA-1, efficiently produced MA when cocultured on a glucose-catechol mixture (Fig. 5B). The toxicity of catechol was, however, a major challenge for this process. In particular, the cellular energy level and ATP yield were identified as critical factors (Kohlstedt et al., 2018). This issue was addressed by different strategies. On the process operation side, defined feed pauses during fed-batch fermentation allowed the regeneration of cellular energy levels. At the onset of catechol feeding, the cells highly efficiently converted catechol into MA to a maximum titer of 64.2 g L^{-1} (Fig. 5B, Table 3). The performance surpassed previously reported values for catechol-based MA production with *P. putida* by a factor of ten (Kohlstedt et al., 2018). Increasing catechol tolerance via systems metabolic engineering appears to be a promising strategy to increase the expression of catechol 1,2-dioxygenase, the catechol-converting enzyme in the microbe. Among various designed and tested genetic constructs, the implementation of a second copy of the *catA2* gene directly downstream of the *catA* gene under control of the native *catA* promoter was most beneficial (Kohlstedt et al., 2018). The resulting mutant, MA-6, exhibited a strongly increased tolerance towards catechol and a significantly higher specific catechol degradation rate. Subsequently, the MA production process was successfully scaled up and provided MA at 98 % purity at the kilogram scale. The MA-9 strain, additionally equipped with a phenol hydroxylase, also converted phenol into MA and furthermore produced methylated variants of MA from cresols. The strain accumulated 13 g L^{-1} MA and small amounts of 3-methyl *cis,cis*-MA from a softwood lignin hydrolysate (Fig. 6B, Table 3). The products were purified and then hydrogenated into adipic acid and its methylated derivative to finally derive bionylon from lignin (Kohlstedt et al., 2018). Another interesting work addressed the biotransformation efficiency in *P. putida* KT2440 on a regulatory level (Johnson et al., 2017). Carbon catabolite repression (Crc) could be identified as a reason for the low MA yield using, e.g., *p*-coumarate and ferulate. A mutant that lacked the *crc* regulator gene exhibited a substantially increased yield when *p*-coumarate and ferulate were used as biotransformation substrates (Johnson et al., 2017). As a common feature, all these studies are based on glucose to support cell growth. In this regard, a recent study reports glucose-independent MA production with engineered *P. putida* KT2440 (Sonoki et al., 2018).

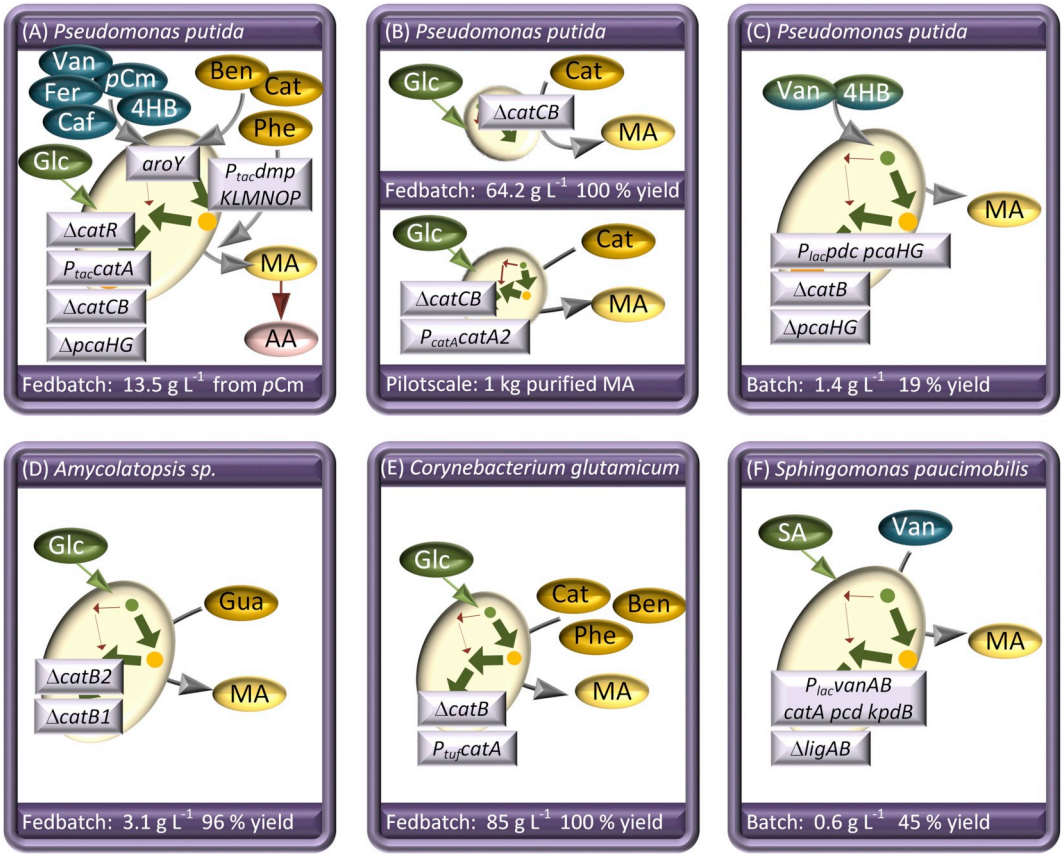

Fig. 5. Production of *cis,cis*-muconate from monolignins. (A) Production of *cis,cis*-muconate from different aromatics using *Pseudomonas putida* with subsequent hydration of muconate to adipic acid (Vardon et al., 2015), (B) Production of *cis,cis*-muconate from catechol using *Pseudomonas putida* (Kohlstedt et al., 2018), (C) Glucose-free production of *cis,cis*-muconate from vanillate and 4-hydroxybenzoate using *Pseudomonas putida* (Sonoki et al., 2018) (D) Production of *cis,cis*-muconate from guaiacol using *Amycolatopsis* species (Barton et al., 2018), (E) Production of *cis,cis*-muconate from catechol, phenol and benzoate using *Corynebacterium glutamicum* (Becker et al., 2018a), (F) glucose-free production of *cis,cis*-muconate from vanillate using *Sphingomonas paucimobilis* (Sonoki et al., 2018). Color code is as follows: dark green: growth substrate, dark turquois: biotransformation substrate (protocatechuate branch), dark gold: biotransformation substrate (catechol branch), light gold: biotransformation product, light purple: genetic modification, light red: products from chemical reaction, grey arrow: biotransformation reaction, green arrow: substrate uptake for growth, red arrow: chemical or hydrothermal reaction. Yields are given on a molar basis.
4HB: 4-hydroxybenzoate, *aroY*: protocatechuate decarboxylase, Ben: benzoate, Caf: caffeate Cat: catechol, *catA*: catechol 1,2-dioxygenase, *catB*: muconate cycloisomerase, *catC*: muconolactone isomerase, *catR*: regulater of *cat*-operon, *p*Cm: *p*-coumarate, *dmpKLMNOP*: phenol monooxidase, Fer: ferulate, Gua: guaiacol, Glc: glucose, *kdpB*: 4-hydroxybenzoate decarboxylase, *ligAB*: protocatechuate 4,5-dioxygenase, MA: *cis,cis*-muconate, *pcaHG*: protocatechuate 3,4-dioxygenase, P_{catA}: promoter of catechol 1,2-dioxygenase, *pdc*: protocatechuate decarboxylase, P_{eftu}: promoter of elongation factor tu, Phe: phenol, P_{lac}: *lac*-promoter, P_{tac}: *tac*-promoter, SA: syringate, Van: vanillin, *vanAB*: vanillin O-demethylase.

First, the chassis strain *P. putida* IDPC was constructed by deletion of *pcaHG* and *catB*. PcaHG activity was then restored by plasmid-based *pcaHG* expression controlled by the *lac* promoter, thereby circumventing the natural expression control. Coexpression of the protocatechuate decarboxylase gene *pcd* from *K. pneumoniae* enabled simultaneous growth and MA production from vanillic acid, 4-hydroxybenzoic acid and mixtures thereof (Fig. 5C), with molar yields of 3 %, 12 % and 20 % (Sonoki et al., 2018). The strain also produced small amounts of MA from softwood hydrolysates (Fig. 6C, Table 3) (Sonoki et al., 2018).

5.1.1.2. Amycolatopsis sp. as a production host. Recently, the actinomycete *Amycolatopsis* sp. ATCC 39116 has been developed into an efficient MA producer. The microbe has been known for many years as an efficient degrader of aromatics, exhibits a comparably high tolerance and even prefers aromatics over sugars during growth (An et al., 2000; Barton et al., 2018). Moreover, it naturally uses guaiacol, an abundant monomer in G-type lignin that was largely unaddressed in lignin-based bioproduction (Beckham et al., 2016). Using a newly established approach for genome-based engineering, the genetically challenging microbe was turned into an MA producer after successive deletion of two putative muconate cycloisomerase genes. The obtained mutant, MA-2, cultured on glucose as a growth substrate and guaiacol as a production substrate, accumulated 3.1 g L^{-1} MA at a molar yield of 96 % (Fig. 5D, Table 3). MA production was also achieved from true lignin hydrolysates (Fig. 6D). To this end, hydrothermal conversion of pine lignin was carried out for 20 min at 330°C – 370°C and 130 – 210 bar, which yielded guaiacol-rich hydrolysates (Barton et al., 2018). The lignin-derived aromatic mixtures were efficiently converted into MA and 2-methyl MA (Table 3), the latter being produced from *o*-cresol (Barton et al., 2018).

5.1.1.3. Corynebacterium glutamicum as a production host. An MA-producing strain of *C. glutamicum* ATCC 13032 was created by deletion of the *catB* gene, which encodes muconate cycloisomerase (Becker et al., 2018a). *C. glutamicum* MA-1 efficiently produced MA from benzoate, catechol and phenol (Fig. 5E), thereby proving high tolerance against the aromatic substrates. Substantial improvement of the MA production rate (25-fold) was achieved by decoupling *catA* expression from its natural induction by benzoate using the constitutive promoter *tuf* to drive *catA* expression (Becker et al., 2018a). In a fed-batch process on catechol, the second generation *C. glutamicum* MA-2

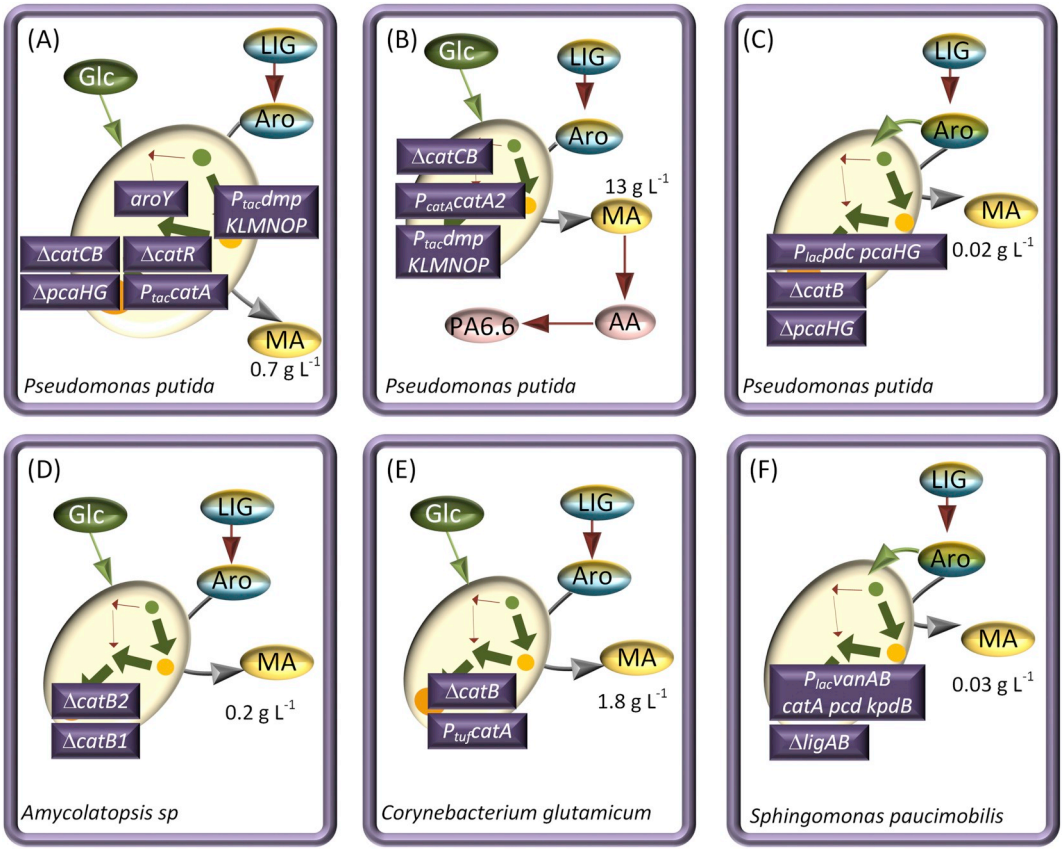

Fig. 6. Biotechnological valorization of lignin. (A) Production of *cis,cis*-muconate from depolymerized softwood lignin using *Pseudomonas putida* (Vardon et al., 2015), (B) Production of *cis,cis*-muconate from depolymerized softwood lignin using *Pseudomonas putida* with subsequent hydration of *cis,cis*-muconate to adipic acid and polymerization to nylon-6.6 (Kohlstedt et al., 2018), (C) Production of *cis,cis*-muconate from depolymerized softwood lignin using *Pseudomonas putida* (Sonoki et al., 2018) (D) production of *cis,cis*-muconate from depolymerized softwood lignin using *Amycolatopsis* sp. (Barton et al., 2018), (E) Production of *cis,cis*-muconate from depolymerized softwood lignin using *Corynebacterium glutamicum* (Becker et al., 2018a), (F) Production of *cis,cis*-muconate from depolymerized hardwood lignin using *Sphingomonas paucimobilis* (Sonoki et al., 2018). Color code is as follows: dark green: growth substrate, dark turquois: substrate of protocatechuate branch, dark gold: substrate of catechol branch, light turquois: biotransformation product (protocatechuate branch), light gold: biotransformation product (catechol branch), purple: genetic modification, light red: products from chemical reaction, grey arrow: biotransformation reaction, green arrow: substrate uptake for growth, red arrow: chemical or hydrothermal reaction.
AA: adipic acid, Aro: aromatic mixture, *aroY*: protocatechuate decarboxylase, *catA*: catechol 1,2-dioxygenase, *catB*: muconate cycloisomerase, *catC*: muconolactone isomerase, *catR*: regulater of *cat*-operon, *dmpKLMNOP*: phenol monooxidase, Glc: glucose, *kdpB*: 4-hydroxybenzoate decarboxylase, Lig: lignin, *ligAB*: protocatechuate 4,5-dioxygenase, MA: *cis,cis*-muconate, *pcaHG*: protocatechuate 3,4-dioxygenase, *pdc*: protocatechuate decarboxylase, P_{lac}: *lac*-promoter, P_{catA}: promoter of catechol 1,2-dioxygenase, P_{eftu}: promoter of elongation factor tu, P_{tac}: *tac*-promoter, *vanAB*: vanillin O-demethylase.

strain accumulated the highest MA titer among all microbes (85 g L^{-1}) and achieved a maximum productivity of 2.4 g L^{-1} h^{-1} (Table 3). As a proof-of-concept, MA production (1.8 g L^{-1}) from softwood lignin hydrolysate was demonstrated (Fig. 6E, Table 3) (Becker et al., 2018a).

5.1.1.4. Escherichia coli as a production host. In *E. coli*, the production of MA was established from vanillin (Table 3) (Sonoki et al., 2014). Because *E. coli* is not equipped with aromatic degradation pathways, substantial genetic engineering was required. The strain design comprised heterologous expression of the vanillin catabolic genes from *P. putida*, expression of *aroY* from *Klebsiella pneumoniae*, and expression of *catA* from *P. putida* (Sonoki et al., 2014). Protocatechuate decarboxylation was identified as a major bottleneck for production. This issue was addressed by the additional expression of *kpdB* from *Klebsiella pneumoniae*, which encodes the β-subunit of 4-hydroxybenzoate decarboxylase. The enzyme likely fulfills the need for a functional flavin mononucleotide prenyltransferase required for protocatechuate decarboxylase activity (Payer et al., 2017; Weber et al., 2017; White et al., 2015). Although protocatechuate decarboxylation activity was increased by 14-fold, no increase in MA production was observed (Sonoki et al., 2014).

5.1.1.5. Sphingobium paucimobilis SYK-6 as a production host. *Sphingobium paucimobilis* SYK-6 is one of the best characterized bacterial lignin-degraders (Bugg et al., 2011; Masai et al., 2007a). This microbe possesses an extensive pathway repertoire for the degradation of lignin-derived biaryls, monoaryls and biphenyls (Higuchi et al., 2018; Kuatsjah et al., 2017; Masai et al., 2012; Masai et al., 1989; Peng et al., 2002; Sonoki et al., 2000; Takahashi et al., 2014), and its aromatic catabolism (Table 2) has been intensively studied (Barry and Taylor, 2013; Hogancamp and Raushel, 2018; Kamimura et al., 2017; Kasai et al., 2012; Masai et al., 2002; Sugimoto et al., 2014). Interestingly, it possesses a rich set of pathways for the degradation of S-lignin compounds, including syringate and gallate, which are largely missing in the above-described production hosts, while lacking a catechol-branch-based catabolism. These metabolic features make *S. paucimobilis* SYK-6 an interesting strain for application in lignin biotechnology for the valorization of S-lignin compounds, as either a production host itself or a heterologous donor strain for enzymes. In this regard, a recent study described MA production from a mixture of S/G-lignin compounds using engineered *S. paucimobilis* SYK-6 (Sonoki et al., 2018). MA production from vanillate (G-lignin) was established by heterologous expression of *vanAB* (vanillate O-demethylase, *P.*

putida KT2440), *pdc* (*aroY,* protocatechuate decarboxylase, *K. pneumoniae*), *kdpB* (4-hydroxybenzoate decarboxylase, *K. pneumoniae*) and *catA* (catechol 1,2-dioxygenase, *P. putida* KT2440), while disrupting native protocatechuate degradation by deletion of *ligAB* (protocatechuate 4,5-dioxygenase) (Fig. 5F). Syringate served as a growth substrate, thus allowing glucose-free MA production (Sonoki et al., 2018). Grown on hardwood lignin hydrolysates, the strain was able to consume vanillin, vanillate, syringate and syringaldehyde for growth and production of MA (Fig. 6F, Table 3), while only adding 0.1-0.2 g L^{-1} tryptone as extra carbon source to support growth (Sonoki et al., 2018).

5.1.2. Pyruvic acid, lactic acid and succinic acid

Lignin and aromatics thereof also found application in *de novo* production of pyruvic acid (PA), lactic acid (LA), and succinic acid (SA) (Table 3). These organic acids are not only central key intermediates of microbial, plant, animal and human metabolism but also chemicals of recognized industrial value, i.e., precursors for various derivatives and polymers and ingredients in diverse commodity products (Becker et al., 2015).

In *P. putida* KT2440, PA production from benzoate (via catechol) and *p*-coumarate (via protocatechuate) was achieved upon deletion of the *aceEF* genes, which encode subunits of pyruvate dehydrogenase (Johnson and Beckham, 2015). The type of aromatic ring cleavage of catechol and protocatechuate, i.e., ortho- or meta-cleavage, had a substantial impact on the production efficiency because the different pathways provided different central intermediates and redox equivalents (Fig. 4). When the natural ortho-cleaving pathways of *P. putida* KT2440 were replaced by the meta-cleaving pathways of *P. putida* mt-2 (catechol pathway) and *Sphingobium* sp. strain SYK-6 (4,5 meta-protocatechuate pathway), PA production was improved by 30 % and 500 %, respectively (Johnson and Beckham, 2015).

In the next step, aerobic LA production was attempted in a PA producer. As overexpression of the endogenous lactate dehydrogenase (LDH) and the heterologous LDH from two LA bacteria failed, a codon-optimized gene with an N109G amino acid exchange from *Bos taurus* was implemented (Johnson and Beckham, 2015). To avoid reuptake and consumption of the produced LA, the degradation pathway was disrupted by deletion of the *lldD* gene. The modifications enabled mixed PA-LA production from benzoate and *p*-coumarate (Johnson and Beckham, 2015).

In addition, a natural lignin degrader—the basidiomycete fungus *Phanerochaete chrysosporium*—was applied to SA production from lignin (Table 3) (Hong et al., 2017). Because the ligninolytic activity of the fungus produced radicals, reducing agents were added as scavengers, allowing the degradation of a synthetic lignin along with the production of aromatic compounds and SA. The titer (18 mg L^{-1}) remained low, but the results can be considered a successful proof of principle for lignin-based production of SA (Hong et al., 2017).

5.1.3. Pyridine-related organic acids

Further interesting examples of lignin valorization include the production of pyridine-2,4-dicarboxylic acid (2,4-PDCA) and pyridine-2,5-dicarboxylic acid (2,5-PDCA) using *Rhodococcus jostii* RHA1 (Table 3) (Mycroft et al., 2015). As dicarboxylic acids, 2,4-PDCA and 2,5-PDCA can serve as building blocks for aromatic polymers, including polyamides and polyesters. *R. jostii* RHA1 is a natural bacterial degrader of lignin, using the β-ketoadipate pathway for further aromatic catabolism. To establish 2,4-PDCA and 2,5-PDCA production, the native ortho-cleavage pathway of protocatechuate was complemented by the two alternative meta-cleavage pathways. The design was realized by insertion of the recombinant genes *ligAB*, encoding protocatechuate 4,5-dioxygenase from *S. paucimobilis*, and *praA*, encoding protocatechuate 2,3-dioxygenase from *Paenibacillus* sp. JJ-1b. The recombinant strain produced 80 mg L^{-1} 2,4-PDCA and 125 mg L^{-1} 2,5-PDCA when grown on minimal medium with 1 % (w/v) wheat straw lignocellulose (Mycroft et al., 2015).

5.2. Materials

5.2.1. Nylon

With an annual global market of approximately 7 million tons, nylons hold the pole position of today´s plastic market and are omnipresent in our everyday life (Becker and Wittmann, 2015; Kind et al., 2014). As described above, the full value chain from lignin to nylon was established only recently, applying a cascade chemical and biochemical conversion of softwood lignin (Kohlstedt et al., 2018). First, softwood lignin was thermally depolymerized using a setup that mainly produced mixtures of catechol and phenol with small amounts of *p*-cresol and *o*-cresol. Within 54 h, the engineered MA-9 (see above) strain converted the stepwise-fed hydrolysate into 13 g L^{-1} MA at a yield close to 100 % (mol mol^{-1}) (Fig. 6B, Table 3) Follow-up purification of MA, hydrogenation into adipic acid and polycondensation with hexamethylendiamine yielded lignin-based nylon (Kohlstedt et al., 2018).

5.2.2. Polyhydroxyalkanoates

P. putida KT2440 was additionally applied to the production of medium-chain-length polyhydroxyalkanoates (mcl-PHAs) using aromatics as a carbon source (Linger et al., 2014). PHAs are polyesters with excellent biodegradability and biocompatibility and thus of high value for various application fields, including tissue engineering, drug delivery or eco-friendly packaging (Poblete-Castro et al., 2012; Poblete-Castro et al., 2013). For the model substrates *p*-coumarate and ferulate, mcl-PHA production was as high as 34 % and 39 % of the cell dry weight (Table 3). Comparable mcl-PHA production (32 % wt wt^{-1}) was achieved directly from alkaline pretreated liquor (APL) (Linger et al., 2014).

APL was also used to screen fourteen bacteria for their ability to depolymerize lignin and to convert APL to value-added coproducts such as PHAs and FAMEs (Salvachua et al., 2015). *P. putida* (PHA, FAME), *Amycolatopsis* sp. (FAME), *R. jostii* (FAME) and *Cupriavidus necator* (PHA, FAME) were found to accumulate intracellular carbon storage compounds (Salvachua et al., 2015). Interestingly, the screening of marine bacteria led to the discovery of lignin-degrading *Oceanimonas doudoroffii*, which is capable of synthesizing PHA directly from lignin and its derivatives (Numata and Morisaki, 2015). More recently, PHA production in *P. putida* strain A514 was established using vanillate as the sole carbon source (Wang et al., 2018c). Targeted overexpression of an enoyl-CoA hydratase (encoded by *phaJ4*), a 3-hydroxyacyl-ACP thioesterase (encoded by *phaG*) and a long-chain fatty acid-CoA ligase (encoded by *alkK*) was found to simultaneously improve cell growth and PHA production. The combination allowed a production of 246 mg L^{-1} PHA (Table 3) (Wang et al., 2018c). PHA production from lignin or lignin-related aromatic compounds was also achieved in other bacteria (Table 3), including a *Pandoraea* sp. (Kumar et al., 2017) and *Cupriavidus basilensis* (Shi et al., 2017).

5.3. Fuels

The demand for biobased fuel production is steadily increasing and expected to grow further due to the shortage of fossil resources and legal assignments. In this regard, lignin bioconversion into lipids has attracted attention as a potential biofuel (Chen and Wan, 2017; Liu et al., 2018). *Rhodococcus opacus* was reported to produce lipids (Table 3) from the pure model aromatics vanillate and 4-hydroxybenzoate (Kosa and Ragauskas, 2012) and from technical lignins, such as kraft lignin (Wei et al., 2015; Zhao et al., 2016) and ethanol organosolv lignin (Kosa and Ragauskas, 2013). The highest lipid production from lignin, 1.8 g L^{-1}, resulted from a combinatorial pretreatment of lignin and additional laccase treatment of the lignin stream, which was then applied in an optimized fed-batch fermentation (Table 3) (Liu et al., 2018). The high production was likely the result of

improved release of aromatic monomers from lignin, reduced inhibition by detoxification of the lignin stream and an optimal reaction environment (adequate oxygen supply, pH control) in the fermenter (Liu et al., 2018).

5.4. Flavors and fragrances

Approximately 20 years ago, initial studies investigated the use of eugenol (Overhage et al., 1999a; Overhage et al., 2002, 2003) and ferulic acid (Narbad and Gasson, 1998) to obtain vanillin, used as a flavor in the food industry and as a fragrance in the production of perfumes. Today, the worldwide production of natural vanillin is approximately 6,500 tons, with the major supplying countries being Indonesia, Madagascar and China (Banerjee and Chattopadhyay, 2019). The supply from vanilla pods can, however, not fulfill the market demands and is thus complemented by another 18,000 tons of chemical or synthetic vanillin (Banerjee and Chattopadhyay, 2019). Despite the highly attractive price (15 \$ kg^{-1} vs. 1200-4000 \$ kg^{-1} for natural vanillin) (Banerjee and Chattopadhyay, 2019), synthetic vanillin does not comply with food safety requirements (Banerjee and Chattopadhyay, 2019). Biotechnological production routes based on eugenol and ferulic acid hence gained importance by having attributes such as “natural”, “bio” and “healthy” (Banerjee and Chattopadhyay, 2019; Priefert et al., 2001).

In the beginning, substantial work was invested to determine the catabolic pathways of eugenol and ferulic acid and the corresponding genes (Narbad and Gasson, 1998; Overhage et al., 1999b; Plaggenborg et al., 2003). Vanillin accumulation in *Pseudomonas* sp. strain HR199 was then achieved by interruption of the *vdh* gene, which encodes NAD-dependent vanillin dehydrogenase (Overhage et al., 1999a). The mutant strain produced up to 2.9 mM vanillin (Table 3) in a two-stage process comprising a growth phase with gluconate as the substrate and a production phase using 6.5 mM eugenol as the substrate (Fig. 7A). After 17 h, the vanillin level dropped from its peak value of 2.9 mM as a result of the activity of another vanillin dehydrogenase (VDH-II) (Overhage et al., 1999a). The eugenol catabolic genes *ehyAB* (eugenol hydroxylase), *calA* (coniferyl alcohol dehydrogenase) and *calB* (coniferyl aldehyde dehydrogenase) of *Pseudomonas* sp. strain HR199 were then successfully transferred as a catabolic gene cassette into *Ralstonia eutropha* H16 (Fig. 7B) using the newly designed broad-host-range vector pBBR1-JO2 (Overhage et al., 2002). The genes were functionally expressed, enabling the production of ferulic acid from eugenol with a molar biotransformation yield of 93.8 % (Overhage et al., 2002).

This gene combination was also tested to establish ferulic acid production in *Escherichia coli* XL1-Blue but failed. Successful biotransformation relied on the replacement of the *ehyAB* genes by the *vaoA* gene, encoding vanillyl alcohol oxidase from *Penicillium simplicissimum* CBS 170.90 (Overhage et al., 2003). Scaled to a 30-liter fermenter, resting cells of the recombinant *E. coli* strain produced 14.7 g L^{-1} ferulic acid within 30 h, thereby achieving a molar yield of 93.3 % (Table 3, Fig. 7C) (Overhage et al., 2003).

In a next step, a two-step biotransformation process for the conversion of eugenol to vanillin was established (Overhage et al., 2003), additionally recruiting a previously constructed recombinant *E. coli* XL1-Blue strain that converted ferulic acid to vanillin upon expression of *fcs* and *ech*, which encode feruloyl-CoA synthase and enoyl-CoA hydratase/aldolase from *Pseudomonas* sp. strain HR199, respectively (Fig. 7C) (Overhage et al., 1999b). After 5 g L^{-1} ferulic acid was produced from eugenol in the first process stage, 0.3 g L^{-1} vanillin accumulated in the second process stage, along with 0.1 g L^{-1} vanillyl alcohol and a residual ferulic acid concentration of 4.6 g L^{-1} (Overhage et al., 2003). Similar approaches were used for the production of vanillin, coniferyl alcohol and ferulic acid using *Amycolatopsis* sp. HR167 (Overhage et al., 2006) and *Rhodococcus* strains (Plaggenborg et al., 2006).

In addition to vanillin, lignin-derived aromatic compounds also appear to be interesting starting molecules for the production of other flavors and fragrances. During fruit ripening, a complex mixture of volatile esters is produced by the activity of alcohol acyltransferases that typically contribute to the specific odor of pineapple (Elss et al., 2005), melon (El-Sharkawy et al., 2005), strawberry (Cumplido-Laso et al., 2012) and kiwi (Günther et al., 2011). Among other compounds, this volatile cocktail also contains esters derived from aromatic compounds. In ripe kiwifruit, ethyl benzoate is one of the major esters (Günther et al., 2011), and the enzyme characterization of alcohol acyltransferases from other fruit sources revealed good activity with benzoate, benzaldehyde or cinnamyl alcohol (Cumplido-Laso et al., 2012; El-Sharkawy et al., 2005; Holland et al., 2005). Lignin-derived aromatics could hence be used as starter molecules for alcohol acyltransferase-based volatile ester production.

6. Conclusion

The development of concepts and strategies for upgrading lignin

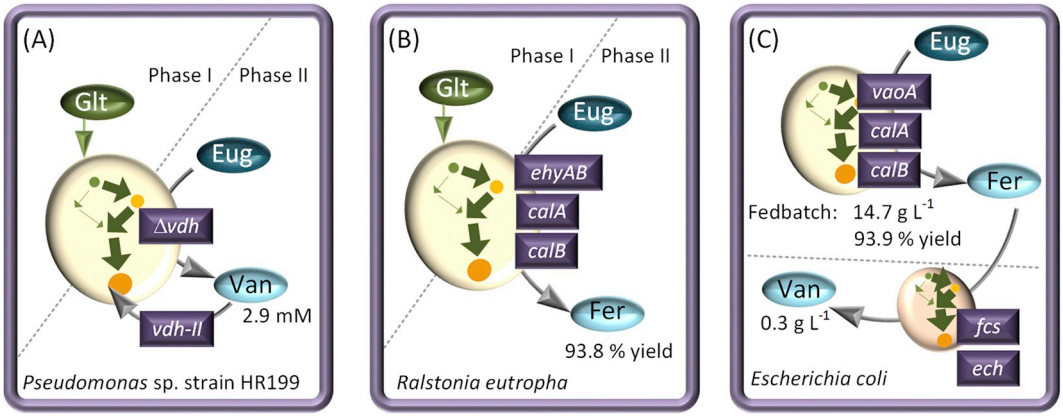

Fig. 7. Production of vanillin and ferulate from monolignins. (A) Production of vanillin from eugenol using *Pseudomonas* species. The process comprised a growth phase on gluconate (phase I) and a production phase using eugenol as biotransformation substrate (phase II) (Overhage et al., 1999a), (B) Production of ferulate from eugenol using *Ralstonia eutropha*. The process comprised a growth phase on gluconate (phase I) and a production phase using eugenol as biotransformation substrate (phase II) (Overhage et al., 2002), (C) Production of ferulate from eugenol with subsequent biotransformation of ferulate to vanillin using *Escherichia coli* (Overhage et al., 2003). Color code is as follows: dark green: growth substrate, dark turquois: biotransformation substrate, light turquois: biotransformation product, purple: genetic modification, grey arrow: biotransformation reaction, green arrow: substrate uptake for growth. Yields are given on a molar basis.
calA: coniferyl alcohol dehydrogenase, *calB*: coniferyl aldehyde dehydrogenase, *ech*: enoyl-CoA hydratase/aldolase, *ehyAB*: eugenol hydroxylase, Eug: eugenol, *fcs*: feruloyl-CoA synthase, Fer: ferulate, Glt: gluconate, Van: vanillin, *vaoA*: vanillyl alcohol oxidase, *vdh*: vanillin dehydrogenase.

into value-added compounds is clearly one of the hot topics in current chemical, biochemical and biotechnological research. As illustrated, metabolic engineering has bred efficient microbial cell factories for the production of relevant industrial goods from lignin at the laboratory scale and even at the pilot scale (Kohlstedt et al., 2018). In this regard, a cornerstone for lignin valorization has been achieved, and it promises exciting possibilities for future upgrading of lignin-containing product streams from the biomass-processing industries. However, for further upscaling, a difficult remaining challenge is the efficient supply of large quantities of lignin in a relatively uniform, purified and biocompatible form (Pye, 2010). Improved processing of lignin for feeding into bioproduction is a key target and might include the use of enzymes of higher efficiency, tailored process operation modes and consolidated bioprocessing concepts (Abdelaziz et al., 2016; Beckham et al., 2016; Hämäläinen et al., 2018; Kohlstedt et al., 2018; Ragauskas et al., 2014; Rodriguez et al., 2017; Salvachua et al., 2015; Schutyser et al., 2018). These approaches will hopefully further increase and diversify the portfolio of products from lignin.

Funding

This work was supported by the German Federal Ministry of Education and Research (BMBF) via the projects “BioNylon” (FKZ 03VO757) and “LignoValue“ (FKZ 01DN17036). The funding body was not involved in study design; collection, analysis and interpretation of data; writing of the manuscript; and the decision to submit the manuscript.

Conflict of interest

The authors have filed a patent application regarding MA production from lignin-based aromatics and have no further competing interests.

References

Abdelaziz, O.Y., Brink, D.P., Prothmann, J., Ravi, K., Sun, M., Garcia-Hidalgo, J., Sandahl, M., Hulteberg, C.P., Turner, C., Liden, G., Gorwa-Grauslund, M.F., 2016. Biological valorization of low molecular weight lignin. Biotechnol. Adv. 1318–1346 2016/10/11 ed.

Abe, T., Masai, E., Miyauchi, K., Katayama, Y., Fukuda, M., 2005. A tetrahydrofolate-dependent O-demethylase, LigM, is crucial for catabolism of vanillate and syringate in *Sphingomonas paucimobilis* SYK-6. J. Bacteriol. 187 (6), 2030–2037.

Adler, P., Bolten, C.J., Dohnt, K., Hansen, C.E., Wittmann, C., 2013. Core fluxome and metafluxome of lactic acid bacteria under simulated cocoa pulp fermentation conditions. Appl. Environ. Microbiol. 79 (18), 5670–5681.

Adler, P., Frey, L.J., Berger, A., Bolten, C.J., Hansen, C.E., Wittmann, C., 2014. The key to acetate: metabolic fluxes of acetic acid bacteria under cocoa pulp fermentation-simulating conditions. Appl. Environ. Microbiol. 80 (15), 4702–4716.

Ahmad, M., Taylor, C.R., Pink, D., Burton, K., Eastwood, D., Bending, G.D., Bugg, T.D., 2010. Development of novel assays for lignin degradation: comparative analysis of bacterial and fungal lignin degraders. Mol. Biosyst. 6 (5), 815–821.

Ahmad, M., Roberts, J.N., Hardiman, E.M., Singh, R., Eltis, L.D., Bugg, T.D., 2011. Identification of DypB from *Rhodococcus jostii* RHA1 as a lignin peroxidase. Biochem. 50 (23), 5096–5107.

Alvarez-Rodriguez, M.L., Belloch, C., Villa, M., Uruburu, F., Larriba, G., Coque, J.J., 2003. Degradation of vanillic acid and production of guaiacol by microorganisms isolated from cork samples. FEMS Microbiol. Lett. 220 (1), 49–55.

An, H.R., Park, H.J., Kim, E.S., 2000. Characterization of benzoate degradation via ortho-cleavage by *Streptomyces setonii*. J. Microbiol. Biotechnol. 10 (1), 111–114.

Arazoe, T., Kondo, A., Nishida, K., 2018. Targeted Nucleotide Editing Technologies for Microbial Metabolic Engineering. Biotechnol. J. 13 (9), e1700596.

Banerjee, G., Chattopadhyay, P., 2019. Vanillin biotechnology: the perspectives and future. J. Sci. Food Agric. 99 (2), 499–506.

Bang, S.G., Choi, C.Y., 1995. DO-stat fed-batch production of *cis, cis*-muconic acid from benzoic acid by *Pseudomonas putida* BM014. J. Ferm. Bioeng. 79 (4), 381–383.

Banno, S., Nishida, K., Arazoe, T., Mitsunobu, H., Kondo, A., 2018. Deaminase-mediated multiplex genome editing in *Escherichia coli*. Nat. Microbiol. 3 (4), 423–429.

Barry, K.P., Taylor, E.A., 2013. Characterizing the promiscuity of LigAB, a lignin catabolite degrading extradiol dioxygenase from *Sphingomonas paucimobilis* SYK-6. Biochem. 52 (38), 6724–6736.

Barton, N., Horbal, L., Starck, S., Kohlstedt, M., Luzhetskyy, A., Wittmann, C., 2018. Enabling the valorization of guaiacol-based lignin: Integrated chemical and biochemical production of *cis*,*cis*-muconic acid using metabolically engineered *Amycolatopsis* sp ATCC 39116. Metab. Eng. 45, 200–210.

Baumgärtner, F., Conrad, J., Sprenger, G.A., Albermann, C., 2014. Synthesis of the human milk oligosaccharide lacto-N-tetraose in metabolically engineered, plasmid-free *E. coli*. Chembiochem 15 (13), 1896–1900.

Becker, J., Wittmann, C., 2015. Advanced Biotechnology: Metabolically engineered cells for the bio-based production of chemicals and fuels, materials, and health-care products. Angew. Chem. Int. Ed. Engl. 54, 3328–3350.

Becker, J., Wittmann, C., 2018. From systems biology to metabolically engineered cells-an omics perspective on the development of industrial microbes. Curr. Opin. Microbiol. 45, 180–188.

Becker, J., Zelder, O., Haefner, S., Schröder, H., Wittmann, C., 2011. From zero to hero–design-based systems metabolic engineering of *Corynebacterium glutamicum* for L-lysine production. Metab. Eng. 159–168 2011/01/19 ed.

Becker, J., Reinefeld, J., Stellmacher, R., Schäfer, R., Lange, A., Meyer, H., Lalk, M., Zelder, O., von Abendroth, G., Schröder, H., Haefner, S., Wittmann, C., 2013a. Systems-wide analysis and engineering of metabolic pathway fluxes in bio-succinate producing *Basfia succiniciproducens*. Biotechnol. Bioeng. 110 (11), 3013–3023.

Becker, J., Schäfer, R., Kohlstedt, M., Harder, B.J., Borchert, N.S., Stöveken, N., Bremer, E., Wittmann, C., 2013b. Systems metabolic engineering of *Corynebacterium glutamicum* for production of the chemical chaperone ectoine. Microb. Cell Fact. 12, 110.

Becker, J., Lange, A., Fabarius, J., Wittmann, C., 2015. Top value platform chemicals: bio-based production of organic acids. Curr. Opin. Biotechnol. 36, 168–175.

Becker, J., Kuhl, M., Kohlstedt, M., Starck, S., Wittmann, C., 2018a. Metabolic engineering of *Corynebacterium glutamicum* for the production of *cis, cis*-muconic acid from lignin. Microb. Cell Fact. 17 (1), 115.

Becker, J., Rohles, C.M., Wittmann, C., 2018b. Metabolically engineered *Corynebacterium glutamicum* for bio-based production of chemicals, fuels, materials, and healthcare products. Metab. Eng. 50, 122–141.

Beckham, G.T., Johnson, C.W., Karp, E.M., Salvachua, D., Vardon, D.R., 2016. Opportunities and challenges in biological lignin valorization. Curr. Opin. Biotechnol. 42, 40–53.

Belda, E., van Heck, R.G., Jose Lopez-Sanchez, M., Cruveiller, S., Barbe, V., Fraser, C., Klenk, H.P., Petersen, J., Morgat, A., Nikel, P.I., Vallenet, D., Rouy, Z., Sekowska, A., Martins Dos Santos, V.A., de Lorenzo, V., Danchin, A., Medigue, C., 2016. The revisited genome of *Pseudomonas putida* KT2440 enlightens its value as a robust metabolic chassis. Environ. Microbiol. 18 (10), 3403–3424.

Bilal, M., Nawaz, M.Z., Iqbal, H.M.N., Hou, J., Mahboob, S., Al-Ghanim, K.A., Cheng, H., 2018. Engineering ligninolytic consortium for bioconversion of lignocelluloses to ethanol and chemicals. Protein Pept. Lett. 25 (2), 108–119.

Blazeck, J., Miller, J., Pan, A., Gengler, J., Holden, C., Jamoussi, M., Alper, H.S., 2014. Metabolic engineering of *Saccharomyces cerevisiae* for itaconic acid production. Appl. Microbiol. Biotechnol. 98 (19), 8155–8164.

Bommareddy, R.R., Chen, Z., Rappert, S., Zeng, A.P., 2014. A de novo NADPH generation pathway for improving lysine production of *Corynebacterium glutamicum* by rational design of the coenzyme specificity of glyceraldehyde 3-phosphate dehydrogenase. Metab. Eng. 25, 30–37.

Brennan, M.A., Trachtenberg, A.M., McClelland, W.D., MacLea, K.S., 2017. Genome Sequence of *Oceanimonas doudoroffii* ATCC 27123(T). Genome Announc. 5 (36).

Brunow, G., 2010. Lignin chemistry and its role in biomass conversion. In: Kamm, B., Gruber, P.R., Kamm, M. (Eds.), Biorefineries - Industrial processes and products. Wiley-VCH Verlag GmbH & Co. KGaA, Weinheim, pp. 151–163.

Bugg, T.D., Ahmad, M., Hardiman, E.M., Singh, R., 2011. The emerging role for bacteria in lignin degradation and bio-product formation. Curr. Opin. Biotechnol. 22 (3), 394–400.

Busche, T., Silar, R., Picmanova, M., Patek, M., Kalinowski, J., 2012. Transcriptional regulation of the operon encoding stress-responsive ECF sigma factor SigH and its anti-sigma factor RshA, and control of its regulatory network in *Corynebacterium glutamicum*. BMC Genomics 13, 445.

Buschke, N., Schröder, H., Wittmann, C., 2011. Metabolic engineering of *Corynebacterium glutamicum* for production of 1,5-diaminopentane from hemicellulose. Biotechnol. J. 6 (3), 306–317.

Buschke, N., Becker, J., Schäfer, R., Kiefer, P., Biedendieck, R., Wittmann, C., 2013a. Systems metabolic engineering of xylose-utilizing *Corynebacterium glutamicum* for production of 1,5-diaminopentane. Biotechnol. J. 557–570 2013/03/01 ed.

Buschke, N., Schäfer, R., Becker, J., Wittmann, C., 2013b. Metabolic engineering of industrial platform microorganisms for biorefinery applications–optimization of substrate spectrum and process robustness by rational and evolutive strategies. Bioresour. Technol. 135, 544–554.

Cao, L., Yu, I.K.M., Liu, Y., Ruan, X., Tsang, D.C.W., Hunt, A.J., Ok, Y.S., Song, H., Zhang, S., 2018. Lignin valorization for the production of renewable chemicals: State-of-the-art review and future prospects. Bioresour. Technol. 269, 465–475.

Chae, T.U., Kim, W.J., Choi, S., Park, S.J., Lee, S.Y., 2015. Metabolic engineering of *Escherichia coli* for the production of 1,3-diaminopropane, a three carbon diamine. Sci. Rep. 5, 13040.

Chai, L.Y., Chen, Y.H., Tang, C.J., Yang, Z.H., Zheng, Y., Shi, Y., 2014. Depolymerization and decolorization of kraft lignin by bacterium *Comamonas* sp. B-9. Appl. Microbiol. Biotechnol. 98 (4), 1907–1912.

Chandra, R., Raj, A., Purohit, H.J., Kapley, A., 2007. Characterisation and optimisation of three potential aerobic bacterial strains for kraft lignin degradation from pulp paper waste. Chemosphere 67 (4), 839–846.

Chen, Z., Wan, C.X., 2017. Biological valorization strategies for converting lignin into fuels and chemicals. Renew. Sust. Energ. Rev. 73, 610–621.

Chen, Y.F., Chao, H., Zhou, N.Y., 2014. The catabolism of 2,4-xylenol and *p*-cresol share the enzymes for the oxidation of para-methyl group in *Pseudomonas putida* NCIMB 9866. Appl. Microbiol. Biotechnol. 98 (3), 1349–1356.

Chen, C., Zhang, Y., Xu, L., Zhu, K., Feng, Y., Pan, J., Si, M., Zhang, L., Shen, X., 2018. Transcriptional control of the phenol hydroxylase gene *phe* of *Corynebacterium*

glutamicum by the AraC-type regulator PheR. Microbiol. Res. 209, 14–20.
Cho, S.W., Lee, J., Carroll, D., Kim, J.S., 2013. Heritable gene knockout in *Caenorhabditis elegans* by direct injection of Cas9-sgRNA ribonucleoproteins. Genetics 195 (3), 1177–1180.
Cho, J.S., Choi, K.R., Prabowo, C.P.S., Shin, J.H., Yang, D., Jang, J., Lee, S.Y., 2017. CRISPR/Cas9-coupled recombineering for metabolic engineering of *Corynebacterium glutamicum*. Metab. Eng. 42, 157–167.
Choi, W.J., Lee, E.Y., Cho, M.H., Choi, C.Y., 1997. Enhanced production of *cis,cis*-muconate in a cell-recycle bioreactor. J. Ferm. Bioeng. 84 (1), 70–76.
Chu, H.S., Kim, Y.S., Lee, C.M., Lee, J.H., Jung, W.S., Ahn, J.H., Song, S.H., Choi, I.S., Cho, K.M., 2015. Metabolic engineering of 3-hydroxypropionic acid biosynthesis in *Escherichia coli*. Biotechnol. Bioeng. 112 (2), 356–364.
Chua, J.W., Hsieh, J.H., 1990. Oxidative bioconversion of toluene to 1,3-butadiene-1,4-dicarboxylic acid (*cis,cis*-muconic acid). World J. Microbiol. Biotechnol. 6 (2), 127–143.
Clarkson, S.M., Giannone, R.J., Kridelbaugh, D.M., Elkins, J.G., Guss, A.M., Michener, J.K., 2017. Construction and optimization of a heterologous pathway for protocatechuate catabolism in *Escherichia coli* enables bioconversion of model aromatic compounds. Appl. Environ. Microbiol. 83 (18).
Constant, S., Wienk, H.L.J., Frissen, A.E., de Peinder, P., Boelens, R., van Es, D.S., Grisel, R.J.H., Weckhuysen, B.M., Huijgen, W.J.J., Gosselink, R.J.A., Bruijnincx, P.C.A., 2016. New insights into the structure and composition of technical lignins: a comparative characterisation study. Green Chem. 18 (9), 2651–2665.
Cook, T.B., Rand, J.M., Nurani, W., Courtney, D.K., Liu, S.A., Pfleger, B.F., 2018. Genetic tools for reliable gene expression and recombineering in *Pseudomonas putida*. J. Ind. Microbiol. Biotechnol. 45 (7), 517–527.
Corona, A., Biddy, M.J., Vardon, D.R., Birkved, M., Hauschild, M.Z., Beckham, G.T., 2018. Life cycle assessment of adipic acid production from lignin. Green Chem. 20 (16), 3857–3866.
Cumplido-Laso, G., Medina-Puche, L., Moyano, E., Hoffmann, T., Sinz, Q., Ring, L., Studart-Wittkowski, C., Caballero, J.L., Schwab, W., Munoz-Blanco, J., Blanco-Portales, R., 2012. The fruit ripening-related gene FaAAT2 encodes an acyl transferase involved in strawberry aroma biogenesis. J. Exp. Bot. 63 (11), 4275–4290.
Curran, K.A., Leavitt, J.M., Karim, A.S., Alper, H.S., 2013. Metabolic engineering of muconic acid production in *Saccharomyces cerevisiae*. Metab. Eng. 15, 55–66.
Dashtban, M., Schraft, H., Syed, T.A., Qin, W., 2010. Fungal biodegradation and enzymatic modification of lignin. Int. J. Biochem. Mol. Biol. 1 (1), 36–50.
Davis, R., Tao, L., Tan, E.C.F., Biddy, M.J., Beckham, G., Scarlata, C., 2013. Process design and economics for the conversion of lignocellulosic biomass to hydrocarbons - dilute-acid and enzymatic deconstruction of biomass to sugars and biological conversion of sugars to hydrocarbons. National Renewable Energy Laboratory.
de Gonzalo, G., Colpa, D.I., Habib, M.H., Fraaije, M.W., 2016. Bacterial enzymes involved in lignin degradation. J. Biotechnol. 236, 110–119.
de Jong, E., van Berkel, W.J., van der Zwan, R.P., de Bont, J.A., 1992. Purification and characterization of vanillyl-alcohol oxidase from *Penicillium simplicissimum*. A novel aromatic alcohol oxidase containing covalently bound FAD. Eur. J. Biochem. 208 (3), 651–657.
Deangelis, K.M., Sharma, D., Varney, R., Simmons, B., Isern, N.G., Markilllie, L.M., Nicora, C., Norbeck, A.D., Taylor, R.C., Aldrich, J.T., Robinson, E.W., 2013. Evidence supporting dissimilatory and assimilatory lignin degradation in *Enterobacter lignolyticus* SCF1. Front. Microbiol. 4, 280.
Donnelly, M.I., Dagley, S., 1980. Production of methanol from aromatic acids by *Pseudomonas putida*. J. Bacteriol. 142 (3), 916–924.
Draths, K.M., Frost, J.W., 1994. Environmentally compatible synthesis of adipic acid from D-glucose. J. Am. Chem. Soc. 116, 399–400.
Du, L., Ma, L., Qi, F., Zheng, X., Jiang, C., Li, A., Wan, X., Liu, S.J., Li, S., 2016. Characterization of a unique pathway for 4-cresol catabolism initiated by phosphorylation in *Corynebacterium glutamicum*. J. Biol. Chem. 291 (12), 6583–6594.
Dvorak, P., Nikel, P.I., Damborsky, J., de Lorenzo, V., 2017. Bioremediation 3.0: Engineering pollutant-removing bacteria in the times of systemic biology. Biotechnol. Adv. 35 (7), 845–866.
Eastwood, D.C., Floudas, D., Binder, M., Majcherczyk, A., Schneider, P., Aerts, A., Asiegbu, F.O., Baker, S.E., Barry, K., Bendiksby, M., Blumentritt, M., Coutinho, P.M., Cullen, D., de Vries, R.P., Gathman, A., Goodell, B., Henrissat, B., Ihrmark, K., Kauserud, H., Kohler, A., LaButti, K., Lapidus, A., Lavin, J.L., Lee, Y.H., Lindquist, E., Lilly, W., Lucas, S., Morin, E., Murat, C., Oguiza, J.A., Park, J., Pisabarro, A.G., Riley, R., Rosling, A., Salamov, A., Schmidt, O., Schmutz, J., Skrede, I., Stenlid, J., Wiebenga, A., Xie, X., Kues, U., Hibbett, D.S., Hoffmeister, D., Hogberg, N., Martin, F., Grigoriev, I.V., Watkinson, S.C., 2011. The plant cell wall-decomposing machinery underlies the functional diversity of forest fungi. Science 333 (6043), 762–765.
El-Sharkawy, I., Manriquez, D., Flores, F.B., Regad, F., Bouzayen, M., Latche, A., Pech, J.C., 2005. Functional characterization of a melon alcohol acyl-transferase gene family involved in the biosynthesis of ester volatiles. Identification of the crucial role of a threonine residue for enzyme activity* Plant Mol. Biol. 59 (2), 345–362.
Elss, S., Preston, C., Hertzig, C., Heckel, F., Richling, E., Schreier, P., 2005. Aroma profiles of pineapple fruit (*Ananas comosus* [L.] Merr.) and pineapple products. Lwt-Food Sci. Technol. 38 (3), 263–274.
Eltis, L.D., Karlson, U., Timmis, K.N., 1993. Purification and Characterization of Cytochrome-P450$_{RR1}$ from *Rhodococcus rhodochrous*. Eur. J. Biochem. 213 (1), 211–216.
Erden, E., Ucar, M.C., Gezer, T., Pazarlioglu, N.K., 2009. Screening for ligninolytic enzymes from autochthonous fungi and applications for decolorization of Remazole Marine Blue. Braz. J. Microbiol. 40 (2), 346–353.
Fache, M., Boutevin, B., Caillol, S., 2016. Vanillin production from lignin and its use as a renewable chemical. ACS Sustain. Chem. Eng. 4 (1), 35–46.
Fernandez-Rodriguez, J., Erdocia, X., Sanchez, C., Alriols, M.G., Labidi, J., 2017. Lignin depolymerization for phenolic monomers production by sustainable processes. J. Energy Chem. 26 (4), 622–631.
Fischer, R., Bleichrodt, F.S., Gerischer, U.C., 2008. Aromatic degradative pathways in *Acinetobacter baylyi* underlie carbon catabolite repression. Microbiology 154 (Pt 10), 3095–3103.
Ghodake, G.S., Kalme, S.D., Jadhav, J.P., Govindwar, S.P., 2009. Purification and partial characterization of lignin peroxidase from *Acinetobacter calcoaceticus* NCIM 2890 and its application in decolorization of textile dyes. Appl. Biochem. Biotechnol. 152 (1), 6–14.
Gibson, D.G., 2009. Synthesis of DNA fragments in yeast by one-step assembly of overlapping oligonucleotides. Nucleic Acids Res. 37 (20), 6984–6990.
Gibson, D.G., Young, L., Chuang, R.Y., Venter, J.C., Hutchison 3rd, C.A., Smith, H.O., 2009. Enzymatic assembly of DNA molecules up to several hundred kilobases. Nat. Methods 6 (5), 343–345.
Glenn, J.K., Gold, M.H., 1985. Purification and characterization of an extracellular Mn (II)-dependent peroxidase from the lignin-degrading basidiomycete, *Phanerochaete chrysosporium*. Arch. Biochem. Biophys. 242 (2), 329–341.
Glenn, J.K., Akileswaran, L., Gold, M.H., 1986. Mn(II) oxidation is the principal function of the extracellular Mn-peroxidase from *Phanerochaete chrysosporium*. Arch. Biochem. Biophys. 251 (2), 688–696.
Gottschalk, L.M., Bon, E.P., Nobrega, R., 2008. Lignin peroxidase from *Streptomyces viridosporus* T7A: enzyme concentration using ultrafiltration. Appl. Biochem. Biotechnol. 147 (1-3), 23–32.
Grant, D.J.W., Patel, J.C., 1969. Non-oxidative decarboxylation of p-hydroxybenzoic acid, gentisic acid, protocatechuic acid and gallic acid by *Klebsiella aerogenes* (*Aerobacter aerogenes*). Anton. Van Lee. J. M. S. 35 (3) 325-&.
Grund, E., Knorr, C., Eichenlaub, R., 1990. Catabolism of benzoate and monohydroxylated benzoates by *Amycolatopsis* and *Streptomyces* spp. Appl. Environ. Microbiol. 56 (5), 1459–1464.
Günther, C.S., Chervin, C., Marsh, K.B., Newcomb, R.D., Souleyre, E.J., 2011. Characterisation of two alcohol acyltransferases from kiwifruit (*Actinidia* spp.) reveals distinct substrate preferences. Phytochemistry 72 (8), 700–710.
Hämäläinen, V., Grönroos, T., Suonpää, A., Heikkilä, M.W., Romein, B., Ihalainen, P., Malandra, S., Birikh, K.R., 2018. Enzymatic processes to unlock the lignin value. Front. Bioeng. Biotechnol. 6, 20.
Harayama, S., Rekik, M., 1990. The meta cleavage operon of TOL degradative plasmid pWW0 comprises 13 genes. Mol. Gen. Genet. 221 (1), 113–120.
Harder, B.J., Bettenbrock, K., Klamt, S., 2016. Model-based metabolic engineering enables high yield itaconic acid production by *Escherichia coli*. Metab. Eng. 38, 29–37.
Heider, S.A., Peters-Wendisch, P., Netzer, R., Stafnes, M., Brautaset, T., Wendisch, V.F., 2014. Production and glucosylation of C50 and C 40 carotenoids by metabolically engineered *Corynebacterium glutamicum*. Appl. Microbiol. Biotechnol. 98 (3), 1223–1235.
Heinaru, E., Truu, J., Stottmeister, U., Heinaru, A., 2000. Three types of phenol and *p*-cresol catabolism in phenol- and *p*-cresol-degrading bacteria isolated from river water continuously polluted with phenolic compounds. FEMS Microbiol. Ecol. 31 (3), 195–205.
Hemme, D., Veyel, D., Muhlhaus, T., Sommer, F., Juppner, J., Unger, A.K., Sandmann, M., Fehrle, I., Schonfelder, S., Steup, M., Geimer, S., Kopka, J., Giavalisco, P., Schroda, M., 2014. Systems-wide analysis of acclimation responses to long-term heat stress and recovery in the photosynthetic model organism *Chlamydomonas reinhardtii*. The Plant cell 26 (11), 4270–4297.
Henson, W.R., Campbell, T., DeLorenzo, D.M., Gao, Y., Berla, B., Kim, S.J., Foston, M., Moon, T.S., Dantas, G., 2018a. Multi-omic elucidation of aromatic catabolism in adaptively evolved *Rhodococcus opacus*. Metab. Eng. 49, 69–83.
Henson, W.R., Hsu, F.F., Dantas, G., Moon, T.S., Foston, M., 2018b. Lipid metabolism of phenol-tolerant *Rhodococcus opacus* strains for lignin bioconversion. Biotechnol. Biofuels 11, 339.
Higuchi, Y., Aoki, S., Takenami, H., Kamimura, N., Takahashi, K., Hishiyama, S., Lancefield, C.S., Ojo, O.S., Katayama, Y., Westwood, N.J., Masai, E., 2018. Bacterial catabolism of beta-hydroxypropiovanillone and beta-hydroxypropiosyringone produced in the reductive cleavage of arylglycerol-beta-aryl ether in lignin. Appl. Environ. Microbiol. 84(7).
Hochman, A., Goldberg, I., 1991. Purification and characterization of a catalase-peroxidase and a typical catalase from the bacterium *Klebsiella pneumoniae*. Biochim. Biophys. Acta 1077 (3), 299–307.
Hoffmann, S.L., Jungmann, L., Schiefelbein, S., Peyriga, L., Cahoreau, E., Portais, J.C., Becker, J., Wittmann, C., 2018. Lysine production from the sugar alcohol mannitol: Design of the cell factory *Corynebacterium glutamicum* SEA-3 through integrated analysis and engineering of metabolic pathway fluxes. Metab. Eng. 47, 475–487.
Hofrichter, M., 2002. Review: lignin conversion by manganese peroxidase (MnP). Enzyme Microb. Technol. 30 (4), 454–466.
Hogancamp, T.N., Raushel, F.M., 2018. Functional annotation of LigU as a 1,3-allylic isomerase during the degradation of lignin in the protocatechuate 4,5-cleavage pathway from the soil bacterium *Sphingobium* sp. SYK-6. Biochem. 57 (19), 2837–2845.
Holland, D., Larkov, O., Bar-Ya'akov, I., Bar, E., Zax, A., Brandeis, E., Ravid, U., Lewinsohn, E., 2005. Developmental and varietal differences in volatile ester formation and acetyl-CoA: alcohol acetyl transferase activities in apple (*Malus domestica* Borkh.) fruit. J. Agric. Food Chem. 53 (18), 7198–7203.
Hong, C.Y., Ryu, S.H., Jeong, H., Lee, S.S., Kim, M., Choi, I.G., 2017. *Phanerochaete chrysosporium* multienzyme catabolic system for in vivo modification of synthetic lignin to succinic acid. ACS Chem. Biol. 12 (7), 1749–1759.
Hong, E.Y., Kim, J.Y., Upadhyay, R., Park, B.J., Lee, J.M., Kim, B.G., 2018. Rational engineering of ornithine decarboxylase with greater selectivity for ornithine over lysine through protein network analysis. J. Biotechnol. 281, 175–182.

Hopper, D.J., Taylor, D.G., 1975. Pathways for the degradation of *m*-cresol and *p*-cresol by *Pseudomonas putida*. J. Bacteriol. 122 (1), 1–6.
Hsieh, J.H., 1984. Continuous fermentation process and bioconversion-product recovery, US Patent No. 4480034.
Hsieh, J.H., 1985. Muconic acid productivity by a stabilized mutant microorganism population, US Patent No. 4535059.
Hsieh, J.H., 1990. Continuous fermentation process for aromatic hydrocarbon bioconversion, US Patent No. 4968612.
Huang, Y., Zhao, K.X., Shen, X.H., Jiang, C.Y., Liu, S.J., 2008. Genetic and biochemical characterization of a 4-hydroxybenzoate hydroxylase from *Corynebacterium glutamicum*. Appl. Microbiol. Biotechnol. 78 (1), 75–83.
Huang, X.F., Santhanam, N., Badri, D.V., Hunter, W.J., Manter, D.K., Decker, S.R., Vivanco, J.M., Reardon, K.F., 2013. Isolation and characterization of lignin-degrading bacteria from rainforest soils. Biotechnol. Bioeng. 110 (6), 1616–1626.
Huang, X., Lu, X., Li, Y., Li, X., Li, J.J., 2014. Improving itaconic acid production through genetic engineering of an industrial *Aspergillus terreus* strain. Microb. Cell Fact. 13 (1), 119.
Imada, Y., Yoshikawa, N., Mizuno, S., Mikawa, T., 1989. Process for preparing muconic acid.
Inokuma, K., Iwamoto, R., Bamba, T., Hasunuma, T., Kondo, A., 2017. Improvement of xylose fermentation ability under heat and acid co-stress in *Saccharomyces cerevisiae* using genome shuffling technique. Front. Bioeng. Biotechnol. 5, 81.
Jayakody, L.N., Turner, T.L., Yun, E.J., Kong, I.I., Liu, J.J., Jin, Y.S., 2018. Expression of Gre2p improves tolerance of engineered xylose-fermenting *Saccharomyces cerevisiae* to glycolaldehyde under xylose metabolism. Appl. Microbiol. Biotechnol. 102 (18), 8121–8133.
Jeschek, M., Gerngross, D., Panke, S., 2016. Rationally reduced libraries for combinatorial pathway optimization minimizing experimental effort. Nat. Commun. 7, 11163.
Jimenez, J.I., Minambres, B., Garcia, J.L., Diaz, E., 2002. Genomic analysis of the aromatic catabolic pathways from *Pseudomonas putida* KT2440. Environ. Microbiol. 4 (12), 824–841.
Jinek, M., Chylinski, K., Fonfara, I., Hauer, M., Doudna, J.A., Charpentier, E., 2012. A programmable dual-RNA-guided DNA endonuclease in adaptive bacterial immunity. Science 337 (6096), 816–821.
Johnson, C.W., Beckham, G.T., 2015. Aromatic catabolic pathway selection for optimal production of pyruvate and lactate from lignin. Metab. Eng. 28, 240–247.
Johnson, C.W., Salvachua, D., Khanna, P., Smith, H., Peterson, D.J., Beckham, G.T., 2016. Enhancing muconic acid production from glucose and lignin-derived aromatic compounds via increased protocatechuate decarboxylase activity. Metab. Eng. Commun. 3, 111–119.
Johnson, C.W., Abraham, P.E., Linger, J.G., Khanna, P., Hettich, R.L., Beckham, G.T., 2017. Eliminating a global regulator of carbon catabolite repression enhances the conversion of aromatic lignin monomers to muconate in *Pseudomonas putida* KT2440. Metab. Eng. Commun. 5, 19–25.
Jojima, T., Noburyu, R., Sasaki, M., Tajima, T., Suda, M., Yukawa, H., Inui, M., 2015. Metabolic engineering for improved production of ethanol by *Corynebacterium glutamicum*. Appl. Microbiol. Biotechnol. 99 (3), 1165–1172.
Kallscheuer, N., Vogt, M., Kappelmann, J., Krumbach, K., Noack, S., Bott, M., Marienhagen, J., 2016. Identification of the *phd* gene cluster responsible for phenylpropanoid utilization in *Corynebacterium glutamicum*. Appl. Microbiol. Biotechnol. 100 (4), 1871–1881.
Kamimura, N., Goto, T., Takahashi, K., Kasai, D., Otsuka, Y., Nakamura, M., Katayama, Y., Fukuda, M., Masai, E., 2017. A bacterial aromatic aldehyde dehydrogenase critical for the efficient catabolism of syringaldehyde. Sci. Rep. 7, 44422.
Kaneko, A., Ishii, Y., Kirimura, K., 2011. High-yield production of cis,cis-muconic acid from catechol in aqueous solution by biocatalyst. Chem. Lett. 40 (4), 381–383.
Kang, S.M., Li, X.L., Fan, J., Chang, J., 2013. Hydrothermal conversion of lignin: A review. Renew. Sust. Energ. Rev. 27, 546–558.
Karlson, U., Dwyer, D.F., Hooper, S.W., Moore, E.R., Timmis, K.N., Eltis, L.D., 1993. Two independently regulated cytochromes P-450 in a *Rhodococcus rhodochrous* strain that degrades 2-ethoxyphenol and 4-methoxybenzoate. J. Bacteriol. 175 (5), 1467–1474.
Kasai, D., Masai, E., Miyauchi, K., Katayama, Y., Fukuda, M., 2005. Characterization of the gallate dioxygenase gene: three distinct ring cleavage dioxygenases are involved in syringate degradation by *Sphingomonas paucimobilis* SYK-6. J. Bacteriol. 187 (15), 5067–5074.
Kasai, D., Fujinami, T., Abe, T., Mase, K., Katayama, Y., Fukuda, M., Masai, E., 2009. Uncovering the protocatechuate 2,3-cleavage pathway genes. J. Bacteriol. 191 (21), 6758–6768.
Kasai, D., Kamimura, N., Tani, K., Umeda, S., Abe, T., Fukuda, M., Masai, E., 2012. Characterization of FerC, a MarR-type transcriptional regulator, involved in transcriptional regulation of the ferulate catabolic operon in *Sphingobium* sp. strain SYK-6. FEMS Microbiol. Lett. 332 (1), 68–75.
Keat, M.J., Hopper, D.J., 1978a. The aromatic alcohol dehydrogenases in *Pseudomonas putida* N.C.I.B. 9869 grown on 3,5-xylenol and *p*-cresol. Biochem J. 175 (2), 659–667.
Keat, M.J., Hopper, D.J., 1978b. *p*-cresol and 3,5-xylenol methylhydroxylases in *Pseudomonas putida* N.C.I.B. 9896. Biochem. J. 175 (2), 649–658.
Khan, A., Nair, V., Colmenares, J.C., Gläser, R., 2018. Lignin-based composite materials for photocatalysis and photovoltaics. Top. Curr. Chem. 376 (3), 20.
Kiefer, P., Heinzle, E., Zelder, O., Wittmann, C., 2004. Comparative metabolic flux analysis of lysine-producing *Corynebacterium glutamicum* cultured on glucose or fructose. Appl. Environ. Microbiol. 70 (1), 229–239.
Kind, S., Jeong, W.K., Schröder, H., Wittmann, C., 2010a. Systems-wide metabolic pathway engineering in *Corynebacterium glutamicum* for bio-based production of diaminopentane. Metab. Eng. 12 (4), 341–351.
Kind, S., Jeong, W.K., Schröder, H., Zelder, O., Wittmann, C., 2010b. Identification and elimination of the competing N-acetyldiaminopentane pathway for improved production of diaminopentane by *Corynebacterium glutamicum*. Appl. Environ. Microbiol. 76 (15), 5175–5180.
Kind, S., Kreye, S., Wittmann, C., 2011. Metabolic engineering of cellular transport for overproduction of the platform chemical 1,5-diaminopentane in *Corynebacterium glutamicum*. Metab. Eng. 13 (5), 617–627.
Kind, S., Neubauer, S., Becker, J., Yamamoto, M., Völkert, M., Abendroth, G.V., Zelder, O., Wittmann, C., 2014. From zero to hero - Production of bio-based nylon from renewable resources using engineered *Corynebacterium glutamicum*. Metab. Eng. 25, 113–123.
Kirk, T.K., Tien, M., Faison, B.D., 1984. Biochemistry of the oxidation of lignin by *Phanerochaete chrysosporium*. Biotechnol. Adv. 2 (2), 183–199.
Kohler, A.C., Simmons, B.A., Sale, K.L., 2018. Structure-based engineering of a plant-fungal Hybrid peroxidase for enhanced temperature and pH tolerance. Cell chemical biology 25 (8), 974–983 e973.
Kohlstedt, M., Becker, J., Wittmann, C., 2010. Metabolic fluxes and beyond-systems biology understanding and engineering of microbial metabolism. Appl. Microbiol. Biotechnol. 88 (5), 1065–1075.
Kohlstedt, M., Sappa, P.K., Meyer, H., Maass, S., Zaprasis, A., Hoffmann, T., Becker, J., Steil, L., Hecker, M., van Dijl, J.M., Lalk, M., Mader, U., Stülke, J., Bremer, E., Völker, U., Wittmann, C., 2014. Adaptation of *Bacillus subtilis* carbon core metabolism to simultaneous nutrient limitation and osmotic challenge: a multi-omics perspective. Environ. Microbiol. 16 (6), 1898–1917.
Kohlstedt, M., Starck, S., Barton, N., Stolzenberger, J., Selzer, M., Mehlmann, K., Schneider, R., Pleissner, D., Rinkel, J., Dickschat, J.S., Venus, J., van Duuren, J.B.J.H., Wittmann, C., 2018. From lignin to nylon: Cascaded chemical and biochemical conversion using metabolically engineered *Pseudomonas putida*. Metab. Eng. 47, 279–293.
Kosa, M., Ragauskas, A.J., 2012. Bioconversion of lignin model compounds with oleaginous *Rhodococci*. Appl. Microbiol. Biotechnol. 93 (2), 891–900.
Kosa, M., Ragauskas, A.J., 2013. Lignin to lipid bioconversion by oleaginous *Rhodococci*. Green Chem. 15 (8), 2070–2074.
Krömer, J.O., Sorgenfrei, O., Klopprogge, K., Heinzle, E., Wittmann, C., 2004. In-depth profiling of lysine-producing *Corynebacterium glutamicum* by combined analysis of the transcriptome, metabolome, and fluxome. J. Bacteriol. 186 (6), 1769–1784.
Krömer, J.O., Bolten, C.J., Heinzle, E., Schröder, H., Wittmann, C., 2008. Physiological response of *Corynebacterium glutamicum* to oxidative stress induced by deletion of the transcriptional repressor McbR. Microbiology 154 (Pt 12), 3917–3930.
Kuatsjah, E., Chen, H.M., Withers, S.G., Eltis, L.D., 2017. Characterization of an extradiol dioxygenase involved in the catabolism of lignin-derived biphenyl. FEBS Lett. 591 (7), 1001–1009.
Kumar, V., Chandra, R., 2018. Characterisation of manganese peroxidase and laccase producing bacteria capable for degradation of sucrose glutamic acid-Maillard reaction products at different nutritional and environmental conditions. World J. Microbiol. Biotechnol. 34 (2), 32.
Kumar, M., Singhal, A., Verma, P.K., Thakur, I.S., 2017. Production and characterization of polyhydroxyalkanoate from lignin derivatives by *Pandoraea* sp. ISTKB. ACS Omega 2 (12), 9156–9163.
Kumari, M., Yadav, R.S., Yadav, K.D., 2002. Secretion of ligninperoxidase by *Penicillium citrinum*, *Fusarium oxysporum* and *Aspergillus terreus*. Indian journal of experimental biology 40 (7), 802–806.
Lange, A., Becker, J., Schulze, D., Cahoreau, E., Portais, J.C., Haefner, S., Schröder, H., Krawczyk, J., Zelder, O., Wittmann, C., 2017. Bio-based succinate from sucrose: High-resolution ^{13}C metabolic flux analysis and metabolic engineering of the rumen bacterium *Basfia succiniciproducens*. Metab. Eng. 44, 198–212.
Larsson, S., Cassland, P., Jonsson, L.J., 2001. Development of a *Saccharomyces cerevisiae* strain with enhanced resistance to phenolic fermentation inhibitors in lignocellulose hydrolysates by heterologous expression of laccase. Appl. Environ. Microbiol. 67 (3), 1163–1170.
Lee, K.H., Park, J.H., Kim, T.Y., Kim, H.U., Lee, S.Y., 2007. Systems metabolic engineering of *Escherichia coli* for L-threonine production. Mol. Syst. Biol. 3, 149.
Lee, J.Y., Seo, J., Kim, E.S., Lee, H.S., Kim, P., 2013. Adaptive evolution of *Corynebacterium glutamicum* resistant to oxidative stress and its global gene expression profiling. Biotechnol. Lett. 35 (5), 709–717.
Linger, J.G., Vardon, D.R., Guarnieri, M.T., Karp, E.M., Hunsinger, G.B., Franden, M.A., Johnson, C.W., Chupka, G., Strathmann, T.J., Pienkos, P.T., Beckham, G.T., 2014. Lignin valorization through integrated biological funneling and chemical catalysis. Proc. Natl. Acad. Sci. 111 (33), 12013–12018.
Liu, W.H., Li, R.M., Kung, K.H., Cheng, T.L., 2003. Bioconversion of benzoic acid to *cis, cis*-muconic acid by *Corynebacterium pseudodiphtheriticum*. Food Sci. Agri. Chem. 5, 7–12.
Liu, X., Zhao, Z., Zhang, W., Sun, Y., Yang, Y., Bai, Z., 2017. Bicistronic expression strategy for high-level expression of recombinant proteins in *Corynebacterium glutamicum*. Eng. Lif. Sci. 17.
Liu, Z.H., Xie, S., Lin, F., Jin, M., Yuan, J.S., 2018. Combinatorial pretreatment and fermentation optimization enabled a record yield on lignin bioconversion. Biotechnol. Biofuels 11, 21.
López, A.M.Q., Silva, A.L.D., Dos Santos, E.C.L., 2017. The fungal ability for biobleaching/biopulping/bioremediation of lignin-like compounds of agro-industrial raw material. Quim. Nova 40 (8), 916–931.
Lv, B., Sun, H., Huang, S., Feng, X., Jiang, T., Li, C., 2018. Structure-guided engineering of the substrate specificity of a fungal beta-glucuronidase toward triterpenoid saponins. J. Biol. Chem. 293 (2), 433–443.
Ma, Q., Zhang, Q., Xu, Q., Zhang, C., Li, Y., Fan, X., Xie, X., Chen, N., 2017. Systems metabolic engineering strategies for the production of amino acids. Synth. Syst. Biotechnol. 2 (2), 87–96.

Majumdar, S., Lukk, T., Solbiati, J.O., Bauer, S., Nair, S.K., Cronan, J.E., Gerlt, J.A., 2014. Roles of small laccases from *Streptomyces* in lignin degradation. Biochem. 53 (24), 4047–4058.
Mallinson, S.J.B., Machovina, M.M., Silveira, R.L., Garcia-Borras, M., Gallup, N., Johnson, C.W., Allen, M.D., Skaf, M.S., Crowley, M.F., Neidle, E.L., Houk, K.N., Beckham, G.T., DuBois, J.L., McGeehan, J.E., 2018. A promiscuous cytochrome P450 aromatic O-demethylase for lignin bioconversion. Nat. Commun. 9 (1), 2487.
Marinovic, M., Nousiainen, P., Dilokpimol, A., Kontro, J., Moore, R., Sipila, J., de Vries, R.P., Makela, M.R., Hilden, K., 2018. Selective cleavage of lignin beta-O-4 aryl ether bond by beta-etherase of the white-rot fungus *Dichomitus squalens*. ACS Sustain. Chem. Eng. 6 (3), 2878–2882.
Martani, F., Beltrametti, F., Porro, D., Branduardi, P., Lotti, M., 2017. The importance of fermentative conditions for the biotechnological production of lignin modifying enzymes from white-rot fungi. FEMS Microbiol. Lett. 364 (13).
Martinez, A.T., Speranza, M., Ruiz-Duenas, F.J., Ferreira, P., Camarero, S., Guillen, F., Martinez, M.J., Gutierrez, A., del Rio, J.C., 2005. Biodegradation of lignocellulosics: microbial, chemical, and enzymatic aspects of the fungal attack of lignin. Int. Microbiol. 8 (3), 195–204.
Martinez-Garcia, E., Nikel, P.I., Aparicio, T., de Lorenzo, V., 2014a. *Pseudomonas* 2.0: genetic upgrading of *P. putida* KT2440 as an enhanced host for heterologous gene expression. Microb. Cell Fact. 13, 159.
Martinez-Garcia, E., Nikel, P.I., Chavarria, M., de Lorenzo, V., 2014b. The metabolic cost of flagellar motion in *Pseudomonas putida* KT2440. Environ. Microbiol. 16 (1), 291–303.
Martins-Santana, L., Nora, L.C., Sanches-Medeiros, A., Lovate, G.L., Cassiano, M.H.A., Silva-Rocha, R., 2018. Systems and synthetic biology approaches to engineer fungi for fine chemical production. Front. Bioeng. Biotechnol. 6, 117.
Masai, E., Katayama, Y., Nishikawa, S., Yamasaki, M., Morohoshi, N., Haraguchi, T., 1989. Detection and localization of a new enzyme catalyzing the beta-aryl ether cleavage in the soil bacterium (*Pseudomonas paucimobilis* SYK-6). FEBS Lett. 249 (2), 348–352.
Masai, E., Harada, K., Peng, X., Kitayama, H., Katayama, Y., Fukuda, M., 2002. Cloning and characterization of the ferulic acid catabolic genes of *Sphingomonas paucimobilis* SYK-6. Appl. Environ. Microbiol. 68 (9), 4416–4424.
Masai, E., Katayama, Y., Fukuda, M., 2007a. Genetic and biochemical investigations on bacterial catabolic pathways for lignin-derived aromatic compounds. Biosci. Biotechnol. Biochem. 71 (1), 1–15.
Masai, E., Yamamoto, Y., Inoue, T., Takamura, K., Hara, H., Kasai, D., Katayama, Y., Fukuda, M., 2007b. Characterization of *ligV* essential for catabolism of vanillin by *Sphingomonas paucimobilis* SYK-6. Biosci. Biotechnol. Biochem. 71 (10), 2487–2492.
Masai, E., Kamimura, N., Kasai, D., Oguchi, A., Ankai, A., Fukui, S., Takahashi, M., Yashiro, I., Sasaki, H., Harada, T., Nakamura, S., Katano, Y., Narita-Yamada, S., Nakazawa, H., Hara, H., Katayama, Y., Fukuda, M., Yamazaki, S., Fujita, N., 2012. Complete genome sequence of *Sphingobium* sp. strain SYK-6, a degrader of lignin-derived biaryls and monoaryls. J. Bacteriol. 194 (2), 534–535.
Maxwell, P.C., 1982. Production of muconic acid, US Patent No. 4355107.
Maxwell, P.C., 1986. Process for the production of muconic acid, US Patent No. 4588688.
Maxwell, P.C., 1988. Process for the production of muconic acid, US Patent No. 4731328.
Maxwell, P.C., 1991. Microbial culture having catechol 1,2-oxygenase activity, US Patent No. 5026648.
Merkens, H., Beckers, G., Wirtz, A., Burkovski, A., 2005. Vanillate metabolism in *Corynebacterium glutamicum*. Curr. Microbiol. 51 (1), 59–65.
Mimitsuka, T., Sawai, H., Hatsu, M., Yamada, K., 2007. Metabolic engineering of *Corynebacterium glutamicum* for cadaverine fermentation. Biosci. Biotechnol. Biochem. 71 (9), 2130–2135.
Minty, J.J., Lesnefsky, A.A., Lin, F., Chen, Y., Zaroff, T.A., Veloso, A.B., Xie, B., McConnell, C.A., Ward, R.J., Schwartz, D.R., Rouillard, J.M., Gao, Y., Gulari, E., Lin, X.N., 2011. Evolution combined with genomic study elucidates genetic bases of isobutanol tolerance in *Escherichia coli*. Microb. Cell Fact. 10, 18.
Mitsunobu, H., Teramoto, J., Nishida, K., Kondo, A., 2017. Beyond Native Cas9: Manipulating Genomic Information and Function. Trends Biotechnol. 35 (10), 983–996.
Mizuno, S., Yoshikawa, N., Seki, M., Mikawa, T., Imada, Y., 1988. Microbial production of *cis,cis*-muconic acid from benzoic acid. Appl. Microbiol. Biotechnol. 28, 20–25.
Moore, S.J., Lai, H.E., Kelwick, R.J., Chee, S.M., Bell, D.J., Polizzi, K.M., Freemont, P.S., 2016. EcoFlex: A Multifunctional MoClo Kit for E. coli Synthetic Biology. ACS Synth. Biol. 5 (10), 1059–1069.
Muheim, A., Lerch, K., 1999. Towards a high-yield bioconversion of ferulic acid to vanillin. Appl. Microbiol. Biotechnol. 51 (4), 456–461.
Mutalik, V.K., Guimaraes, J.C., Cambray, G., Lam, C., Christoffersen, M.J., Mai, Q.A., Tran, A.B., Paull, M., Keasling, J.D., Arkin, A.P., Endy, D., 2013. Precise and reliable gene expression via standard transcription and translation initiation elements. Nat. Methods 10 (4), 354–360.
Muthu, M., Ophir, Y., Macdonald, L.J., Vaidya, A., Lloyd-Jones, G., 2018. Versatile catechol dioxygenases in *Sphingobium scionense* WP01(T). Anton, Van Lee.
Mycroft, Z., Gomis, M., Mines, P., Law, P., Bugg, T.D.H., 2015. Biocatalytic conversion of lignin to aromatic dicarboxylic acids in *Rhodococcus jostii* RHA1 by re-routing aromatic degradation pathways. Green Chem. 17 (11), 4974–4979.
Narbad, A., Gasson, M.J., 1998. Metabolism of ferulic acid via vanillin using a novel CoA-dependent pathway in a newly-isolated strain of *Pseudomonas fluorescens*. Microbiology 144 (Pt 5), 1397–1405.
Naseem, A., Tabasum, S., Zia, K.M., Zuber, M., Ali, M., Noreen, A., 2016. Lignin-derivatives based polymers, blends and composites: A review. Int. J. Biol. Macromol. 93 (Pt A), 296–313.
Nikel, P.I., de Lorenzo, V., 2014. Robustness of *Pseudomonas putida* KT2440 as a host for ethanol biosynthesis. N. Biotechnol. 31 (6), 562–571.
Nikel, P.I., de Lorenzo, V., 2018. *Pseudomonas putida* as a functional chassis for industrial biocatalysis: From native biochemistry to trans-metabolism. Metab. Eng. 50, 142–155.
Nikel, P.I., Martinez-Garcia, E., de Lorenzo, V., 2014. Biotechnological domestication of pseudomonads using synthetic biology. Nat. Rev. Microbiol. 12 (5), 368–379.
Nishikawa, S., Sonoki, T., Kasahara, T., Obi, T., Kubota, S., Kawai, S., Morohoshi, N., Katayama, Y., 1998. Cloning and sequencing of the *Sphingomonas* (*Pseudomonas*) *paucimobilis* gene essential for the O demethylation of vanillate and syringate. Appl. Environ. Microbiol. 64 (3), 836–842.
Nishizaki, T., Tsuge, K., Itaya, M., Doi, N., Yanagawa, H., 2007. Metabolic engineering of carotenoid biosynthesis in *Escherichia coli* by ordered gene assembly in *Bacillus subtilis*. Appl. Environ. Microbiol. 73 (4), 1355–1361.
Noda, Y., Nishikawa, S., Shiozuka, K., Kadokura, H., Nakajima, H., Yoda, K., Katayama, Y., Morohoshi, N., Haraguchi, T., Yamasaki, M., 1990. Molecular cloning of the protocatechuate 4,5-dioxygenase genes of *Pseudomonas paucimobilis*. J. Bacteriol. 172 (5), 2704–2709.
Nogales, J., Canales, A., Jimenez-Barbero, J., Garcia, J.L., Diaz, E., 2005. Molecular characterization of the gallate dioxygenase from *Pseudomonas putida* KT2440. The prototype of a new subgroup of extradiol dioxygenases. J. Biol. Chem. 280 (42), 35382–35390.
Numata, K., Morisaki, K., 2015. Screening of marine bacteria to synthesize poly-hydroxyalkanoate from lignin: Contribution of lignin derivatives to biosynthesis by *Oceanimonas doudoroffii*. ACS Sustain. Chem. Eng. 3 (4), 569–573.
Oide, S., Gunji, W., Moteki, Y., Yamamoto, S., Suda, M., Jojima, T., Yukawa, H., Inui, M., 2015. Thermal and solvent stress cross-tolerance conferred to *Corynebacterium glutamicum* by adaptive laboratory evolution. Appl. Environ. Microbiol. 81 (7), 2284–2298.
Orellana, R., Chaput, G., Markillie, L.M., Mitchell, H., Gaffrey, M., Orr, G., DeAngelis, K.M., 2017. Multi-time series RNA-seq analysis of *Enterobacter lignolyticus* SCF1 during growth in lignin-amended medium. PLoS One 12 (10), e0186440.
Overhage, J., Priefert, H., Rabenhorst, J., Steinbüchel, A., 1999a. Biotransformation of eugenol to vanillin by a mutant of *Pseudomonas* sp. strain HR199 constructed by disruption of the vanillin dehydrogenase (*vdh*) gene. Appl. Microbiol. Biotechnol. 52 (6), 820–828.
Overhage, J., Priefert, H., Steinbüchel, A., 1999b. Biochemical and genetic analyses of ferulic acid catabolism in *Pseudomonas* sp. Strain HR199. Appl. Environ. Microbiol. 65 (11), 4837–4847.
Overhage, J., Steinbüchel, A., Priefert, H., 2002. Biotransformation of eugenol to ferulic acid by a recombinant strain of *Ralstonia eutropha* H16. Appl. Environ. Microbiol. 68 (9), 4315–4321.
Overhage, J., Steinbüchel, A., Priefert, H., 2003. Highly efficient biotransformation of eugenol to ferulic acid and further conversion to vanillin in recombinant strains of *Escherichia coli*. Appl. Environ. Microbiol. 69 (11), 6569–6576.
Overhage, J., Steinbüchel, A., Priefert, H., 2006. Harnessing eugenol as a substrate for production of aromatic compounds with recombinant strains of *Amycolatopsis* sp. HR167. J. Biotechnol. 125 (3), 369–376.
Paddon, C.J., Westfall, P.J., Pitera, D.J., Benjamin, K., Fisher, K., McPhee, D., Leavell, M.D., Tai, A., Main, A., Eng, D., Polichuk, D.R., Teoh, K.H., Reed, D.W., Treynor, T., Lenihan, J., Fleck, M., Bajad, S., Dang, G., Dengrove, D., Diola, D., Dorin, G., Ellens, K.W., Fickes, S., Galazzo, J., Gaucher, S.P., Geistlinger, T., Henry, R., Hepp, M., Horning, T., Iqbal, T., Jiang, H., Kizer, L., Lieu, B., Melis, D., Moss, N., Regentin, R., Secrest, S., Tsuruta, H., Vazquez, R., Westblade, L.F., Xu, L., Yu, M., Zhang, Y., Zhao, L., Lievense, J., Covello, P.S., Keasling, J.D., Reiling, K.K., Renninger, N.S., Newman, J.D., 2013. High-level semi-synthetic production of the potent antimalarial artemisinin. Nature 496 (7446), 528–532.
Palazzolo, M.A., Kurina-Sanz, M., 2016. Microbial utilization of lignin: available biotechnologies for its degradation and valorization. World J. Microbiol. Biotechnol. 32 (10), 173.
Park, H.J., Kim, E.S., 2003. An inducible *Streptomyces* gene cluster involved in aromatic compound metabolism. FEMS Microbiol. Lett. 226 (1), 151–157.
Park, S.H., Kim, H.U., Kim, T.Y., Park, J.S., Kim, S.S., Lee, S.Y., 2014. Metabolic engineering of *Corynebacterium glutamicum* for L-arginine production. Nat. Commun. 5, 4618.
Payer, S.E., Marshall, S.A., Barland, N., Sheng, X., Reiter, T., Dordic, A., Steinkellner, G., Wuensch, C., Kaltwasser, S., Fisher, K., Rigby, S.E.J., Macheroux, P., Vonck, J., Gruber, K., Faber, K., Himo, F., Leys, D., Pavkov-Keller, T., Glueck, S.M., 2017. Regioselective para-carboxylation of catechols with a prenylated flavin dependent decarboxylase. Angew. Chem. Int. Ed. Engl. 56 (44), 13893–13897.
Peng, X., Egashira, T., Hanashiro, K., Masai, E., Nishikawa, S., Katayama, Y., Kimbara, K., Fukuda, M., 1998. Cloning of a *Sphingomonas paucimobilis* SYK-6 gene encoding a novel oxygenase that cleaves lignin-related biphenyl and characterization of the enzyme. Appl. Environ. Microbiol. 64 (7), 2520–2527.
Peng, X., Masai, E., Katayama, Y., Fukuda, M., 1999. Characterization of the meta-cleavage compound hydrolase gene involved in degradation of the lignin-related biphenyl structure by *Sphingomonas paucimobilis* SYK-6. Appl. Environ. Microbiol. 65 (6), 2789–2793.
Peng, X., Masai, E., Kitayama, H., Harada, K., Katayama, Y., Fukuda, M., 2002. Characterization of the 5-carboxyvanillate decarboxylase gene and its role in lignin-related biphenyl catabolism in *Sphingomonas paucimobilis* SYK-6. Appl. Environ. Microbiol. 68 (9), 4407–4415.
Pfeifer, E., Gatgens, C., Polen, T., Frunzke, J., 2017. Adaptive laboratory evolution of *Corynebacterium glutamicum* towards higher growth rates on glucose minimal medium. Sci. Rep. 7 (1), 16780.
Pinkowska, H., Wolak, P., Zlocinska, A., 2012. Hydrothermal decomposition of alkali lignin in sub- and supercritical water. Chem. Eng. J. 187, 410–414.
Plaggenborg, R., Overhage, J., Steinbüchel, A., Priefert, H., 2003. Functional analyses of

genes involved in the metabolism of ferulic acid in *Pseudomonas putida* KT2440. Appl. Microbiol. Biotechnol. 61 (5-6), 528–535.
Plaggenborg, R., Overhage, J., Loos, A., Archer, J.A., Lessard, P., Sinskey, A.J., Steinbüchel, A., Priefert, H., 2006. Potential of *Rhodococcus* strains for biotechnological vanillin production from ferulic acid and eugenol. Appl. Microbiol. Biotechnol. 72 (4), 745–755.
Poblete-Castro, I., Becker, J., Dohnt, K., dos Santos, V.M., Wittmann, C., 2012. Industrial biotechnology of *Pseudomonas putida* and related species. Appl. Microbiol. Biotechnol. 93 (6), 2279–2290.
Poblete-Castro, I., Binger, D., Rodrigues, A., Becker, J., Martins Dos Santos, V.A., Wittmann, C., 2013. In-silico-driven metabolic engineering of *Pseudomonas putida* for enhanced production of poly-hydroxyalkanoates. Metab. Eng. 15, 113–123.
Polen, T., Spelberg, M., Bott, M., 2013. Toward biotechnological production of adipic acid and precursors from biorenewables. J. Biotechnol. 167 (2), 75–84.
Pometto, A.L., Sutherland, J.B., Crawford, D.L., 1981. *Streptomyces setonii*: catabolism of vanillic acid via guaiacol and catechol. Can. J. Microbiol. 27 (6), 636–638.
Ponnusamy, V.K., Nguyen, D.D., Dharmaraja, J., Shobana, S., Banu, J.R., Saratale, R.G., Chang, S.W., Kumar, G., 2019. A review on lignin structure, pretreatments, fermentation reactions and biorefinery potential. Bioresour. Technol. 271, 462–472.
Portnoy, V.A., Bezdan, D., Zengler, K., 2011. Adaptive laboratory evolution–harnessing the power of biology for metabolic engineering. Curr. Opin. Biotechnol. 22 (4), 590–594.
Priefert, H., Rabenhorst, J., Steinbüchel, A., 1997. Molecular characterization of genes of *Pseudomonas* sp. strain HR199 involved in bioconversion of vanillin to protocatechuate. J. Bacteriol. 179 (8), 2595–2607.
Priefert, H., Rabenhorst, J., Steinbüchel, A., 2001. Biotechnological production of vanillin. Appl. Microbiol. Biotechnol. 56 (3-4), 296–314.
Pye, E.K., 2010. Industrial lignin production and application. In: Kamm, B., Gruber, P.R., Kamm, M. (Eds.), Biorefineries - Industrial processes and products. Wiley-VCH Verlag GmbH & Co. KGaA, Weinheim, pp. 165–200.
Qian, Z.G., Xia, X.X., Lee, S.Y., 2009. Metabolic engineering of *Escherichia coli* for the production of putrescine: a four carbon diamine. Biotechnol. Bioeng. 104 (4), 651–662.
Qian, Z.G., Xia, X.X., Lee, S.Y., 2011. Metabolic engineering of *Escherichia coli* for the production of cadaverine: a five carbon diamine. Biotechnol. Bioeng. 108 (1), 93–103.
Ragauskas, A.J., Beckham, G.T., Biddy, M.J., Chandra, R., Chen, F., Davis, M.F., Davison, B.H., Dixon, R.A., Gilna, P., Keller, M., Langan, P., Naskar, A.K., Saddler, J.N., Tschaplinski, T.J., Tuskan, G.A., Wyman, C.E., 2014. Lignin valorization: improving lignin processing in the biorefinery. Science 344 (6185), 1246843.
Raivio, T.L., Leblanc, S.K., Price, N.L., 2013. The *Escherichia coli* Cpx envelope stress response regulates genes of diverse function that impact antibiotic resistance and membrane integrity. J. Bacteriol. 195 (12), 2755–2767.
Ramos, J.L., Sol Cuenca, M., Molina-Santiago, C., Segura, A., Duque, E., Gomez-Garcia, M.R., Udaondo, Z., Roca, A., 2015. Mechanisms of solvent resistance mediated by interplay of cellular factors in *Pseudomonas putida*. FEMS Microbiol. Rev. 39 (4), 555–566.
Rampioni, G., D'Angelo, F., Leoni, L., Stano, P., 2019. Gene-Expressing Liposomes as Synthetic Cells for Molecular Communication Studies. Front. Bioeng. Biotechnol. 7, 1.
Rey, D.A., Pühler, A., Kalinowski, J., 2003. The putative transcriptional repressor McbR, member of the TetR-family, is involved in the regulation of the metabolic network directing the synthesis of sulfur containing amino acids in *Corynebacterium glutamicum*. J. Biotechnol. 103 (1), 51–65.
Rey, D.A., Nentwich, S.S., Koch, D.J., Rückert, C., Pühler, A., Tauch, A., Kalinowski, J., 2005. The McbR repressor modulated by the effector substance S-adenosylhomocysteine controls directly the transcription of a regulon involved in sulphur metabolism of *Corynebacterium glutamicum* ATCC 13032. Mol. Microbiol. 56 (4), 871–887.
Rinaldi, R., Jastrzebski, R., Clough, M.T., Ralph, J., Kennema, M., Bruijnincx, P.C., Weckhuysen, B.M., 2016. Paving the way for lignin valorisation: recent advances in bioengineering, biorefining and catalysis. Angew. Chem. Int. Ed. Engl. 55 (29), 8164–8215.
Roberts, J.N., Singh, R., Grigg, J.C., Murphy, M.E., Bugg, T.D., Eltis, L.D., 2011. Characterization of dye-decolorizing peroxidases from *Rhodococcus jostii* RHA1. Biochem. 50 (23), 5108–5119.
Rodrigues, A.L., Trachtmann, N., Becker, J., Lohanatha, A.F., Blotenberg, J., Bolten, C.J., Korneli, C., de Souza Lima, A.O., Porto, L.M., Sprenger, G.A., Wittmann, C., 2013. Systems metabolic engineering of *Escherichia coli* for production of the antitumor drugs violacein and deoxyviolacein. Metab. Eng. 20, 29–41.
Rodrigues, A.L., Becker, J., de Souza Lima, A.O., Porto, L.M., Wittmann, C., 2014. Systems metabolic engineering of *Escherichia coli* for gram scale production of the antitumor drug deoxyviolacein from glycerol. Biotechnol. Bioeng. 111 (11), 2280–2289.
Rodriguez, A., Salvachúa, D., Katahira, R., Black, B.A., Cleveland, N.S., Reed, M., Smith, H., Baidoo, E.E.K., Keasling, J.D., Simmons, B.A., Beckham, G.T., Gladden, J.M., 2017. Base-catalyzed depolymerization of solid lignin-rich streams enables microbial conversion. ACS Sustain. Chem. Eng. 5, 8171–8180.
Rohles, C.M., Giesselmann, G., Kohlstedt, M., Wittmann, C., Becker, J., 2016. Systems metabolic engineering of *Corynebacterium glutamicum* for the production of the carbon-5 platform chemicals 5-aminovalerate and glutarate. Microb. Cell Fact. 15 (1), 154.
Rohles, C.M., Gläser, L., Kohlstedt, M., Giesselmann, G., Pearson, S., del Campo, A., Becker, J., Wittmann, C., 2018. A bio-based route to the carbon-5 chemical glutaric acid and to bionylon-6,5 using metabolically engineered *Corynebacterium glutamicum*. Green Chem. 20 (20), 4662–4674.
Rorrer, N.A., Dorgan, J.R., Vardon, D.R., Martinez, C.R., Yang, Y., Beckham, G.T., 2016. Renewable unsaturated polyesters from muconic acid. ACS Sustain. Chem. Eng. 4 (12), 6867–6876.
Rorrer, N.A., Vardon, D.R., Dorgan, J.R., Gjersing, E.J., Beckham, G.T., 2017. Biomass-derived monomers for performance-differentiated fiber reinforced polymer composites. Green Chem. 19 (12), 2812–2825.
Rumbold, K., van Buijsen, H.J., Overkamp, K.M., van Groenestijn, J.W., Punt, P.J., van der Werf, M.J., 2009. Microbial production host selection for converting second-generation feedstocks into bioproducts. Microb. Cell Fact. 8, 64.
Rytter, J.V., Helmark, S., Chen, J., Lezyk, M.J., Solem, C., Jensen, P.R., 2014. Synthetic promoter libraries for *Corynebacterium glutamicum*. Appl. Microbiol. Biotechnol. 98 (6), 2617–2623.
Sainsbury, P.D., Hardiman, E.M., Ahmad, M., Otani, H., Seghezzi, N., Eltis, L.D., Bugg, T.D., 2013. Breaking down lignin to high-value chemicals: the conversion of lignocellulose to vanillin in a gene deletion mutant of *Rhodococcus jostii* RHA1. ACS Chem. Biol. 8 (10), 2151–2156.
Saitoh, S., Ishida, N., Onishi, T., Tokuhiro, K., Nagamori, E., Kitamoto, K., Takahashi, H., 2005. Genetically engineered wine yeast produces a high concentration of L-lactic acid of extremely high optical purity. Appl. Environ. Microbiol. 71 (5), 2789–2792.
Salvachua, D., Karp, E.M., Nimlos, C.T., Vardon, D.R., Beckham, G.T., 2015. Towards lignin consolidated bioprocessing: simultaneous lignin depolymerization and product generation by bacteria. Green Chem. 17 (11), 4951–4967.
Sanderson, K., 2011. Lignocellulose: A chewy problem. Nature 474 (7352), S12–S14.
Sankaran, S., Becker, J., Wittmann, C., Del Campo, A., 2019. Optoregulated drug release from an engineered living material: self-replenishing drug depots for fong-term, light-regulated delivery. Small 15 (5), e1804717.
Sauer, U., 2001. Evolutionary engineering of industrially important microbial phenotypes. Adv. Biochem. Eng. Biotechnol. 73, 129–169.
Schmidt, E., Knackmuss, H.J., 1984. Production of *cis,cis*-muconate from benzoate and 2-fluoro-*cis,cis*-muconate from 3-fluorobenzoate by 3-chlorobenzoate degrading bacteria. Appl. Microbiol. Biotechnol. 20 (5), 351–355.
Schneider, J., Wendisch, V.F., 2010. Putrescine production by engineered *Corynebacterium glutamicum*. Appl. Microbiol. Biotechnol. 88 (4), 859–868.
Schuler, J., Hornung, U., Kruse, A., Dahmen, N., Sauer, J., 2017. Hydrothermal liquefaction of lignin. Journal of Biomaterials and Nanobiotechnology 8, 96–108.
Schutyser, W., Renders, T., Van den Bosch, S., Koelewijn, S.F., Beckham, G.T., Sels, B.F., 2018. Chemicals from lignin: an interplay of lignocellulose fractionation, depolymerisation, and upgrading. Chem. Soc. Rev. 47 (3), 852–908.
Schwechheimer, S.K., Becker, J., Peyriga, L., Portais, J.C., Sauer, D., Müller, R., Hoff, B., Haefner, S., Schröder, H., Zelder, O., Wittmann, C., 2018a. Improved riboflavin production with *Ashbya gossypii* from vegetable oil based on ^{13}C metabolic network analysis with combined labeling analysis by GC/MS, LC/MS, 1D, and 2D NMR. Metab. Eng. 47, 357–373.
Schwechheimer, S.K., Becker, J., Peyriga, L., Portais, J.C., Wittmann, C., 2018b. Metabolic flux analysis in *Ashbya gossypii* using ^{13}C-labeled yeast extract: industrial riboflavin production under complex nutrient conditions. Microb. Cell Fact. 17 (1), 162.
Schwille, P., Spatz, J., Landfester, K., Bodenschatz, E., Herminghaus, S., Sourjik, V., Erb, T.J., Bastiaens, P., Lipowsky, R., Hyman, A., Dabrock, P., Baret, J.C., Vidakovic-Koch, T., Bieling, P., Dimova, R., Mutschler, H., Robinson, T., Tang, T.Y.D., Wegner, S., Sundmacher, K., 2018. MaxSynBio: Avenues Towards Creating Cells from the Bottom Up. Angewandte Chemie-International Edition 57 (41), 13382–13392.
Shen, X., Liu, S., 2005. Key enzymes of the protocatechuate branch of the beta-ketoadipate pathway for aromatic degradation in *Corynebacterium glutamicum*. Sci. China C. Life Sci. 48 (3), 241–249.
Shen, X.H., Huang, Y., Liu, S.J., 2005. Genomic analysis and identification of catabolic pathways for aromatic compounds in *Corynebacterium glutamicum*. Microb. Environ. 20 (3), 160–167.
Shen, C.R., Lan, E.I., Dekishima, Y., Baez, A., Cho, K.M., Liao, J.C., 2011. Driving forces enable high-titer anaerobic 1-butanol synthesis in *Escherichia coli*. Appl. Environ. Microbiol. 77 (9), 2905–2915.
Shen, X.H., Zhou, N.Y., Liu, S.J., 2012. Degradation and assimilation of aromatic compounds by *Corynebacterium glutamicum*: another potential for applications for this bacterium? Appl. Microbiol. Biotechnol. 95 (1), 77–89.
Shi, Y., Yan, X., Li, Q., Wang, X., Liu, M.R., Xie, S.X., Chai, L.Y., Yuan, J.S., 2017. Directed bioconversion of Kraft lignin to polyhydroxyalkanoate by *Cupriavidus basilensis* B-8 without any pretreatment. Pro. Biochem. 52, 238–242.
Shin, J.H., Park, S.H., Oh, Y.H., Choi, J.W., Lee, M.H., Cho, J.S., Jeong, K.J., Joo, J.C., Yu, J., Park, S.J., Lee, S.Y., 2016. Metabolic engineering of *Corynebacterium glutamicum* for enhanced production of 5-aminovaleric acid. Microb. Cell Fact. 15 (1), 174.
Shrestha, R., Huang, G., Meekins, D.A., Geisbrecht, B.V., Li, P., 2017. Mechanistic insights into dye-decolorizing peroxidase revealed by solvent isotope and viscosity effects. ACS Catal. 7 (9), 6352–6364.
Smith, K.M., Cho, K.M., Liao, J.C., 2010. Engineering *Corynebacterium glutamicum* for isobutanol production. Appl. Microbiol. Biotechnol. 87 (3), 1045–1055.
Sonoki, T., Obi, T., Kubota, S., Higashi, M., Masai, E., Katayama, Y., 2000. Coexistence of two different O demethylation systems in lignin metabolism by *Sphingomonas paucimobilis* SYK-6: cloning and sequencing of the lignin biphenyl-specific O-demethylase (LigX) gene. Appl. Environ. Microbiol. 66 (5), 2125–2132.
Sonoki, T., Morooka, M., Sakamoto, K., Otsuka, Y., Nakamura, M., Jellison, J., Goodell, B., 2014. Enhancement of protocatechuate decarboxylase activity for the effective production of muconate from lignin-related aromatic compounds. J. Biotechnol. 192 (Pt A), 71–77.
Sonoki, T., Takahashi, K., Sugita, H., Hatamura, M., Azuma, Y., Sato, T., Suzuki, S., Kamimura, N., Masai, E., 2018. Glucose-free *cis,cis*-muconic acid production via new metabolic designs corresponding to the heterogeneity of lignin. ACS Sustain. Chem. Eng. 6 (1), 1256–1264.
Sparnins, V.L., Dagley, S., 1975. Alternative routes of aromatic catabolism in *Pseudomonas acidovorans* and *Pseudomonas putida*: gallic acid as a substrate and inhibitor of

dioxygenases. J. Bacteriol. 124 (3), 1374–1381.
Storch, M., Casini, A., Mackrow, B., Ellis, T., Baldwin, G.S., 2017. BASIC: A Simple and Accurate Modular DNA Assembly Method. Methods Mol. Biol. 1472, 79–91.
Suastegui, M., Matthiesen, J.E., Carraher, J.M., Hernandez, N., Rodriguez Quiroz, N., Okerlund, A., Cochran, E.W., Shao, Z., Tessonnier, J.P., 2016. Combining metabolic engineering and electrocatalysis: application to the production of polyamides from sugar. Angew. Chem. Int. Ed. Engl. 55 (7), 2368–2373.
Sugimoto, K., Senda, M., Kasai, D., Fukuda, M., Masai, E., Senda, T., 2014. Molecular mechanism of strict substrate specificity of an extradiol dioxygenase, DesB, derived from *Sphingobium* sp. SYK-6. PLoS One 9 (3) e92249.
Sutherland, J.B., Crawford, D.L., Pometto 3rd, A.L., 1983. Metabolism of cinnamic, *p*-coumaric, and ferulic acids by *Streptomyces setonii*. Can. J. Microbiol. 29 (10), 1253–1257.
Takahashi, K., Kamimura, N., Hishiyama, S., Hara, H., Kasai, D., Katayama, Y., Fukuda, M., Kajita, S., Masai, E., 2014. Characterization of the catabolic pathway for a phenylcoumaran-type lignin-derived biaryl in *Sphingobium* sp. strain SYK-6. Biodegradation 25 (5), 735–745.
Takahashi, K., Miyake, K., Hishiyama, S., Kamimura, N., Masai, E., 2018. Two novel decarboxylase genes play a key role in the stereospecific catabolism of dehydrodiconiferyl alcohol in *Sphingobium* sp. strain SYK-6. Environ. Microbiol. 20 (5), 1739–1750.
Tien, M., Kirk, T.K., 1984. Lignin-degrading enzyme from *Phanerochaete chrysosporium*: Purification, characterization, and catalytic properties of a unique H(2)O(2)-requiring oxygenase. Proc. Natl. Acad. Sci. 81 (8), 2280–2284.
Tsuge, Y., Hasunuma, T., Kondo, A., 2015. Recent advances in the metabolic engineering of *Corynebacterium glutamicum* for the production of lactate and succinate from renewable resources. J. Ind. Microbiol. Biotechnol. 42 (3), 375–389.
Tsuruta, H., Paddon, C.J., Eng, D., Lenihan, J.R., Horning, T., Anthony, L.C., Regentin, R., Keasling, J.D., Renninger, N.S., Newman, J.D., 2009. High-level production of amorpha-4,11-diene, a precursor of the antimalarial agent artemisinin, in *Escherichia coli*. PLoS One 4 (2), e4489.
Ukibe, K., Hashida, K., Yoshida, N., Takagi, H., 2009. Metabolic engineering of *Saccharomyces cerevisiae* for astaxanthin production and oxidative stress tolerance. Appl. Environ. Microbiol. 75 (22), 7205–7211.
Van den Bosch, S., Koelewijn, S.F., Renders, T., Van den Bossche, G., Vangeel, T., Schutyser, W., Sels, B.F., 2018. Catalytic Strategies Towards Lignin-Derived Chemicals. Top. Curr. Chem. 376 (5), 36.
van Duuren, J.B., Wijte, D., Leprince, A., Karge, B., Puchalka, J., Wery, J., Dos Santos, V.A., Eggink, G., Mars, A.E., 2011. Generation of a *catR* deficient mutant of *P. putida* KT2440 that produces *cis*, *cis*-muconate from benzoate at high rate and yield. J. Biotechnol. 156 (3), 163–172.
van Duuren, J.B., Wijte, D., Karge, B., dos Santos, V.A., Yang, Y., Mars, A.E., Eggink, G., 2012. pH-stat fed-batch process to enhance the production of cis, cis-muconate from benzoate by *Pseudomonas putida* KT2440-JD1. Biotechnol. Prog. 28 (1), 85–92.
Vardon, D.R., Franden, M.A., Johnson, C.W., Karp, E.M., Guarnieri, M.T., Linger, J.G., Salm, M.J., Strathmann, T.J., Beckham, G.T., 2015. Adipic acid production from lignin. Energ. Environ. Sci. pp. 617-628.
Vardon, D.R., Rorrer, N.A., Salvachua, D., Settle, A.E., Johnson, C.W., Menart, M.J., Cleveland, N.S., Ciesielski, P.N., Steirer, K.X., Dorgan, J.R., Beckham, G.T., 2016. *cis,cis*-Muconic acid: separation and catalysis to bio-adipic acid for nylon-6,6 polymerization. Green Chem. 18 (11), 3397–3413.
Varman, A.M., Follenfant, R., Liu, F., Davis, R.W., Lin, Y.K., Singh, S., 2018. Hybrid phenolic-inducible promoters towards construction of self-inducible systems for microbial lignin valorization. Biotechnol. Biofuels 11, 182.
Vasudevan, N., Mahadevan, A., 1990. Degradation of labelled lignins and veratrylglycerol-beta-guaiacyl ether by *Acinetobacter* sp. Ital. J. Biochem. 39 (5), 285–293.
Vasudevan, N., Mahadevan, A., 1992. Degradation of non-phenolic beta-o-4 lignin substructure model compounds by *Acinetobacter* sp. Res. Microbiol. 143 (3), 333–339.
Vignali, E., Tonin, F., Pollegioni, L., Rosini, E., 2018. Characterization and use of a bacterial lignin peroxidase with an improved manganese-oxidative activity. Appl. Microbiol. Biotechnol. 102 (24), 10579–10588.
Vyas, P., Kumar, A., Singh, S., 2018. Biomass breakdown: A review on pretreatment, instrumentations and methods. Front. Biosci. 10, 155–174.
Wahyudiono Sasaki, M., Goto, M., 2011. Thermal decomposition of guaiacol in sub- and supercritical water and its kinetic analysis. J. Mater. Cycles Waste 13 (1), 68–79.
Wang, K., Yang, H., Yao, X., Xu, F., Sun, R.C., 2012. Structural transformation of hemicelluloses and lignin from triploid poplar during acid-pretreatment based biorefinery process. Bioresour. Technol. 116, 99–106.
Wang, J.P., Matthews, M.L., Williams, C.M., Shi, R., Yang, C., Tunlaya-Anukit, S., Chen, H.C., Li, Q., Liu, J., Lin, C.Y., Naik, P., Sun, Y.H., Loziuk, P.L., Yeh, T.F., Kim, H., Gjersing, E., Shollenberger, T., Shuford, C.M., Song, J., Miller, Z., Huang, Y.Y., Edmunds, C.W., Liu, B., Sun, Y., Lin, Y.J., Li, W., Chen, H., Peszlen, I., Ducoste, J.J., Ralph, J., Chang, H.M., Muddiman, D.C., Davis, M.F., Smith, C., Isik, F., Sederoff, R., Chiang, V.L., 2018a. Improving wood properties for wood utilization through multi-omics integration in lignin biosynthesis. Nat. Commun. 9 (1), 1579.
Wang, X., Khushk, I., Xiao, Y., Gao, Q., Bao, J., 2018b. Tolerance improvement of *Corynebacterium glutamicum* on lignocellulose derived inhibitors by adaptive evolution. Appl. Microbiol. Biotechnol. 102 (1), 377–388.
Wang, X., Lin, L., Dong, J., Ling, J., Wang, W., Wang, H., Zhang, Z., Yu, X., 2018c. Simultaneous improvements of *Pseudomonas* cell growth and polyhydroxyalkanoate production from a lignin derivative for lignin-consolidated bioprocessing. Appl. Environ. Microbiol. 84 (18).
Weber, H., Polen, T., Heuveling, J., Wendisch, V.F., Hengge, R., 2005. Genome-wide analysis of the general stress response network in Escherichia coli: sigmaS-dependent genes, promoters, and sigma factor selectivity. J. Bacteriol. 187 (5), 1591–1603.
Weber, H.E., Gottardi, M., Bruckner, C., Oreb, M., Boles, E., Tripp, J., 2017. Requirement of a functional flavin mononucleotide prenyltransferase for the activity of a bacterial decarboxylase in a heterologous muconic acid pathway in *Saccharomyces cerevisiae*. Appl. Environ. Microbiol. 83 (10).
Wei, Z., Zeng, G.M., Huang, F., Kosa, M., Huang, D.L., Ragauskas, A.J., 2015. Bioconversion of oxygen-pretreated Kraft lignin to microbial lipid with oleaginous *Rhodococcus opacus* DSM 1069. Green Chem. 17 (5), 2784–2789.
Wengel, M., Kothe, E., Schmidt, C.M., Heide, K., Gleixner, G., 2006. Degradation of organic matter from black shales and charcoal by the wood-rotting fungus *Schizophyllum commune* and release of DOC and heavy metals in the aqueous phase. The Science of the total environment 367 (1), 383–393.
White, M.D., Payne, K.A., Fisher, K., Marshall, S.A., Parker, D., Rattray, N.J., Trivedi, D.K., Goodacre, R., Rigby, S.E., Scrutton, N.S., Hay, S., Leys, D., 2015. UbiX is a flavin prenyltransferase required for bacterial ubiquinone biosynthesis. Nature 522 (7557), 502–506.
Wittmann, C., Heinzle, E., 2002. Genealogy profiling through strain improvement by using metabolic network analysis: metabolic flux genealogy of several generations of lysine-producing Corynebacteria. Appl. Environ. Microbiol. 68 (12), 5843–5859.
Wittmann, C., Hans, M., Bluemke, W., 2002. Metabolic physiology of aroma-producing *Kluyveromyces marxianus*. Yeast 19 (15), 1351–1363.
Wittmann, C., Kiefer, P., Zelder, O., 2004. Metabolic fluxes in *Corynebacterium glutamicum* during lysine production with sucrose as carbon source. Appl. Environ. Microbiol. 70 (12), 7277–7287.
Wu, Y.R., He, J., 2013. Characterization of anaerobic consortia coupled lignin depolymerization with biomethane generation. Bioresour. Technol. 139, 5–12.
Wu, C.M., Wu, C.C., Su, C.C., Lee, S.N., Lee, Y.A., Wu, J.Y., 2006. Microbial synthesis of *cis,cis*-muconic acid from benzoate by *Sphingobacterium* sp mutants. Biochem. Eng. J. 29 (1-2), 35–40.
Wu, W., Liu, F., Singh, S., 2018. Toward engineering *E. coli* with an autoregulatory system for lignin valorization. Proc. Natl. Acad. Sci. 115 (12), 2970–2975.
Xiao, W., Duan, X., Lin, Y., Cao, Q., Li, S., Guo, Y., Gan, Y., Qi, X., Zhou, Y., Guo, L., Qin, P., Wang, Q., Shui, W., 2018. Distinct proteome remodeling of industrial *Saccharomyces cerevisiae* in response to prolonged thermal stress or transient heat shock. J. Proteome Res. 17 (5), 1812–1825.
Xie, N.Z., Wang, Q.Y., Zhu, Q.X., Qin, Y., Tao, F., Huang, R.B., Xu, P., 2014. Optimization of medium composition for *cis,cis*-muconic acid production by a *Pseudomonas* sp. mutant using statistical methods. Prep. Biochem. Biotechnol. 44 (4), 342–354.
Xu, C.P., Arancon, R.A.D., Labidi, J., Luque, R., 2014. Lignin depolymerisation strategies: towards valuable chemicals and fuels. Chem. Soc. Rev. 43 (22), 7485–7500.
Xu, Z., Qin, L., Cai, M., Hua, W., Jin, M., 2018. Biodegradation of kraft lignin by newly isolated *Klebsiella pneumoniae*, *Pseudomonas putida*, and *Ochrobactrum tritici* strains. Environ. Sci. Pollut. Res. Int. 25 (14), 14171–14181.
Xu, N., Wei, L., Liu, J., 2019. Recent advances in the applications of promoter engineering for the optimization of metabolite biosynthesis. World J. Microbiol. Biotechnol. 35 (2), 33.
Yim, S.S., An, S.J., Kang, M., Lee, J., Jeong, K.J., 2013. Isolation of fully synthetic promoters for high-level gene expression in *Corynebacterium glutamicum*. Biotechnol. Bioeng. 110 (11), 2959–2969.
Yim, S.S., Choi, J.W., Lee, R.J., Lee, Y.J., Lee, S.H., Kim, S.Y., Jeong, K.J., 2016. Development of a new platform for secretory production of recombinant proteins in *Corynebacterium glutamicum*. Biotechnol. Bioeng. 113 (1), 163–172.
Yoneda, A., Henson, W.R., Goldner, N.K., Park, K.J., Forsberg, K.J., Kim, S.J., Pesesky, M.W., Foston, M., Dantas, G., Moon, T.S., 2016. Comparative transcriptomics elucidates adaptive phenol tolerance and utilization in lipid-accumulating *Rhodococcus opacus* PD630. Nucleic Acids Res. 44 (5), 2240–2254.
York-Duran, M.J., Godoy-Gallardo, M., Labay, C., Urquhart, A.J., Andresen, T.L., Hosta-Rigau, L., 2017. Recent advances in compartmentalized synthetic architectures as drug carriers, cell mimics and artificial organelles. Colloid. Surface B. 152, 199–213.
Yoshida, T., Inami, Y., Matsui, T., Nagasawa, T., 2010. Regioselective carboxylation of catechol by 3,4-dihydroxybenzoate decarboxylase of *Enterobacter cloacae* P. Biotechnol. Lett. 32 (5), 701–705.
Yoshikata, T., Suzuki, K., Kamimura, N., Namiki, M., Hishiyama, S., Araki, T., Kasai, D., Otsuka, Y., Nakamura, M., Fukuda, M., Katayama, Y., Masai, E., 2014. Three-component O-demethylase system essential for catabolism of a lignin-derived biphenyl compound in *Sphingobium* sp. strain SYK-6. Appl. Environ. Microbiol. 80 (23), 7142–7153.
Yu, J.L., Xia, X.X., Zhong, J.J., Qian, Z.G., 2014. Direct biosynthesis of adipic acid from a synthetic pathway in recombinant *Escherichia coli*. Biotechnol. Bioeng. 111 (12), 2580–2586.
Zhang, B., Zhou, N., Liu, Y.M., Liu, C., Lou, C.B., Jiang, C.Y., Liu, S.J., 2015. Ribosome binding site libraries and pathway modules for shikimic acid synthesis with *Corynebacterium glutamicum*. Microb. Cell Fact. 14, 71.
Zhao, C., Xie, S.X., Pu, Y.Q., Zhang, R., Huang, F., Ragauskas, A.J., Yuan, J.S., 2016. Synergistic enzymatic and microbial lignin conversion. Green Chem. 18 (5), 1306–1312.
Zhou, L.B., Zeng, A.P., 2015. Exploring lysine riboswitch for metabolic flux control and improvement of L-lysine synthesis in *Corynebacterium glutamicum*. ACS Synth. Biol. 4 (6), 729–734.
Zhou, Y., Yang, B., Yang, Y., Jia, R., 2014. Optimization of manganese peroxidase production from *Schizophyllum* sp. F17 in solid-state fermentation of agro-industrial residues. Chin. J. Biotechnol. 30 (3), 524–528.